

## **UC Merced**

### **UC Merced Electronic Theses and Dissertations**

#### **Title**

The role of glial glutamate transporter and its impact on amyloid-beta and tau pathology in Alzheimer's disease

#### **Permalink**

<https://escholarship.org/uc/item/85n0q68w>

#### **Author**

Zumkehr, Joannee

#### **Publication Date**

2017

Peer reviewed|Thesis/dissertation

UNIVERSITY OF CALIFORNIA, MERCED

The role of glial glutamate transporter and its impact on amyloid-beta and tau pathology  
in Alzheimer's disease

A dissertation submitted in partial satisfaction of the requirements for the degree of  
Doctor of Philosophy

in

Quantitative and Systems Biology

by

Joannee Mae Zumkehr

2017

Committee in charge:

Professor Patricia LiWang, Chair  
Professor Masashi Kitazawa  
Professor Fredrick Wolf  
Professor Ramen Saha

Copyright

Joanee Mae Zumkehr, 2017

All rights reserved

The Dissertation of Joannee Mae Zumkehr is approved, and it is acceptable  
in quality and form for publication on microfilm and electronically:

---

Professor Masashi Kitazawa

---

Professor Fredrick Wolf

---

Professor Ramen Saha

---

Professor Patricia LiWang (Chair)

University of California, Merced

2017

## Table of Contents

List of Tables .....	vii
List of Figures .....	viii
Acknowledgments.....	xiii
Curriculum Vita .....	xv
Abstract.....	xvii
Chapter 1: Introduction.....	1
1.1 Dissertation Statement.....	1
1.2 Motivation .....	1
1.3 Background .....	2
1.3.1 A $\beta$ pathology: breakdown of APP to understand A $\beta$ .....	4
1.3.2 Versatile role of inflammation: A $\beta$ regulator and neuron-glia mediator .....	6
1.3.3 Tau pathology: key contributor to neuronal damage .....	7
1.3.4 Synaptic loss: the significant correlate to cognitive decline.....	7
1.4 Premise.....	8
1.4.1 Astrocytes: role in glutamatergic system.....	8
1.4.2 GLT-1 in AD.....	9
1.4.3 GLT-1 .....	10
1.4.4 The loss of GLT-1 and its impact on AD neuropathology .....	10
1.5 Hypothesis.....	11
1.6 Dissertation Contribution.....	11
1.7 Conclusion.....	12
Chapter 2: Ceftriaxone ameliorates tau pathology and cognitive decline via restoration of glial glutamate transporter in a mouse model of Alzheimer’s disease. ....	13
2.1 Abstract .....	13
2.2 Introduction .....	13
2.3 Materials and Methods.....	14
2.3.1 Animals.....	14
2.3.2 Cognitive tests.....	15
2.3.3 Quantitative A $\beta$ ELISA analysis.....	15
2.3.4 Western blot and analysis .....	16
2.3.5 Real-time PCR (RT-PCR).....	16
2.3.6 Immunohistochemical (IHC) and immunofluorescence (IF) staining .....	17

2.3.7	Thioflavin S staining.....	17
2.3.8	Quantitative analysis of synaptic proteins, plaque burden and tau pathology. 17	
2.3.9	Astrocyte and neuron primary cell co-culture .....	18
2.3.10	7PA2 –Chinese Hamster Ovary (CHO) cell culture .....	18
2.3.11	Statistical analysis.....	18
2.4	Results .....	18
2.5	Discussion .....	27
2.6	Conclusion.....	29
Chapter 3: Inflammatory cytokine, IL-1 $\beta$ , regulates glial glutamate transporter via microRNA-181a in vitro.....		30
3.1	Abstract .....	30
3.2	Introduction .....	30
3.3	Materials and Methods.....	32
3.3.1	Primary astrocyte and neuron co-culture .....	32
3.3.2	Chinese hamster ovary and 7PA2 cell cultures.....	32
3.3.3	Quantitative measurement of secreted cytokines via cytokine multiplex assay	32
3.3.4	Western Blot .....	32
3.3.5	RNA Isolation, Reverse Transcription, and Real-time Polymerase Chain Reaction .....	33
3.3.6	TaqMan Detection .....	33
3.3.7	MiR-181a Mimic Transfection .....	33
3.3.8	Statistics .....	33
3.4	Results .....	34
3.4.1	Inflammatory cytokines, IL-1 $\beta$ or TNF $\alpha$ , upregulate GLT-1 in astrocytes	34
3.4.2	MicroRNA-181a mediates IL-1 $\beta$ -induced GLT-1 upregulation in astrocytes 36	
3.4.3	Primary and mature miR-181a in human AD brain.....	38
3.5	Discussion .....	40
3.6	Conclusion.....	42
Chapter 4: Future projects .....		43
4.1	Abstract .....	43
4.2	Introduction .....	43
4.3	Methods.....	44

4.3.1	Animals .....	44
4.3.2	Immunostaining .....	46
4.3.3	Thioflavin S staining.....	46
4.3.4	Golgi Staining .....	46
4.3.5	Statistics .....	47
4.4	Results .....	47
4.4.1	Breeding scheme to generate GLT-1 knockdown with A $\beta$ or tau pathology. 47	
4.4.2	A $\beta$ pathology.....	48
4.4.3	Tau pathology .....	51
4.5	Discussion .....	51
4.6	Conclusion.....	53
Chapter 5:	Conclusion .....	54
References	.....	56

## **List of Tables**

Table 1. Human samples information.....	40
Table 2. Mouse acronym.....	45



## List of Figures

- Figure 1-1. Canonical processing of APP. A $\beta$  peptides are generated from ~100 kDa type one transmembrane protein, APP, and range from 38-43 amino acids. APP is cleaved by known proteases called the  $\alpha$ - or  $\beta$ - secretase then  $\gamma$ - secretases.  $\alpha$ -secretase prevents A $\beta_{42}$  generation by cleaving in the middle of the A $\beta$  domain while the sequential cleavage by  $\beta$ - then  $\gamma$ - secretase produce the amyloidogenic A $\beta_{40}$  or A $\beta_{42}$  by cleavage of the N- and C-terminal domains of A $\beta$  respectively. A $\beta_{40}$  and A $\beta_{42}$  are the predominant species, A $\beta_{42}$  being the most amyloidogenic. PSEN1 and PSEN2 are the catalytic components of  $\gamma$ -secretase and mutations in these genes increase A $\beta_{42}$ /A $\beta_{40}$  ratio..... 4
- Figure 1-2. Glutamatergic tripartite synapse (simplified). Depolarization of the presynaptic neuron, releases calcium-dependent glutamate-containing vesicles to release glutamate in the synaptic space. Glutamate binds to both ionotropic and metabotropic receptors (not shown). Binding of glutamate to ionotropic receptors leads to an influx of sodium and calcium ions into the post-synaptic neuron causing its depolarization. Excess glutamate is taken up by glutamate transporters – majorly regulated by GLT-1 expressed mainly on astrocytes. In astrocytes, glutamate is metabolized; glutamine synthetase converts glutamate to glutamine. Glutamine is returned to the pre-synaptic neuron where it is converted to glutamate by glutaminase. .... 9
- Figure 2-1. GLT-1 decreases in an age-dependent manner in 3xTg-AD mice. (A) RT-PCR analysis of GLT-1 mRNA levels in wild type (WT) and 3xTg-AD mice at 2, 6 and 23 month (mo) old mice. (B) RT-PCR analysis of GFAP mRNA levels in WT and 3xTg-AD 2, 6 and 23 month old mice. (C) Western blot analysis of protein extracts from 3, 12 and 23 month old WT and 3xTg-AD mice using GLT-1, GFAP and GAPDH antibodies. The densitometric analysis of the GLT-1 (D), GLAST (E) and GFAP (F) bands normalized to GAPDH shown in the graphs. Each bar is expressed as mean  $\pm$  standard error mean (S.E.M); \* $p < 0.05$  and \*\* $p < 0.01$  compared to the WT group or 2-3 months old 3xTg-AD group. The number of mice analyzed was  $n = 5-7$  per group. .... 20
- Figure 2-2. Naturally secreted A $\beta$  decrease GLT-1 steady state levels. (A) Experimental scheme for investigating GLT-1 expression in the primary astrocyte and neuron co-culture. Astrocytes extracted from the cortex and hippocampus of postnatal day 0 – day 3 (P0-P3) and detected with the GFAP antibody. Neurons were extracted from embryonic day 14 – 16 (E14 – E16) and detected with tau5 or SYP antibodies. 1.85 nM of naturally secreted A $\beta_{42}$  and 4.4 nM of naturally secreted A $\beta_{40}$  present in 7PA2-CM (quantified by ELISA) were added to the co-culture for 48 hours. (B)

RT-PCR analysis of GLT-1 and GLAST mRNA levels from neuron and astrocyte co-cultures treated with CHO conditioned media (CHO-CM) or 7PA2 conditioned media (7PA2-CM) for 48 hrs. (C) Western blot of protein extracts from neuron and astrocyte co-cultures treated with 7PA2-CM or CHO-CM for 48 hours using GLT-1 and tubulin antibodies. The densitometric analysis of the 70 kDa and 140 kDa band from GLT shown in the graph. Each bar is expressed as mean  $\pm$  S.E.M.; \*\*\* $p < 0.0001$  7PA2-CM compared to CHO-CM. Three independent experiments performed each time in triplicates..... 21

Figure 2-3. Chronic ceftriaxone-treatment increases GLT-1 expression levels in 3xTg-AD mice. (A) Western blot analysis of protein extracts from hippocampal tissue of 12 month old 3xTg-AD mice using GLT-1 and GAPDH (housekeeping) antibodies. Densitometric analysis of the GLT1 bands normalized to GAPDH shown in the graph. Each bar is expressed as mean  $\pm$  S.E.M.; \* $p < 0.05$ , ceftriaxone-treated 3xTg-AD mice compared with the vehicle-treated 3xTg-AD mice (n = 5 mice per group). Molecular weight markers are in kDa. Veh = vehicle or saline-treatment and Cef = ceftriaxone treatment. .... 22

Figure 2-4. Upregulation of GLT-1 by ceftriaxone ameliorates cognitive decline in 3xTg-AD mice. (A) Acquisition curve during training of MWM expressed as average of all mice in each group. Arrowheads show the first training of the day. (B) Escape latency and (C) number of crosses on platform location for 24-hour retention trial in MWM. (D) NOR for the first minute of the test. Each bar is expressed as mean  $\pm$  S.E.M.; \* $p < 0.05$  and \*\* $p < 0.01$ , ceftriaxone-treated 3xTg-AD mice compared with the vehicle-treated 3xTg-AD mice (n = 5 mice per group). .... 23

Figure 2-5. Effect of GLT-1 up-regulation on A $\beta$  pathology in 3xTg-AD mice. (A) Quantitative A $\beta$  ELISA in detergent-insoluble (formic acid soluble) brain hippocampal fraction and detergent soluble brain hippocampal fraction. (B) Western blot analysis of APP processing in the hippocampus of the brain. The densitometric analysis of C99 and C83 fragments shown in the graph. (C) Dot blot analysis of soluble pre-fibrillar and fibrillar A $\beta$  oligomers in the cortical soluble fractions detected by the A11 and OC antibodies respectively. (D) Qualitative representation of the immunohistochemical staining with 4G8 and Thioflavin S to detect A $\beta$  plaques. Each bar is expressed in mean  $\pm$  S.E.M.; \*\* $p < 0.01$ , ceftriaxone-treated 3xTg-AD mice compared with the vehicle-treated 3xTg-AD mice (n = 4-5 mice per group). .... 24

Figure 2-6. Effect of GLT-1 up-regulation on tau pathology in 3xTg-AD mice. (A) Representative IHC or IF staining with tau antibodies HT7, PHF-1 and CP13 antibodies. The mean intensities of HT7 and PHF-1 from immunofluorescence staining are shown in the graph along with the CP-13 positive neuron analysis. Arrows point to tau-positive neurons. (B) Representative western blot image of total human tau using HT7 antibody from the sarkosyl – insoluble cortical protein fraction. The densitometric analysis of all bands are shown in the graph. (C) Western blot analysis of total human tau using HT7 antibody and various phosphor-

specific tau using PHF1, AT8, CP13, AT180 and GAPDH (housekeeping protein) from the detergent-soluble hippocampal protein fraction. The densitometric analysis of PHF1, AT8, CP13 and AT180 are shown in the graph. (D) Western blot analysis of known tau kinases: p25, p35, phosphor-GSK3 $\beta$  (pGSK3 $\beta$ ), GSK3 $\beta$  and Tubulin (housekeeping protein) on detergent soluble hippocampal protein fraction. The densitometric analysis of p25, p35, phosphor-GSK3 $\beta$  and GSK3 $\beta$  are shown in the graph. Each bar is expressed as mean  $\pm$  S.E.M.; \*p<0.05, ceftriaxone-treated 3xTg-AD mice compared with the vehicle-treated 3xTg-AD mice (n = 4-5 mice per group)..... 26

Figure 2-7. Synaptic proteins restored in ceftriaxone-treated 3xTg-AD mice. (A) Representative IF images of SYP in the CA3 region of the hippocampus and quantitative analysis of the average mean intensities from five IF (20  $\mu$ m) stained sections in the dentate gyrus (DG), CA1 and CA3 of the hippocampus. (B) Representative IF images of PSD95 in the CA3 region of the hippocampus and quantitative analysis of the average mean intensities from five IF (20  $\mu$ m) stained sections in the DG, CA1 and CA3 of the hippocampus. (C) Escape latency as a function of synaptic protein mean intensity graphs in the designated region of the hippocampus. Each shape represents one mouse and each bar is expressed as mean  $\pm$  S.E.M.; \*p<0.05 and \*\*\*p<0.001, ceftriaxone-treated 3xTg-AD mice compared with the vehicle-treated 3xTg-AD mice (n = 3-5 mice per group). Sec = seconds . 27

Figure 3-1 Primary astrocyte and neuron co-culture treated with CHO-CM elevated GLT-1 steady state levels while 7PA2-CM decreased GLT-1 steady state levels relative to regular neurobasal growth media (control) after 48 hours treatment. GLT-1 mean  $\pm$  std. error: Control = 1.01  $\pm$  0.00816, CHO-CM = 1.48  $\pm$  0.111, 7PA2-CM= 0.645  $\pm$  .0506, Control vs CHO p = 0.0023, Control vs 7PA2-CM p = 0.0051 and CHO-CM vs 7PA2-CM p < 0.0001, n = 4 independent experiments in triplicates. p  $\leq$  0.05 considered significant by one-way ANOVA followed by Holm-Sidak's post hoc multiple comparisons test. Abbreviations: CHO = Chinese hamster ovary; 7PA2 = CHO cells that express the V717F AD mutation in APP751 (an APP isoform that is 751 amino acids in length); CM = conditioned media; GLT-1 = glutamate transporter 1. .... 35

Figure 3-2 Significant differences in cytokine profile between CHO- and 7PA2- CM after 48 hours exposure. (A) No significant differences in cytokine profile between Neurobasal, CHO-CM and 7PA2-CM prior to incubation. 48 hours exposure showed significant levels (pg/mL) of (B) IL-1 $\beta$  (mean  $\pm$  std. error: Control = 0.170  $\pm$  0.0422, CHO-CM = 1.13  $\pm$  0.182, 7PA2-CM = 0.0969  $\pm$  0.0165, (C) IL-6 mean  $\pm$  std. error: Control = 154  $\pm$  4.79 CHO-CM = 3320  $\pm$  607, 7PA2 = 75.2  $\pm$  5.03, (D) TNF- $\alpha$  mean  $\pm$  std. error: Control = 147  $\pm$  8.17 CHO-CM = 833  $\pm$  166, 7PA2 = 46.5  $\pm$  5.92. n = 3-4 independent experiments in duplicates. p  $\leq$  0.05 considered significant by one-way ANOVA followed by Sidak's posthoc multiple comparison's test. .... 35

Figure 3-3 48 hours of 20ng/mL IL-1 $\beta$  or TNF- $\alpha$  increases GLT-1 while IL-6 has no effect. GLT-1 mean  $\pm$  std. error: Control = 1.01  $\pm$  0.00332, IL-1 $\beta$  = 1.36  $\pm$  0.0797; p = 0.0427, TNF- $\alpha$  = 1.71  $\pm$  0.271; p = 0.0128, IL-6 = 1.07  $\pm$  0.0172; p > 0.9999. n = 2-4 independent experiments in duplicates or triplicates. p  $\leq$  0.05 considered significant by one-way ANOVA followed by Dunn's post hoc multiple comparison's test. .... 36

Figure 3-4 miR-181a decreases after 20ng/mL IL-1b expression. 48-hour exposure of 20ng/mL IL-1b on primary astrocyte and neuron co-culture. (A) SYBR® Chemistry for Real-Time PCR using miRNA primers known to regulate GLT-1 or synaptic function. GLT-1 mean  $\pm$  std. mean error: GLT-1 mean  $\pm$  std. error: Control = 1.05  $\pm$  0.234 and IL-1 $\beta$  = 0.324  $\pm$  0.117, p = 0.0498. n = 2-3 independent experiments with 1-3 samples per group. p  $\leq$  0.05 considered significant by unpaired t-test performed for each microRNA between control and IL-1 $\beta$  (presented on a single graph for presentation). (B) TaqMan® Chemistry for Real-Time PCR using miR-181a primer confirms IL-1 $\beta$  downregulates miR-181a; GLT-1 mean  $\pm$  std. mean error: Control = 1.31  $\pm$  0.0980 and IL-1 $\beta$  = 0.864  $\pm$  0.113, p = 0.0249. n = 4 independent experiments in triplicates. p  $\leq$  0.05 considered significant by unpaired t-test. (C) miR-181a mimic decreases GLT-1 expression in a concentration-dependent manner after 48 hours. GLT-1 mean  $\pm$  std. error: Vehicle = 1.03  $\pm$  0.0102, Control = 1.02  $\pm$  0.0882, 15nM = 1.056  $\pm$  0.0813, 30nM = 0.875  $\pm$  0.0149, 70nM = 0.701  $\pm$  0.0509 (p = 0.0102), negative control = 0.953  $\pm$  .0983. n = 5 independent experiments with duplicates or triplicates for 3 experiments, 1 exploratory experiment and 1 experiment with vehicle and 70nM miR-181a mimic for confirmation. p  $\leq$  0.05 considered significant by one-way ANOVA followed by Dunn's post hoc multiple comparison's test. (D) Co-treatment of 70nM hsa-miR-181a-5p mimic with 20 ng/mL IL-1 $\beta$  after 48 hours returned GLT-1 steady state levels relatively close to control levels. GLT-1 mean  $\pm$  std. error: Control = 1.00  $\pm$  0.00241, IL-1 $\beta$  = 1.81  $\pm$  0.280, IL-1 $\beta$  and miR-181a mimic = 0.935  $\pm$  0.0705; Control vs IL-1 $\beta$  (p = 0.0149), IL-1 $\beta$  vs IL-1 $\beta$  and 70nM miR-181a mimic (p = 0.0143). n = 4 independent experiments in duplicates or triplicates. p  $\leq$  0.05 considered significant by one-way ANOVA followed by Holm-Sidak's post hoc multiple comparison's test. miR-181a mimic = mirVana hsa-miR-181a-5p and scramble = mirVana Negative Control #1 microRNA mimic. .... 37

Figure 3-5 GLT-1 steady state levels and microRNA levels from hippocampal human AD patients compared to age-matched controls. (A) GLT-1 steady state levels significantly decrease in AD human patients compared to age-matched human controls. GLT-1 mean  $\pm$  std. mean error: Control = 1.32  $\pm$  0.489 and AD = 0.370  $\pm$  0.0975 (p = 0.0127). p = 0.0127. (B) no significant differences between mature miR-181a levels from AD patients compared to age-matched control. miR-181a mean  $\pm$  std. mean error: Control = 0.967  $\pm$  0.162 and AD = 0.837  $\pm$  0.179 (p = 0.7789). (C) Decrease of immature miR-181a levels in AD compared to age matched control. pri-miR-181a-1 mean  $\pm$  std. mean error: Control = 0.533  $\pm$  0.0919, AD = 0.2857  $\pm$  0.0962 (p = 0.0927) (D) Ratio of mature miR-181a and pri-

miR181a-1 is higher in AD compared to age matched control groups. Control =  $1.92 \pm 0.469$ , AD =  $3.95 \pm 0.944$  ( $p = 0.228$ ). (E) no differences in pri-miR-181a-2 levels between AD and age matched controls. pri-miR-181a-2 mean  $\pm$  std. mean error: Control =  $0.540 \pm 0.103$ , AD =  $0.563 \pm 0.166$  ( $p = 0.758$ ) and (F) ratio of miR-181a and pri-miR-181-a-2  $\pm$  std. mean error: Control =  $1.70 \pm 0.410$ , AD =  $2.70 \pm 0.748$  ( $p = 0.622$ ). Each symbol represents 1 human sample with an ID corresponding to the number next to the symbol (ntotal = 5 – 8 samples).  $p \leq 0.05$  considered significant by unpaired t-test. Immature miR-181a corresponds to primary miR-181a..... 39

Figure 4-1 A $\beta$  and GLT-1 knockdown breeding scheme. Double transgenic mice were born from heterozygous crosses at the frequency predicted by Mendelian ratios. Expected 25% heterozygous GLT-1 knockdown and hemizygous A $\beta$ , 25% wild type, 25% GLT-1 knockdown and 25% hemizygous A $\beta$ . Tg/0 = hemizygous for the mutated APP transgene; 0 = no transgene. .... 48

Figure 4-2 Tau pathology and GLT-1 knockdown breeding scheme; Double transgenic mice were born from heterozygous crosses at the frequency predicted by Mendelian ratios. Expected 25% heterozygous GLT-1 knockdown and hemizygous human tau, 25% wild type, 25% GLT-1 knockdown and 25% hemizygous human tau. Tg/0 = hemizygous for the mutated APP transgene; 0 = no transgene..... 48

Figure 4-3 Effect of GLT-1 knock down on A $\beta$  pathology in double transgenic mice. Qualitative representation of the immunostaining with (A) Thioflavin S (green) and (b) 82E1 antibody (red) to detect A $\beta$  plaques in the cortex and hippocampus. n = 4-5 mice per group; blind experiment to detect plaques. GLT1KD = NST-GLT-1(+/-) and J20 = APP<sup>sweind</sup>(Tg/0) ..... 49

Figure 4-4 Spine densities (spines/100 $\mu$ m) in stratum radiatum area of CA1. (A) Light microscopy images of dendritic spines on pyramidal cells in CA1 subfield of in wildtype, GLT-1 knockdown, J20 and GLT-1 knockdown with A $\beta$  mice at 6-7 months of age. (B) Quantification of spine density (spines/ $\mu$ m) based on types of spines (including mushroom, thin and stubby). The framed area is 100x. sr = stratum radiatum. GLT1KD = NST-GLT-1(+/-) and J20 = APP<sup>sweind</sup>(Tg/0)..... 50

Figure 4-5 Tau pathology preliminary assessment using PHF-1 antibody found in the dentate gyrus. Phosphorylation at serine 396 and 404<sup>237</sup>. n = 2 mice per group (indicated by symbol). GLT-1KD = NST-GLT-1(+/-) Scale bar: 200 $\mu$ m..... 51

## Acknowledgments

I would like to acknowledge the full support that I received from my family, friends, colleagues, advisors, University of California, Merced (UCM) and University of California, Irvine (UCI) to successfully complete my dissertation project described here. Also, I would like to thank my funding sources: The National Institute of Health and National Institute of Aging F31 pre-doctoral fellowship (AG048705, J.Z.), UCM's Graduate Division, UCM's Faculty Mentor Fellowship, and UCM's Quantitative and Systems Biology's Summer Fellowships for continuing support during my graduate work.

I would like to thank Elsevier for granting permission to use copyrighted material in Chapter 2 of this dissertation.

My deepest gratitude to my advisor, Professor Masashi Kitazawa, for giving me the opportunity to work in his lab. His support and guidance has been instrumental to the development of my technical and professional skills. I could not have asked for a better advisor!

I would like to thank Professor Patricia LiWang, Professor Fredrick Wolf, and Professor Ramen Saha for their constructive input and guidance throughout my research career at UCM. Thank you, Professor Wolf for adopting me into your lab and Professor LiWang for the opportunity to work in yours.

I would like to thank Professor Frank LaFerla for his mentorship during my F31. I would also like to thank Professor Frank LaFerla's lab for their help while I was at UCI.

I would like to thank the dream team of the Kitazawa lab: Dr. Carlos Rodriguez-Ortiz, Dr. Sharon Lim, Dr. Heng Wei Hsu, Jason Killian, and Dr. Hitomi Hoshino for helping me throughout my graduate work.

I would like to thank Professor David Ojcius for meeting with me four days before my wedding and opened the opportunity for graduate school at UCM, Professor James Youngblom (CSU Stanislaus) for encouraging me to pursue a Ph.D. and taking his class to a conference where I listened to Dr. Francis Collins give a speech on the importance of biomedical research and Dr. My Lo Thao (CSU Stanislaus) for giving me my first research experience investigating the world of microbes.

I would like to thank all my incredible undergraduate researchers at UCM who have helped with my projects: Zanett Kieu, Thin Wai, Charlesice Hawkins, Tina Truong, Karina Arroyo, Eliaz Lynch, Alexis Miranda (Chapman University), and Jayetha Panakkadan (Chapman University).

I would like to thank my mom and brother for the constant inspiration and encouragement, my grandparents for instilling a deep foundation of faith, Fr. Butch Malana, M.D. for

constant prayers and guidance, my cousins, aunts, and uncles who have been so supportive and constantly reminding me to laugh.

To my best friend and husband, Andrew Zumkehr – thank you for all that you do.

# Curriculum Vita

Joannee Zumkehr

Irvine, CA 92620 – (209) 201 – 8816

joanneezumkehr@gmail.com

---

## EDUCATION

---

**Ph.D.** – Quantitative and Systems Biology (2017), University of California, Merced

**B.S.** – Biological Sciences (2010), California State University, Stanislaus

---

## SKILLS SUMMARY

---

**Molecular Biology Methods:** RT-PCR, immunoblot, ELISA, cell culture, genotyping, murine CSF extraction, behavioral tests, immunostaining, transfections, gel electrophoresis, DNA and RNA extraction, perfusion, Golgi staining and stereology.

---

## RESEARCH EXPERIENCE

---

*Visiting Graduate Researcher, University of California, Irvine* **2016-2017**

- Showed that inflammatory cytokine, IL-1 $\beta$ , upregulates glial glutamate transporter by suppressing microRNA-181a in primary murine astrocyte and neuron co-culture; a potential pathway to target in Alzheimer's disease (AD).
- Measured glial glutamate transporter and microRNA levels from human hippocampal samples.

*Graduate Researcher, University of California, Merced* **2012 - 2017**

- Investigated the role of glial glutamate transporter in AD pathology utilizing a mouse model.
- One semester rotation with Professor Patricia LiWang; assisted in engineering the backbone of 5p12-linker-T2635 by performing mini-prep, PCR, agarose gel electrophoresis, transformation, and mini-prep of 16S rDNA.

*Undergraduate Researcher, California State University, Stanislaus* **2009 - 2010**

- Helped identify and characterize microbial population in sewage water of the Salida Sanitary District. Performed gram stain and wet mount techniques to physically observe microorganisms. Operated an Olympus microscope digital camera DP20 to capture slide images. Conducted mini-prep, PCR, agarose gel electrophoresis, transformation, and mini-prep of 16S rDNA.

---

## PEER-REVIEWED PUBLICATIONS

---

**Zumkehr, J.**, Rodriguez-Ortiz, C.J., Kitazawa, M. (2017) IL-1 $\beta$  regulates glial glutamate transporter via microRNA. Manuscript in preparation.

Rodriguez-Ortiz, C. J., Flores, J. C., Valenzuela, J. A., Rodriguez, G. J., **Zumkehr, J.**, Tran, D. N., . . . Kitazawa, M. (2016). The Myoblast C2C12 Transfected with Mutant Valosin-Containing Protein Exhibits Delayed Stress Granule Resolution on Oxidative Stress. *The American Journal of Pathology*, 186(6), 1623-1634.

**Zumkehr, J.**, Rodriguez-Ortiz, C. J., Cheng, D., Kieu, Z., Wai, T., Hawkins, C., . . . Kitazawa, M. (2015). Ceftriaxone ameliorates tau pathology and cognitive decline via restoration of glial glutamate transporter in a mouse model of Alzheimer's disease. *Neurobiology of Aging*, 36(7), 2260-2271.

Leung, W., Shaffer, C. D., Reed, L. K., Smith, S. T., Barshop, W., Dirkes, W., . . . **Zumkehr, J.**, . . . Xiong, D. (2015). Drosophila Muller F elements maintain a distinct set of genomic properties over 40 million years of evolution. *G3: Genes| Genomes| Genetics*, 5(5), 719-740.

---

## PROFESSIONAL AND TEACHING EXPERIENCE

---

*Mentor, University of California, Merced and Irvine* **2014 – 2017**

- Mentored eight undergraduate students in molecular biology data collection and analysis.

*Teaching Assistant, University of California, Merced* **2012 – 2013**

- Led and guided Biochemistry 1 discussions or Molecular Biology laboratory sessions.

*Microbiologist I, Dole Packaged Foods, LLC. Analytical Laboratory* **2011 – 2012**

- Performed ELISA and plating methods to test frozen food products for the presence of E. coli, other coliforms, S. aureus, yeast, mold, Listeria species, and Salmonella species; Performed environmental analysis and calibration procedures.



---

---

**CONFERENCE PRESENTATIONS**

- Zumkehr, J.,** Rodriguez-Ortiz, C., and Kitazawa, M. (2017). Inflammatory cytokines regulate glial glutamate transporter via microRNA. Poster. AD/PD International Conference. Vienna, Austria.
- Zumkehr, J.,** Rodriguez-Ortiz, C., and Kitazawa, M. (2017). Inflammatory cytokines regulate glial glutamate transporter via microRNA. Invited Speaker. Research & Education in Memory Impairments & Neurological Disorders 8th annual emerging scientist symposium, Irvine, CA.
- Zumkehr, J.,** Hawkins, C., and Kitazawa, M. (2014). Sustained oligomeric A $\beta$  exposure decreases GLT-1 steady state levels in astrocytes without altering its transcription. Poster. Society for Neuroscience, Washington, D.C.
- Zumkehr J.,** Medeiros, R., Cheng, D., and Kitazawa, M. (2013) Upregulation of glutamate transporter by ceftriaxone ameliorates Alzheimer's disease-associated cognitive impairment in 3xTg-AD mice. Poster. 43rd annual meeting of the Society for Neuroscience, San Diego, CA.

---

---

**FELLOWSHIPS**

<b>NIH, Ruth L. Kirschstein National Research Award (F31)</b> (\$31,982)	<b>2016 - 2017</b>
<b>UC Merced's President's Dissertation Year Fellowship</b> (\$36,070) – declined conflict with F31	<b>2015</b>
<b>UC Merced's Grad Slam Runner-up</b> (\$1,000)	<b>2015</b>
<b>UC Merced's Outstanding Graduate Student of the Year Award</b>	<b>2014</b>
<b>Quantitative and System's Biology Summer Fellowship</b> (\$12,500)	<b>2013-2014</b>
<b>Quantitative and Systems Biology Travel Award</b> (\$1,800)	<b>2013-2014</b>
<b>UC Merced's Graduate Student Research Poster Competition Winner</b> (\$250)	<b>2014</b>
<b>UC Merced's Faculty Mentored Research Fellowship</b> (\$34,894)	<b>2013 – 2014</b>

---

---

**SERVICES**

- Graduate Recruitment Committee Member, University of California, Merced** **2016-2017**
- Invited and hosted potential graduate students for University of California, Merced's graduate programs.
- Walk to End Alzheimer's Booth Coordinator, Alzheimer's Association** **2013-2015**
- Coordinated University of California, Merced's booth during the Walk to End Alzheimer's events
  - Provided scientific information about Alzheimer's disease to the community.

---

---

**PROFESSIONAL MEMBERSHIPS**

- Society for Neuroscience
- American Association for the Advancement of Science

---

---

**LANGUAGES**

- English (speak fluently and read/write with high proficiency)
- Filipino (Viasayan: native language and Tagalog: speak, read and write with basic competence)

---

---

**REFERENCES**

Upon Request

## Abstract

### The role of glial glutamate transporter and its impact on amyloid-beta and tau pathology in Alzheimer's disease

Joannee Mae Zumkehr

Doctor of Philosophy in Quantitative and Systems Biology  
University of California, Merced

2017

Patricia LiWang, Chair

Alzheimer's disease (AD) is the leading cause of dementia among elderly in the United States. There is no effective treatment available, in part due to lack of understanding of the full spectrum of the disease mechanisms. Brain is structured in highly heterogeneous and complex way, and the number of different cell lineages, such as neurons, astrocytes, microglia, oligodendrocytes, perivascular macrophages, and capillary endothelial cells, interact with each other and functionally integrate into one highly hierarchical and organized unit. Traditionally, neurodegeneration has been centered for investigation on neurodegenerative diseases like AD. However, recent rapidly growing evidence strongly implicates the pathogenic involvement of non-neuronal cell lineages, such as astrocytes and microglia, and this work may uncover key disease mechanisms. The purpose of this dissertation is to elucidate the role of glutamate transporter 1 (GLT-1) primarily expressed in astrocytes in the progression or initiation of AD pathology. In humans, its loss is evident even in early or prodromal stages of AD and correlates well with cognitive impairment. The loss of GLT-1 causes glutamate dyshomeostasis in the synaptic cleft, which eventually leads to glutamate-induced excitotoxicity and neurodegeneration. While glutamate excitotoxicity has long been a suspected cause of progressive neurodegeneration in AD, it remains unclear whether the loss of the glutamate transporter directly contributes to the pathological buildup of amyloid  $\beta$  ( $A\beta$ ) and neurofibrillary tau tangles (NFTs) - two key pathological hallmarks of AD. Thus, we hypothesize that **the  $A\beta$ -induced GLT-1 downregulation links  $A\beta$  pathology to tau pathology, synaptic loss, and cognitive decline**. To test this hypothesis, we utilized both *in vitro* and *in vivo* models of AD and thoroughly performed biochemical and histopathological examinations. We show an age-dependent decrease of GLT-1 in animal models and GLT-1 decrease in human hippocampal samples. In addition, pharmacological restoration of GLT-1 can ameliorate AD-like pathology in an animal model of AD. We also present a possible molecular mechanism that regulates GLT-1 independent of  $A\beta$ . The contribution of this research includes a better understanding on the role of astrocyte dysfunction in the early stages of AD and its consequences on the progression of the disease.

# Chapter 1: Introduction

## 1.1 Dissertation Statement

Astrocyte dysfunction, represented by GLT-1 downregulation, is a critical link between A $\beta$ , tau and synaptic loss in Alzheimer's disease.

## 1.2 Motivation

First characterized by Dr. Alois Alzheimer in 1906, this “peculiar” disease is rightfully justified and should be considered as a national public health crisis. AD is now the leading cause of dementia among the elderly and the 6<sup>th</sup> leading cause of deaths in the United States (U.S.). It is the only one in the top ten leading cause of deaths that cannot be prevented, slowed or cured<sup>1,2</sup>. Today, over 5 million individuals in the U.S. or 35 million worldwide suffer from AD, and it is projected to increase up to nearly 16 million in the U.S. by 2050 as the proportion of aging population (65 years or older) increases from 15% to 23% of the population<sup>3</sup>. As the disease progresses for many years, the irreversible memory loss and cognitive impairment over time consequently render the patient completely dependent on others. Such an intensive and daily demand of care has an overwhelming socio-economic impact. In 2016, more than 15 million Americans provided unpaid care for people with AD and other dementias, and an estimated 18.2 billion hours of care valued at \$230 billion were provided by these caregivers<sup>4</sup>. As the number of AD patients and duration of the disease stage increase, these costs could rise as high as \$1.1 trillion by 2050<sup>5</sup>.

Understanding the underlying molecular and cellular mechanisms of the disease will allow the development of mechanism-based therapeutic interventions to treat, slow, and possibly cure AD. Even by delaying the average disease onset by one year would reduce the disease prevalence by more than nine million cases in 2050<sup>6</sup>. Furthermore, an estimated \$83 billion could be saved if we could delay the neuropathological progression of AD by five years<sup>7</sup>. For the last two decades, significant progress in AD research has substantially advanced our understanding of AD. Neuropathological hallmarks have been well characterized by the extracellular buildup of amyloid-beta (A $\beta$ ) plaques and intracellular accumulation of neurofibrillary tangles (NFTs). In addition, extensive neuronal loss, gliosis, and inflammatory responses are evident around these pathological hallmarks. All identified genetic mutations recognize A $\beta$  as the primary culprit that trigger neurodegeneration resulting in dementia. This idea has been formulated into the leading hypothesis called the amyloid cascade hypothesis, stating that A $\beta$  is the indisputable culprit upstream of NFT and neuronal loss<sup>8</sup>. Hence global effort to develop A $\beta$  lowering strategies targeting its metabolism, aggregation, and clearance are ongoing. Despite the remarkable success of A $\beta$ -based therapies in preclinical studies, overwhelmingly these therapies have failed in clinical trials<sup>9-11</sup>. These results strongly implicate the presence of multifactorial mechanisms and heterogeneity of the disease phenotypes thus emphasizing the critical importance of AD research.

Current therapeutic interventions only provide symptomatic relief but do not halt the pathological progression of AD. The U.S. Food and Drug Administration (FDA) approved four medications for AD patients: galantamine (Razadyne®), donepezil (Aricept®), rivastigmine (Exelon®), and memantine (Namenda®). Recently, a combination therapy of donepezil and memantine (Namzaric®) has been added to the FDA-approved list and given to moderate to severe AD patients. The original four medications are grouped into two classes based on its pharmacological mechanism of action; acetylcholinesterase inhibitors (AChEIs) and N-methyl-D-aspartate receptor (NMDAR) antagonist, which serve to increase acetylcholine-mediated neurotransmission or decrease NMDAR-mediated neurotransmission, respectively. AChEIs alone are not entirely effective over time and often require the NMDAR antagonist, memantine, medication as the disease progresses<sup>12</sup>. Therapeutic efficacy of memantine highlights glutamate-induced excitotoxicity as a critical component in AD pathogenesis and further provides motivation for this research.

### 1.3 Background

AD is the leading cause of dementia among the elderly over 65 years old. AD cases are classified into two categories based on age of onset: familial or sporadic. Familial or young-onset AD consists of less than 5% of AD cases and caused purely by known genetic mutations in the amyloid precursor protein (APP), presenilin-1 (PSEN1) and presenilin-2 (PSEN2)<sup>13</sup>. In comparison, sporadic or late-onset AD represents over 95% of AD cases with no definitive cause except that aging is the strongest risk factor. Other than the age of onset, clinical manifestations and pathological observations are indistinguishable between the two forms. Additionally, extensive neuropsychological assessments and laboratory tests are conducted to rule out other forms of dementia.

The neuropsychological assessments show progressive memory loss and cognitive deficits in clinically diagnosed AD patients. One of the most commonly used tools to assess mental function is the Mini-Mental State Examination (MMSE)<sup>14</sup>. MMSE is a brief 30 point questionnaire utilized to diagnose and track cognitive impairment throughout the course of disease. The exam tests multiple cognitive areas impaired in AD including spatial and episodic memory<sup>15</sup>. Its scoring system allows to differentiate the different stages associated with dementia. Generally, scores greater than 27 reflects no cognitive impairment, 19-24 represents mild impairment, 10-18 indicates moderate impairment and a score below 9 demonstrates severe cognitive impairment<sup>15</sup>. MMSE has been utilized in longitudinal studies and its reproducibility renders it dependable in clinical assessments<sup>16</sup>. Overall, the assessments above provide opportunity to quantitatively assess and define levels of cognitive impairment as the disease progresses.

In addition to cognitive assessments, cerebral imaging techniques show decrease in brain activity and progressive brain atrophy in clinically diagnosed AD patients. These techniques include magnetic resonance imaging (MRI) to assess cerebral atrophy or volume changes in characterized anatomic locations<sup>17</sup>. In clinically diagnosed AD,

accelerated brain atrophy is initially seen in the entorhinal cortex followed by the hippocampus, amygdala and parahippocampus – all regions important for memory and cognition<sup>18</sup>. Additionally, positron emission tomography (PET) show altered brain activity in the same areas. PET imaging with radiotracers such [18F] fluoro-2-Deoxy-D-glucose (FDG) measure synaptic activity<sup>19</sup>. In normal physiological conditions, neuronal activity requires high amounts of glucose as a substrate for energy, however, AD patients show decrease in FDG uptake indicative of low activity or neuronal injury<sup>18,20,21</sup>. Thus neuronal activity decrease and brain tissue atrophy occurs in critical areas required for memory and cognition in clinically diagnosed AD patients.

Accurate AD diagnosis is confirmed in post-mortem histopathological studies that show the presence of senile plaques, NFTs, synaptic loss, and extensive neuronal loss. Postmortem studies with synaptic markers, for example, show that AD patients display significant synaptic loss in cortex<sup>22-24</sup>, hippocampal dentate gyrus<sup>25</sup> and hippocampus<sup>26-30</sup>. The results from post-mortem analyses further contribute to clinical and pathological correlation AD studies.

The longitudinal studies found that the best pathological correlate of cognitive decline in AD is synapse loss<sup>8 31,32</sup>. In contrast, neuronal loss best correlates with the spread of NFTs<sup>33,34</sup>. Nevertheless genetics indicate that A $\beta$  is the primary culprit of AD<sup>13</sup>. Taken together, synapse loss is initiated by A $\beta$  but essentially carried out by inflammation, tau and possible glutamate-induced excitotoxicity. The exact molecular mechanism that links A $\beta$  to subsequent pathological hallmarks is unknown.

To test mechanistic hypotheses, animal models, particularly mouse models, have become invaluable in AD research. Mice have comparable brain networks, neurobiological processes, and brain anatomy with humans<sup>15</sup> making them suitable models. They are relatively economical to maintain than larger models and have shorter gestation period allowing feasibility for resource and time constrained projects. Mice do not develop AD naturally<sup>35</sup> but genetic human mutations discovered from familial AD<sup>36</sup> or microtubule associated protein (MAPT) can be introduced to drive AD-like pathology making them valuable to biomedical research. Like many non-human or transgenic models, results obtained from mouse models must be taken with caution. First, no single mouse model fully recapitulates human AD – progressive cognitive deficits, pathological hallmarks, and neuronal loss<sup>15,37</sup>. Second, genetic mutations represent the smallest population of AD cases thus may not make them suitable for sporadic AD. Third, promoters to drive transgenes target a specific region in the brain which may compromise the natural temporal and spatial development of pathology. Lastly, the background strain or the genetic makeup of a produced transgenic mouse may differ from when the transgenic mouse was originally described; extensive breeding history may produce variable phenotypes<sup>38</sup>. Thus, careful consideration must be taken when choosing a model to test a hypothesis and drawing conclusions from results. Furthermore, reproducibility in more than one specific mouse model implicates stronger reliability. With these caveats in mind, the following sections will provide an overview of human and animal data that strongly support the deceptively simple amyloid cascade hypothesis.

### 1.3.1 A $\beta$ pathology: breakdown of APP to understand A $\beta$

Senile plaques are composed of aggregated A $\beta$  peptides produced by the sequential cleavage of the amyloid precursor protein (APP)<sup>39</sup>. The *APP* gene, located on chromosome 21 undergoes alternative splicing that results in three major isoforms containing 695, 751 and 770 amino acids<sup>40-42</sup>. These isoforms are a type I transmembrane protein in which certain isoforms (e.g. APP695) are primarily expressed in the brain and neurons<sup>43</sup>. APP consists of a long extracellular N-terminal domain, a transmembrane region and an intracellular C-terminal APP intracellular domain (AICD)<sup>40,44</sup>. APP is transported through the secretory pathway from the trans golgi network, down the axon to the cell surface<sup>45,46</sup>. At the cell surface, APP undergoes either the non-amyloidogenic or amyloidogenic pathway (**Fig. 1**). In the non-amyloidogenic pathway, cleavage by  $\alpha$ -secretases (ADAM) followed by  $\gamma$ -secretase complex produces sAPP $\alpha$ , AICD, and P3 fragment. On the other hand, in amyloidogenic pathway, APP is cleaved into sAPP $\beta$ , AICD, and A $\beta$  peptides by  $\beta$ -secretase (BACE) then by the  $\gamma$ -secretase complex<sup>46</sup>. A $\beta$  peptides produced by this pathway vary from 38 to 43 amino acids in length and are capable of aggregating with other A $\beta$  peptides to form various highly toxic oligomeric species<sup>46,47</sup>. A $\beta$ <sub>1-42</sub> has higher propensity to aggregate and has been shown to be the more toxic peptide than A $\beta$ <sub>1-40</sub>, but generally produced in ten-fold lower amounts than A $\beta$ <sub>1-40</sub> in the brain under physiological conditions<sup>48</sup>. Thus A $\beta$ <sub>1-42</sub> aggregation leads to senile A $\beta$  plaque production.

APP processing through the amyloidogenic pathway explains the pathogenesis of familial AD. First, disease-causing mutations among familial onset cases are all connected to an

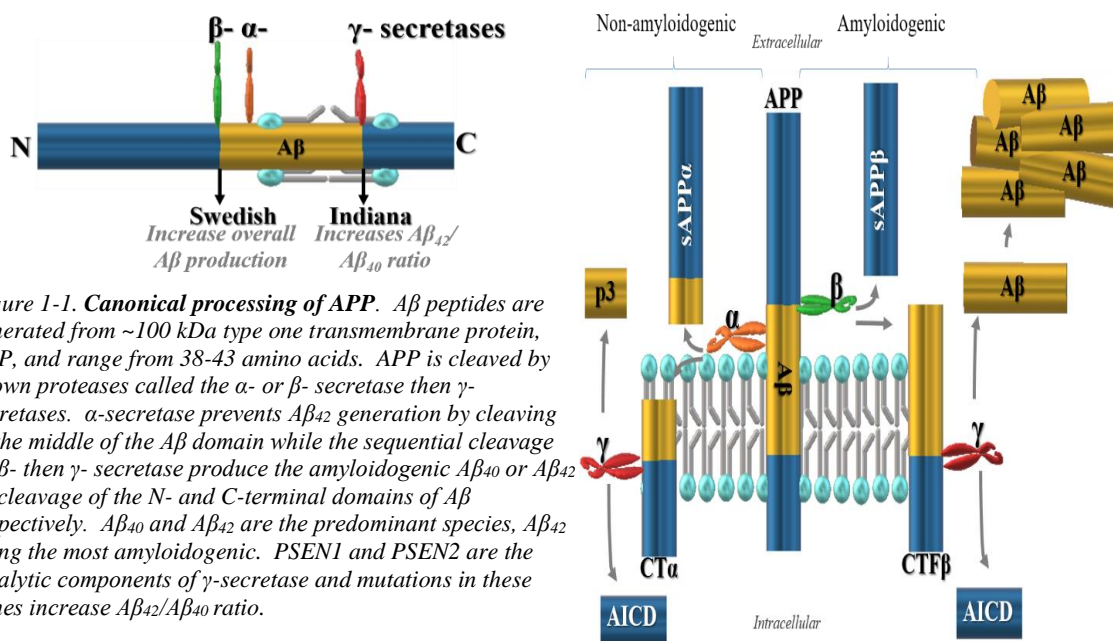


**Figure 1-1. Canonical processing of APP.** A $\beta$  peptides are generated from ~100 kDa type one transmembrane protein, APP, and range from 38-43 amino acids. APP is cleaved by known proteases called the  $\alpha$ - or  $\beta$ - secretase then  $\gamma$ -secretases.  $\alpha$ -secretase prevents A $\beta$ <sub>42</sub> generation by cleaving in the middle of the A $\beta$  domain while the sequential cleavage by  $\beta$ - then  $\gamma$ - secretase produce the amyloidogenic A $\beta$ <sub>40</sub> or A $\beta$ <sub>42</sub> by cleavage of the N- and C-terminal domains of A $\beta$  respectively. A $\beta$ <sub>40</sub> and A $\beta$ <sub>42</sub> are the predominant species, A $\beta$ <sub>42</sub> being the most amyloidogenic. PSEN1 and PSEN2 are the catalytic components of  $\gamma$ -secretase and mutations in these genes increase A $\beta$ <sub>42</sub>/A $\beta$ <sub>40</sub> ratio.

increase in the overall A $\beta$  production, aggregation, or the production of more toxic form

by changing the  $A\beta_{1-42}/A\beta_{1-40}$  ratio<sup>13,49-56</sup>. Second, the pathogenic role of APP or  $A\beta$  is further supported by Down syndrome patients having significantly higher risk for developing senile plaques and early onset AD-like dementia due to 1.5-fold increase in APP expression located on the chromosome 21<sup>57-59</sup>. Third, a duplication of APP gene significantly increases  $A\beta$  deposits and the onset of AD<sup>60</sup>. Finally, a A673T coding mutation on APP right on the BACE cleavage site is protective against AD, presumably by inhibiting BACE cleavage<sup>61</sup>. In summary, human genetic mutations strongly prove that  $A\beta$  dyshomeostasis initiates AD.

Autopsy observations with animal and cell culture studies led to the idea that  $A\beta$  forms various assembly states prior to plaque formation that may contribute more on the pathogenesis of AD<sup>47</sup>. For example, the number of amyloid deposits in the brain does not correlate well with the degree of cognitive impairment and there are individuals that do not meet the criteria for AD diagnosis yet the brain of those individuals contained amyloid plaques<sup>62</sup>. In addition, memory impairment in mice models appear before amyloid plaques<sup>63</sup>. Thus, initial events in  $A\beta$  aggregation of unknown assembly states, likely soluble oligomeric forms, may be the initial culprit of AD<sup>8,47,48,64-66</sup>.

Laboratory techniques to isolate  $A\beta$  followed by application studies further support the hypothesis that unknown assembly states of  $A\beta$  prior to plaque formation drive tau and other AD-like pathology. First, soluble  $A\beta$  oligomers or species are generally defined as  $A\beta$  assembly states that are not pelleted from physiological fluids at high speed centrifugation<sup>47</sup>. These oligomers are characterized by many factors including length, structure, and resistance to solvent<sup>46,47</sup>. Another way to classify  $A\beta$  is by conformational antibodies. For example, A11 antibodies recognize pre-fibrillar oligomers (intermediates of fibril assembly) and OC antibodies recognize fibril intermediates (small pieces of fibril or fibril “seeds”)<sup>67</sup>. These antibodies were utilized to report a correlation between OC-positive oligomers and cognitive decline<sup>68</sup> implying that soluble  $A\beta$  can drive AD pathology. Walsh and colleagues also established a protocol to obtain naturally secreted  $A\beta$  species from transfected Chinese hamster ovary cells providing another powerful tool to study  $A\beta$  in cell cultures and animal models of AD<sup>69</sup>. From these techniques, soluble  $A\beta_{42}$  oligomers have been shown to trigger tau-like alterations<sup>70,71</sup> and neuritic dystrophy<sup>72</sup>.  $A\beta_{42}$  (dimers or trimers) oligomers isolated from AD brain can dose-dependently decrease synapse number and function and impair memory *in vivo*<sup>71</sup>. Therefore,  $A\beta$  oligomers are hypothesized to be the primary culprit for AD pathogenesis.

Processing and effects of  $A\beta$  have been extensively studied but the physiological function of APP or its cleaved products has not been fully elucidated. APP has been associated with neurotrophic signaling and metal homeostasis in the CNS<sup>40,41</sup>. Physiological importance of APP is in part evident from studies characterizing APP knockout (KO) mouse. APP-KO mice are viable but older mice showed significant reduction of dendritic spine density in the CA1 hippocampal neurons<sup>73</sup>. APP-KO mice also display reduced forelimb grip strength and locomotor activity<sup>74</sup>. The phenotypic abnormalities of APP-KO mice suggests that APP may be essential for synapse development, maturation and maintenance.

The smaller secretory fragments (sAPP $\alpha$ , sAPP $\beta$ ), A $\beta$ , and AICD generated from APP (Fig. 1) also have various physiological functions. sAPP $\alpha$  and sAPP $\beta$  fragments contain many domains for signal transduction including growth like binding domains, heparin binding sites and copper binding domains<sup>41</sup>. sAPP $\alpha$  has neurotrophic and neuroprotective effects *in vitro*<sup>75,76</sup> and enhances learning performance and long term potentiation (LTP), a molecular correlate of learning and memory<sup>77</sup>, *in vivo*<sup>78-80</sup>. sAPP $\alpha$  also restores spine density and dendritic integrity in APP-KO mice<sup>73</sup>. Compared to sAPP $\alpha$ , sAPP $\beta$  is 16 amino acids shorter and does not play a role in LTP or memory but is involved in neurite outgrowth<sup>81,82</sup>. AICD acts as a nuclear transcription regulator<sup>83-86</sup>. Under physiological conditions, AICD initiates gene expression encoding proteins involved in Ca<sup>2+</sup> homeostasis<sup>84,87</sup>, neprilysin<sup>88</sup>, and transthyretin<sup>85,86</sup> proteins involved in A $\beta$  degradation and clearance. A $\beta$  however also has potential physiological function. At picomolar concentrations, monomeric A $\beta$  stimulates LTP, regulates neurotransmitter release, and may be neuroprotective in hippocampal neurons<sup>89-94</sup> thus further complicating matters.

The physiological roles of APP and its derivatives, taken together with genetic and pathologic evidence implicate that the abnormal accumulation of A $\beta$  is deleterious and causes the development of AD. In the case of familial AD, increased A $\beta$  production clearly contributes to the early onset of the disease. In the case of sporadic AD, the balance between A $\beta$  production and clearance may uncover key pathogenic mechanisms of the disease<sup>95,96</sup>. Failure to properly regulate A $\beta$  can be detrimental to neuronal health because direct exposure of isolated human A $\beta$  decreases synaptic density, inhibits LTP and induces AD-like tau hyperphosphorylation *in vitro* and *in vivo*<sup>71,72</sup>. In conclusion, the amyloid cascade hypothesis that posits A $\beta$  as the initiating factor while other aspects of the disease are responsible for synapse loss and dementia<sup>8,97</sup> continues to gain overwhelming support.

### 1.3.2 Versatile role of inflammation: A $\beta$ regulator and neuron-glia mediator

A growing body of evidence strongly implicates a fundamental role for neuroinflammation (inflammation in the central nervous system) in the pathological buildup and clearance of A $\beta$ . Genome wide association studies reveal that genes which increase the risk for late-onset AD also encode for immune receptors involved in A $\beta$  clearance<sup>98-100</sup> suggesting a critical role of non-neuronal cells specifically microglia and astrocytes. Microglia are the resident phagocytes of the CNS and their physiological role is to survey and phagocytose debris from the microenvironment<sup>101</sup>. A $\beta$  or misfolded proteins bind to microglia or astrocytes on cell surface receptors<sup>102-105</sup>. These receptors include scavenger receptors, toll like receptors, triggering receptor expressed on myeloid cells 2, and lipoprotein receptor-related proteins 1<sup>106,107</sup>. Subsequent digestion by proteases or autophagy occurs once inside the cell<sup>108-110</sup>. These proteases include metalloendopeptidases such as neprilysin, insulin-degrading enzyme and endothelin-converting enzymes-1 and -2 expressed on astrocytes, microglia, and neurons<sup>108,111,112</sup>. Therefore, microglia cells in the brain are fully equipped to clear out A $\beta$  peptides that are constantly generated through chaperone- or receptor-mediated endocytosis.



Immune activation can turn from acute to chronic thus switching microglia roles from protective to harmful. For example, microglia can induce functional changes on astrocytes via cytokines and complement C1q<sup>113</sup>. Chronic inflammation has been shown to exacerbate tau-like pathology in AD or tauopathy mouse models possibly through microglia- and astrocyte crosstalk<sup>37,114,115</sup>. Sustained neuroinflammation therefore can cause 1) functional changes on surrounding neuronal or non-neuronal cells, and 2) downstream AD pathology (e.g. tau pathology).

### 1.3.3 Tau pathology: key contributor to neuronal damage

Tau pathology is a key contributor to other many neurodegenerative diseases collectively known as tauopathies that differ by affected brain region<sup>116</sup>. Mutations on MAPT gene are known to cause several tauopathies including Pick's disease, frontotemporal dementia, corticobasal degeneration, and progressive supranuclear palsy<sup>117</sup>. These tauopathies do not induce A $\beta$  pathology further supporting the hypothesis that tau is downstream of A $\beta$ . In AD, NFTs appear in the entorhinal cortex then the hippocampus and spread to the limbic and association cortices<sup>33</sup>. Recent *in vivo* and *in vitro* studies implicate exosome-mediated propagation of pathological tau from one neuron to anatomically connected neurons<sup>118-120</sup>. Thus, tau propagation further enhances tau-induced synaptic damage as it is continuously spread.

Neurons become vulnerable to damage because of tau pathology during disease. Under normal physiological conditions, tau serves as a microtubule stabilizing protein that is abundant in neuronal axons<sup>121</sup>. Multiple serine and threonine residues on tau make them susceptible to hyperphosphorylation by a variety of calcium-dependent kinases<sup>116,121</sup>. Under pathological conditions, aberrant phosphorylation of tau proteins voids their normal microtubule supportive function. As hyperphosphorylated tau accumulates, they form insoluble filaments and ultimately NFTs inside the neuron<sup>121</sup>. These NFTs mislocalize from the axons to the neuronal cell bodies and dendritic spines<sup>121,122</sup>. At the dendritic spines, Ittner and colleagues demonstrated that one of the dendritic functions of tau is to facilitate Fyn kinase to postsynaptic compartments where Fyn phosphorylates one of the subunits of the NMDAR, GluN2B, thereby stabilizing their interaction with the scaffolding protein, post-synaptic density protein 95<sup>123</sup>. This leaves the post synapse susceptible to glutamate excitotoxicity and over activation of calcium-dependent tau kinases. The therapeutic efficacy of mentioned memantine, the partial antagonist for NMDAR supports this critical pathological role of glutamate and possible glutamate-induced synaptic degeneration in AD. Overall implicating pathological pathways of tau may be through the glutamatergic pathway.

### 1.3.4 Synaptic loss: the significant correlate to cognitive decline

Progression of A $\beta$  pathology, sustained neuroinflammation, and propagation of NFTs are hypothesized to promote degenerative mechanisms in synapses and neurons. The exact molecular mechanism is still unknown. Growing lines of evidence indicate the answer may be found in the neuron and glia crosstalk<sup>113,124,125</sup>. For example, neuroinflammation

has been associated with plaque clearance and maintenance (mentioned above). However, recent evidence shows its involvement at the synapse. In an animal model of AD, Hong et. al., demonstrated that over active microglia phagocytose synapses prior to plaque formation when challenged with A $\beta$  oligomers through the complement-dependent pathway<sup>124</sup>. This study implicates that neuroinflammation plays an active role in synapse loss during early stages of AD.

The relationship between astrocytes and neurons is vital for synapse preservation as they are intimately associated at the synapse. Furthermore, this relationship may be compromised by aging, the strongest risk factor for sporadic AD<sup>125,126</sup>. In conclusion, the mechanisms in neuron and astrocyte crosstalk may be compromised in AD and thus warrants further investigation.

## 1.4 Premise

### 1.4.1 Astrocytes: role in glutamatergic system

Astrocytes are the most predominant glial cells found in the central nervous system and encompass a variety of versatile roles. Nursing and providing nutrients to neurons has long been thought to be the primary physiological role of astrocytes<sup>127,128</sup>. Recent studies reveal astrocytes' highly versatile functions that include 1) immune-related activities, 2) phagocytosis, 3) pruning, maturation, and maintenance of synapses, and 4) communication between themselves as well as neurons via glial transmitters<sup>129-131</sup>. Therefore, astrocytes are now being recognized as integral and essential component to maintain the brain structure, functions, and homeostatic microenvironment of the CNS.

Processes of astrocytes form part of the tripartite synapse – the intimate and functional integration of astrocytes with the glutamatergic synapses, where astrocytes maintain homeostasis of glutamate and various ions<sup>132</sup>. Astrocytes partake in the glutamate-glutamine cycle at the tripartite synapses during synaptic activity to remove and recycle glutamate at synaptic terminal<sup>133</sup> (**Fig. 2**). Glutamate is stored in synaptic vesicles located in the presynaptic neuron. Upon depolarization of the pre-synaptic neuron, glutamate is released to the synaptic cleft in a calcium-dependent manner<sup>134</sup>. Once released to the synaptic cleft, glutamate then binds to ionotropic and metabotropic receptors. Binding to the ionotropic receptors, such as  $\alpha$ -amino-3-hydroxy-5-methyl-4-isoxazolepropionic acid (AMPA) receptors, NMDAR and Kainate receptors, on the post-synaptic neuron stimulates the influx of Na<sup>+</sup> and Ca<sup>2+</sup> ions. This depolarizes the post-synaptic neuron and triggers Ca<sup>2+</sup> - induced signaling cascades<sup>135</sup>. Released glutamate is quickly cleared from the synaptic cleft by astrocytes and neurons through excitatory amino acid transporters (EAATs) to prevent glutamate leakage and overstimulation, which potentially triggers excitotoxicity. Glutamate is then converted to glutamine by glutamine synthetase<sup>136</sup> and transported to the presynaptic neuron for recycle<sup>137</sup>. Vesicular glutamate transporters then transport the glutamate in the synaptic vesicles awaiting the next depolarization<sup>138,139</sup>.

In the human brain, five high-affinity glutamate EAATs are differentially expressed in astrocytes and neurons<sup>138</sup>. EAATs transport glutamate with three Na<sup>+</sup> and one H<sup>+</sup> coupled to counter-transport of one K<sup>+</sup> ion. Transporting down their concentration gradients result in low extracellular levels of glutamate at the synapse<sup>138</sup>. Among the EAATs is EAAT2 or its mouse homolog GLT-1, herein collectively referred to as GLT-1, is responsible for clearing almost 90% of released glutamate in the synaptic cleft<sup>135,140</sup>. GLT-1 is present in all areas of the hippocampus and almost exclusively on astrocytes<sup>138,141</sup>. For these reasons, GLT-1 is an important transporter in glutamatergic synapses.

#### 1.4.2 GLT-1 in AD

The glutamatergic system is clearly highlighted as one of the critical components altered in AD. More than half of synapses found in hippocampus, the most vulnerable regions affected in AD, are glutamatergic synapses<sup>45,142,143</sup> and play an important role in memory and cognition. Hyperexcitability of neurons is observed in MCI and early AD brains, followed by the loss of glutamatergic synapses, which correlates well with the severity of AD and cognitive decline<sup>144,145</sup>. Lastly, high glutamate levels in the CSF of AD patients suggest an impairment in glutamate regulation<sup>6</sup>. Thus, a possible dysfunction in glutamate uptake or clearance at the synapse is implicated in AD.

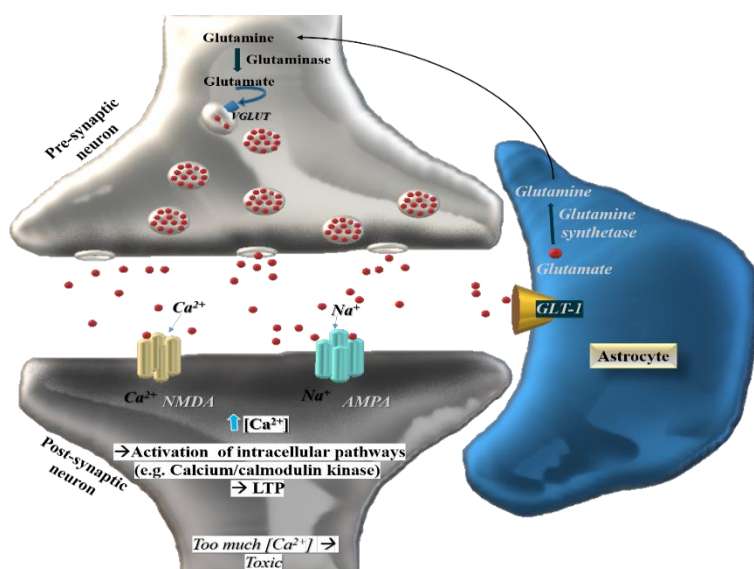


**Figure 1-2. Glutamatergic tripartite synapse (simplified).** Depolarization of the presynaptic neuron, releases calcium-dependent glutamate-containing vesicles to release glutamate in the synaptic space. Glutamate binds to both ionotropic and metabotropic receptors (not shown). Binding of glutamate to ionotropic receptors leads to an influx of sodium and calcium ions into the post-synaptic neuron causing its depolarization. Excess glutamate is taken up by glutamate transporters – majorly regulated by GLT-1 expressed mainly on astrocytes. In astrocytes, glutamate is metabolized; glutamine synthetase converts glutamate to glutamine. Glutamine is returned to the pre-synaptic neuron where it is converted to glutamate by glutaminase.

decline<sup>150,151</sup>. In conclusion, astrocytic GLT-1 dysfunction significantly plays an important role in human AD pathogenesis.

GLT-1 is compromised in AD which indicates consequences that can lead to synapse loss and AD-related pathology. Significant reduction of GLT-1 activity has been reported in the early stages of the disease as well as mild cognitive impaired human patients implicating an early event<sup>146-148</sup>. Separate reports demonstrated that GLT-1 protein levels are significantly reduced in the hippocampus of AD patients<sup>147-149</sup>. In addition, studies using animal models of AD further support these findings from humans by showing the haploinsufficiency of GLT-1 exacerbates cognitive

### 1.4.3 GLT-1

GLT-1 expression can be regulated transcriptionally, post-transcriptionally and post-translationally through pharmacological or endogenous stimuli<sup>135,152-154</sup>. The GLT-1 gene has 11 exons that form 3 major splice variants and yields a protein with 8 transmembrane domains<sup>135</sup>. For transcriptional regulation, studies of cultured fetal astrocytes and small promoter fragments show that the GLT-1 promoter sequence has several transcription factor-sequence including NFκB, N-myc and N-FAT<sup>155,156</sup>. NFκB, for example, serves as a GLT-1 activator when activated by ceftriaxone or epidermal growth factor through the canonical or non-canonical pathway respectively<sup>153,157</sup>. Neurons can send trophic factors to induce GLT-1 transcriptional regulation. Interestingly, site-directed mutagenesis and deletion studies on the 2.5 kb upstream promoter region of GLT-1 identified 10 base pairs essential for GLT-1 promoter activation *in vitro* and *in vivo*<sup>158</sup>. In the same study, Yang et al., found that kappa B-motif binding phosphoprotein, the mouse homologue of human heterogeneous nuclear ribonucleoprotein K, binding to the 10-base pair region induced GLT-1 expression in murine astrocytes during synaptogenesis<sup>158</sup>. Thus, GLT-1 regulation occurs through a neuron and astrocyte dependent pathway.

GLT-1 mRNA expression in human AD brains is found unchanged, thus the loss of GLT-1 may be explained by post-transcriptional modulations<sup>138,146</sup>. One of the endogenous post-transcriptional controls is microRNA-mediated gene silencing. MicroRNAs are 20-25 nucleotide non-coding RNAs that regulate expression by binding to the target sites in either 3' untranslated region of mRNA to inhibit translation or the coding regions to degrade the mRNA<sup>159</sup>. Unlike transcriptional regulation of the gene in the cell, microRNA-mediated post-transcriptional gene regulation could control the specific gene expression in spatial, temporal, and/or stimulation-dependent manners. This spatially and temporally restricted gene regulation may be a key for highly diverse functional versatility in polarized cells, such as neurons. The sequential steps in the canonical processing of mammalian miRNAs are 1) primary miRNA (pri-miRNA) transcript is produced in the nucleus by RNA polymerase II or III, 2) pri-miRNA is then cleaved by the microprocessor complex Drosha-DGCR8 (Pasha) resulting in the production of a precursor hairpin, pre-miRNA, 3) pre-miRNA is then exported from the nucleus to the cytoplasm by Exportin-5-Ran-GTP and transported to various cellular compartments, 4) pre-miRNA hairpin is cleaved to its mature length by RNase Dicer complex with transactivating response RNA-binding protein, 6) the passenger strand is degraded and the functional strand of mature miRNA is then loaded into the RNA-inducing silencing complex with argonaute proteins to target and regulate mRNAs<sup>159,160</sup>. GLT-1 expression has previously been shown to be controlled by microRNA-124a, 107, 29a and 181<sup>161-163</sup>. *Chapter 3 of this dissertation investigates the role miRNAs on GLT-1 expression.*

### 1.4.4 The loss of GLT-1 and its impact on AD neuropathology

The loss of glutamate transporter in astrocytes may lead to sustained excitability and subsequent excitotoxicity in glutamatergic synapses. In clinical studies, a pattern of high

neuronal activity in MCI patients or prodromal phase is detected<sup>164-166</sup>, suggesting that abnormal hyperactivity of neurons may be an early disease phenomenon and be triggered by a loss of GLT-1 and subsequent glutamate dyshomeostasis. Such abnormal neuronal activity and its consequence in AD neuropathology were recently examined using optogenetics in mice. Light-triggered neuronal hyperactivity in hippocampus significantly exacerbates A $\beta$  production in an animal model of AD<sup>167</sup>. In cell culture models, A $\beta$  oligomers promote functional impairment of GLT-1 by downregulating or internalizing the transporter<sup>126,168,169</sup>. As a result, A $\beta$  induces aggravated neuronal excitability<sup>170,171</sup>. These findings from clinical, animal models and cell culture studies strongly implicate that a loss of GLT-1 can generate a vicious feedback loop to increase the production, secretion, and propagation of toxic A $\beta$  in the brain and further induces excitotoxicity to lead progressive synaptic and neuronal loss, characteristics in AD. *Chapter 4 of this dissertation tests the hypothesis that GLT-1 downregulation can increase A $\beta$  pathology in a mouse model of AD.*

Similarly, hyperexcitability of neurons may exacerbate tau pathology. Recent studies report a possible link between hyperexcitable neurons and the propagation of pathological tau in anatomically-connected neuronal network. As mentioned earlier, aberrant neuronal activity greatly enhances the release of tau *in vitro* and *in vivo*<sup>119,172,173</sup>. Thus, the loss of GLT-1 and subsequent hyperexcitation of glutamatergic synapses may promote tau propagation. *Chapter 2 of this dissertation tests the hypothesis that GLT-1 restoration can ameliorate tau pathology in a mouse model of AD.*

## 1.5 Hypothesis

A $\beta$ -induced GLT-1 downregulation links A $\beta$  pathology to tau pathology, synaptic loss, and cognitive decline.

## 1.6 Dissertation Contribution

- Temporal decrease in GLT-1 levels in the hippocampus of AD mouse model
- GLT-1 decrease in hippocampus of human AD patients (further supporting current findings)
- Pharmacological up-regulation of GLT-1:
  - Significantly ameliorates the age-dependent pathological tau accumulation
  - Restores synaptic density
  - Rescues cognitive decline
  - Minimal effects on A $\beta$  pathology.
  - GLT-1 restoration is neuroprotective and partially rescues AD like neuropathology and cognitive decline in an AD mouse model.
  - A $\beta$ -induced astrocyte dysfunction represented by a functional loss of GLT-1 may serve as one of the major pathological links between A $\beta$  and tau pathology.

- IL-1 $\beta$  induces GLT-1 levels via miRNA 181a in primary murine neuron and astrocyte co-culture providing a potential protective mechanism during acute exposures of IL-1 $\beta$ :
  - Synthetic 20ng/mL IL-1 $\beta$  increase GLT-1 expression levels after 48 hours of exposure
  - Synthetic 20ng/mL IL-1 $\beta$  decreases miR-181a expression levels after 48 hours of exposure
  - miR-181a decreases GLT-1 levels in a concentration-dependent manner after 48 hours of exposure
  - miR-181a lowers GLT-1 expression to control levels when co-exposed with IL-1  $\beta$ .

### 1.7 Conclusion

- GLT-1 is a key player in the progression of AD and its restoration may ameliorate AD pathology.
- GLT-1 is regulated post-transcriptionally by IL-1 $\beta$
- miR-181a is a key regulator of GLT-1

## **Chapter 2: Ceftriaxone ameliorates tau pathology and cognitive decline via restoration of glial glutamate transporter in a mouse model of Alzheimer's disease.**

### 2.1 Abstract

Glial glutamate transporter, GLT-1, is the major Na<sup>+</sup>-driven glutamate transporter to control glutamate levels in synapses and prevent glutamate-induced excitotoxicity implicated in neurodegenerative disorders including Alzheimer's disease (AD). Significant functional loss of GLT-1 has been reported to correlate well with synaptic degeneration and severity of cognitive impairment among AD patients, yet the underlying molecular mechanism and its pathological consequence in AD are not well understood. Here, we find the temporal decrease in GLT-1 levels in the hippocampus of the 3xTg-AD mouse model and that the pharmacological upregulation of GLT-1 significantly ameliorates the age-dependent pathological tau accumulation, restores synaptic proteins, and rescues cognitive decline with minimal effects on A $\beta$  pathology. In primary neuron and astrocyte co-culture, naturally secreted A $\beta$  species significantly downregulate GLT-1 steady state and expression levels. Taken together, our data strongly suggest that GLT-1 restoration is neuroprotective and A $\beta$ -induced astrocyte dysfunction represented by a functional loss of GLT-1 may serve as one of the major pathological links between A $\beta$  and tau pathology.

### 2.2 Introduction

Alzheimer's disease (AD) is the most common progressive neurodegenerative disease associated with dementia. Neuropathological hallmarks include extracellular amyloid-beta (A $\beta$ ) plaques and intracellular neurofibrillary tangles (NFTs) composed of A $\beta$  peptides and hyperphosphorylated tau proteins, respectively. Buildup of these pathological lesions are believed to trigger complex, multi-factorial neurodegenerative cascades in AD leading to synaptic loss and neurodegeneration. Dementia severity among AD patients correlates well with synaptic loss and oligomeric A $\beta$  species, and to a lesser extent, with A $\beta$  plaques in the brain<sup>27,32,47,62,68,97</sup>. Moreover, increasing A $\beta$  levels has been suggested to be an initiating factor in AD pathology<sup>47</sup>. The exact molecular mechanism that links A $\beta$  and tau pathology in AD, however, remains largely unknown.

Clinical and pre-clinical evidence suggests disruption of glutamate homeostasis contributes to the development of neuropathological hallmarks and cognitive decline in AD. Glutamate neurotransmission is critically involved in learning and memory, and its synapses are densely concentrated in the hippocampus, a vulnerable region affected in AD. Its neurotransmission is tightly controlled by five different glutamate transporters within the vicinity of glutamatergic synapses in humans to prevent prolonged glutamate input and subsequent glutamate-induced excitotoxicity in neurons. Among these transporters, the excitatory amino acid transporter 2 (EAAT-2) or its mouse homologue glutamate

transporter 1 (GLT-1, herein collectively referred to as GLT-1) expressed predominantly on astrocytes is responsible for regulating 90% of glutamate levels in the synapses<sup>135</sup>. A significant reduction of GLT-1 activity has been reported to occur in an early stage of AD and correlates well with synaptic loss and cognitive decline in patients<sup>146</sup>. In addition, GLT-1 gene expression and protein levels are altered in the hippocampus of AD patients<sup>149</sup>. Recent studies further support the involvement of GLT-1 in AD by showing that the heterozygous knockdown of GLT-1 in an AD mouse model exacerbates cognitive decline without affecting A $\beta$  pathology and that astrocytic GLT-1 dysfunction plays an important role in human AD pathogenesis<sup>150,151</sup>. These studies evidently show that impairment in GLT-1 is not only part of the initial stages of AD pathology but that it also plays an important role in the progression of cognitive decline.

In this study, we investigate whether compensation for the age- and pathology-dependent loss of GLT-1 would significantly impact AD-like neuropathology and cognitive decline in the triple transgenic mouse model of AD (3xTg-AD). We hypothesize that a loss of GLT-1, representative of functional impairments of astrocytes, mediates A $\beta$ -induced neurotoxicity and precedes post-synaptic degeneration and cognitive decline in AD, and its restoration rescues functional synapses and halts the disease progression. Here, we show that the chronic up-regulation of GLT-1 by ceftriaxone significantly attenuates tau pathology, restores synaptic proteins and rescues cognition without affecting A $\beta$  pathology in 3xTg-AD mice. Our *in vitro* studies uncover that naturally secreted A $\beta$  species significantly downregulate GLT-1 expression. Taken together, loss of GLT-1 may in part mediate A $\beta$ -triggered tau pathology in AD.

## 2.3 Materials and Methods

### 2.3.1 Animals

All experiments were carried out in accordance with the Institutional Animal Care and Use Committee at the University of California and were consistent with Federal guidelines. All mice were housed on a 12 hour light/dark schedule with ad libitum access to food and water. The 3xTg-AD mice express the Swedish (K670N/M671L), PS1M146V and tau (P301L; found in frontotemporal dementia patients) mutations which increase the overall production of A $\beta$ , increases the ratio of A $\beta$ <sub>42</sub>/A $\beta$ <sub>40</sub> and promotes tau tangle formation respectively<sup>174</sup>. A total of five to seven 3xTg-AD mice and five to seven strain-matched C57BL6/129SvJ non-transgenic mice were used for the aging study. A total of 15 3xTg-AD mice were treated; 4 females and 4 males for the vehicle group and 3 females and 4 males for the ceftriaxone-treated group.

#### 2.3.1.1 Animal treatment paradigm

Ten months old 3xTg-AD mice were treated intraperitoneally (i.p.) with 200 mg/kg ceftriaxone (Santa Cruz Biotechnology, Santa Cruz, CA) or 0.8% sodium chloride (Vehicle) daily for 2 months<sup>157</sup>. Upon completion of the treatment period and cognitive evaluation, mice were anesthetized, and perfused with ice-cold phosphate buffered saline,



and brains were collected. One hemisphere of the brain was fixed with 4% paraformaldehyde for immunostaining. The other hemisphere was micro-dissected into the hippocampus and cortex. The hippocampus was homogenized in T-PER buffer containing protease and phosphatase inhibitors followed by the centrifugation at 100,000 x g for 1 hr to separate the detergent-soluble fraction and insoluble pellets. Pellets were subsequently homogenized in 70% formic acid and the detergent-insoluble fractions were collected. Samples were stored at -80°C until further analysis.

### 2.3.2 Cognitive tests

Following the 2 months of ceftriaxone treatment, all mice were subjected to cognitive evaluation in the Morris water maze (MWM) and novel object recognition test (NOR). As described previously<sup>175</sup>, the apparatus used for the MWM task was a circular aluminum tank (1.2 m diameter) painted white and filled with water maintained at 22 to 24°C. The maze was located in a room containing several simple visual extramaze cues. Mice were trained to swim and find a 14-cm-diameter circular clear Plexiglas platform submerged 1.5 cm beneath the surface of the water and invisible to the mice while swimming. On each training trial, mice were placed into the tank at one of four designated start points in a pseudorandom order. Mice were allowed to find and escape onto the platform. If mice failed to find the platform within 60 sec, they were manually guided to the platform and allowed to remain there for 10 sec. Each day, mice received four training sessions separated by intervals of 25 sec under a warming lamp. The training period ended when all groups of mice reached criterion (<25 sec mean escape latency). The probe trial to examine retention memory was assessed 24 hrs after the last training trial. In the probe trials, the platform was removed from the pool, and mice were monitored by a ceiling-mounted camera directly above the pool during the 1 minute period. All trials were recorded for subsequent analysis. The parameters measured during the probe trial included 1) latency to cross the platform location and 2) number of platform location crosses.

The NOR was performed as described previously<sup>176</sup>. Briefly, mice were habituated in the test environment for 3 days (5 minutes per day). In the acquisition of familiar objects, mice were exposed to 2 identical objects separated in a specific location in a square cage. Twenty-four hours later, mice were placed in the test cage with one familiar object and one novel object. The total amount of time the mice explored each object was recorded separately for 3 minutes, and the recognition index ( $[\text{time spent on novel object}] / \{[\text{time spent on novel object}] + [\text{time spent on a familiar object}]\}$ ) was calculated in %).

### 2.3.3 Quantitative A $\beta$ ELISA analysis

Soluble and insoluble A $\beta_{1-40}$  and A $\beta_{1-42}$  levels were measured by ELISA as previously described<sup>175</sup>. Briefly, 96-well plates (Immulon 2HB, Fisher Scientific, Waltham, MA) were coated with 25  $\mu\text{g/mL}$  of the mouse anti-A $\beta$  monoclonal antibody (clone 20.1) in carbonate coating buffer pH 9.6 (Sigma-Aldrich, St. Louis, MO) and incubated overnight at 4°C. The wells were washed and blocked with 3% BSA overnight at 4°C with shaking. After washing, serial dilutions of A $\beta_{40}$  and A $\beta_{42}$  were added to the wells and plates were

sealed then incubated overnight at 4°C with shaking. After washing, HRP-conjugated affinity anti-A $\beta$ 40 or anti-A $\beta$ 42 antibodies were added at 1:2000 and 1:1000 dilutions, respectively, and incubated overnight at 4°C with shaking. Wells were then washed and incubated with streptavidin-HRP (1:4000 dilution) for 4 hrs at room temperature, washed then Ultra-TMB ELISA substrate (Pierce, Rockford, IL) was added for 5-10 minutes to develop the reaction. The reaction was stopped by adding 2N H<sub>2</sub>PO<sub>4</sub> and plates were analyzed on a SpectraMax Spectrophotometer (Molecular Devices, Sunnyvale, CA) at 450 nm. The plasma end-point titer was defined as the maximal plasma dilution in which the O.D. for the antibodies was 3 times higher than the O.D. values of the blank wells.

### 2.3.4 Western blot and analysis

Protein concentrations of detergent-soluble fractions from half brain (hippocampus or cortex) were determined by the Bradford protein assay. These fractions (9  $\mu$ g of protein) were subsequently immunoblotted with the following antibodies: HT7 (total human tau, Pierce Biotechnology, Rockford, IL), AT8 (phosphorylated tau at S202/T205, Pierce Biotechnology), PHF-1 (phosphorylated tau at S396/S404; a kind gift from Dr. Peter Davies, Albert Einstein College of Medicine), CP13 (phosphorylated at S202/T205; a kind gift from Dr. Peter Davies, Albert Einstein College of Medicine), AT100 (phosphorylated tau at S212/T214, Pierce Biotechnology), GLT-1 (a kind gift from Dr. Jeffrey David Rothstein, Johns Hopkins University), GFAP (Dako, Carpinteria, CA) cdk5 (Calbiochem, La Jolla, CA), p35/p25 (Santa Cruz Biotechnology), GSK-3 $\beta$  (BD transduction laboratories, San Jose, CA) and phospho-GSK-3 $\beta$  (phosphorylation at S9, Cell Signaling Technology, Beverly, MA). GAPDH, (Santa Cruz Biotechnology), tubulin and/or actin (Abcam, Cambridge, MA) were used to control for protein loading or to confirm no cross-contamination of each fraction. Band intensity was measured using the Odyssey Image station and Image Studio (version 2.1, Li-Cor Biosciences, Lincoln, Nebraska) and normalized by corresponding loading control proteins.

### 2.3.5 Real-time PCR (RT-PCR)

Total RNA was isolated from 3xTg-AD or WT hippocampal tissue using TRI reagent (Molecular Research Center, Cincinnati, OH). Total RNA was isolated from untreated and treated neuron and astrocyte primary cells using Direct-zol RNA MiniPrep (Zymo Research Corp., Irvine, CA). Briefly, 1  $\mu$ g of total RNA was used for one-cycle reverse transcriptase reaction to make cDNA by random hexamers using 5x iScript<sup>TM</sup> Reaction Mix and iScript<sup>TM</sup> Reverse Transcriptase (BioRad, Hercules, CA). 2  $\mu$ l of resulting cDNA was subjected to a PCR reaction for the detection of GLT-1, GLAST, and GFAP using Power SYBR Green PCR Master Mix (Applied Biosystems, Life-Technologies). Sequences of GLT-1 primers were 5'-TTCCAAGCCTGGATCACT GCTC-3' (forward) and 5'- GGACGAATCTGGTCACACGCTT -3' (reverse) (Origene, NM\_001077514). GLAST primers were 5'-GCGATTGG TCGCGGTGATAATG-3' (forward) and 5'-CGACAATGACTGTACCGGTGTAC-3' (reverse) (Origene, NM\_148938). GFAP primers were 5'-CACCTACAGGAAATTGCTGGAGG-3' (forward) and 5'-CCACGATGTTCTTCTTGAGGTG-3' (reverse) (Origene, NM\_010277). GAPDH was

used for normalizing the GLT-1, GLAST and GFAP expression levels in each treatment, and the primer sequences were 5'-AACTTTGGCATTGTGGAAGG-3' and 5'-ACACATTGGGGGTAGGAACA-3'. The PCR cycle parameters were as follows: denaturing step (95 °C for 15 sec), annealing step (60 °C for 60 sec) and extension step (72 °C for 30 sec). The cycle threshold (Ct) values were determined by SDS Software v1.3.1 (Applied Biosystems), and  $\Delta\text{Ct}$  for each treatment group was calculated as follows:  $\Delta\text{Ct} = \text{Ct (GLT-1, GLAST1 or GFAP)} - \text{Ct (GAPDH)}$ <sup>177</sup>.

### 2.3.6 Immunohistochemical (IHC) and immunofluorescence (IF) staining

Each half brain was cut into 20  $\mu\text{m}$  slices using a microtome and stored in PBS with 0.05% sodium azide. Free-floating sections were washed with TBS, permeablized with 0.1% triton X-100 and blocked with 3% BSA in TBS. For A $\beta$  plaque burden and certain tau staining, free-floating sections were pre-treated with 90% formic acid for 3 minutes prior to the incubation with primary antibodies. Sections were then incubated with antibodies against synaptophysin (SYP; presynaptic marker; Abcam; 1:1000), post-synaptic density protein 95 kDa (PSD95; postsynaptic marker; Neuromab; 1:1000), AT8 (1:2000), AT100 (1:2000), CP13 (1:1000), PHF1 (1:1000), MC1 (1:1000), HT7 (1:2000), Iba-1 (1:400), 4G8 (1:400), or biotinylated antibody against A $\beta$ <sub>42</sub> (clone D32 from Drs. Vasilevko and Cribbs, 1:400) overnight. Sections were washed the following day and incubated with 3% BSA and 1% triton X-100 in TBS then 1 hr incubation with corresponding secondary antibody conjugated with Alexa Fluor 488, Alexa Fluor 555 and/or Alexa Fluor 633 with DAPI for nuclear staining. For immunohistochemistry, after the incubation with primary antibodies, sections were incubated with corresponding biotinylated secondary antibodies, followed by ABC treatment and DAB staining according to the manufacturer's specifications.

### 2.3.7 Thioflavin S staining

For immunofluorescent staining with thioflavin S (Sigma, St. Louis, MO), free-floating sections were mounted on a Superfrost Plus™ microscope slide (Fisher Scientific, Waltham, MA) to dry overnight. To hydrate, fixed sections were immersed twice in 100% ethanol for 2 minutes, twice in 95% ethanol for 2 minutes, once in 70% ethanol for two minutes then once in 50% ethanol for two minutes. Sections were then incubated with 0.5% thioflavin S in 50% ethanol for 10 minutes (in the dark). Sections were washed twice with 50% ethanol for 3 minutes and twice with water for 3 minutes. Staining was visualized using a digital inverted microscope (EVOS-*fl*, Advanced Microscopy Group).

### 2.3.8 Quantitative analysis of synaptic proteins, plaque burden and tau pathology.

Synapse proteins in the CA1 and CA3 regions of the hippocampus and dentate gyrus (DG) were quantified by Image J software. Briefly, 6 brain sections (20 $\mu\text{m}$  thickness) from each animal were IF stained with SYP or PSD95 antibodies described above and images were captured using a digital inverted microscope (EVOS-*fl*, Advanced Microscopy Group). PSD95 or SYP IF signal were counted in the subfield of the hippocampus and dentate

gyrus. SYP and PSD95 protein levels were calculated independently. For each 20  $\mu\text{m}$  brain section, 3 different areas from the CA1 and CA3 regions of the hippocampus and DG were captured. From those images, 3 random 100  $\mu\text{m}^2$  sections were chosen (each representative of that area) from each image and the mean intensity was measured using ImageJ software. An average of all the areas from each region was calculated and represented synapse intensity for DG, CA1 or CA3 of the hippocampus. Staining with 4G8, HT7 or PHF-1 was also analyzed in the same manner. For the CP-13, HT7 and PHF-1 analysis, the entire area of the hippocampus and cortex (separately) was chosen of 2-5 brain sections (20 $\mu\text{m}$  thickness) and positive soma were counted from each area.

### 2.3.9 Astrocyte and neuron primary cell co-culture

As described by Yang and colleagues<sup>158</sup>, primary astrocytes were extracted from the cortex and hippocampus of postnatal day 2-3 (P2-P3) mice from wildtype (WT) mice. Primary cells were grown in Dulbecco's modified Eagle's medium (DMEM) containing 10% fetal bovine serum (FBS), 1% penicillin/streptomycin (P/S). Primary neurons were extracted from embryonic day 14-16 (E14-16) of WT mice. Primary neurons were added to confluent primary astrocytes in Neurobasal media with B27 supplement, glutamine, and 5% FBS (plating media) for the first 24 hrs then the medium was changed to media of similar contents but with only 2.5% FBS (growth media). Primary cells were treated after day 7 (of neuron addition)<sup>158</sup>. The purity of primary astrocytes and the presence of neurons were consistently monitored by IF staining with GFAP and Tau5 respectively.

### 2.3.10 7PA2 –Chinese Hamster Ovary (CHO) cell culture

Naturally secreted A $\beta$  monomers and oligomers were obtained from the conditioned medium (CM) of 7PA2 CHO cells that express the V717F AD mutation in APP751 (an APP isoform that is 751 amino acids in length, a kind gift from Dr. Edward Koo, UCSD)<sup>69</sup>. Both control CHO cells and 7PA2 cells were grown in the DMEM containing 10% FBS and 1% P/S until ~90% confluency. Cells were washed and medium replaced with neuronal growth media (described above) for ~18 hrs. CM was collected and centrifuged at 1,000 x g for 10 minutes at 4°C to remove cell debris then used for treatment of astrocyte and neuron primary cell co-culture. CM from CHO cells and fresh growth media were used as controls.

### 2.3.11 Statistical analysis

All immunoblot and immunohistochemical data were quantitatively analyzed using Image Studio (version 2.1) software or Image J software. Statistics were carried out using one-way ANOVA with post-hoc tests or unpaired t-test and  $p < 0.05$  or lower was considered to be significant. Pearson correlation coefficient was calculated for linear regression graphs.

## 2.4 Results

To determine whether the expression of GLT-1 in astrocytes changed with age and/or the progression of the AD-like pathological hallmarks in 3xTg-AD mouse model, we assessed levels of GLT-1 in the hippocampus from 2-3 (pre-pathological), 6 (early pathology), 12-13 (mild/moderate pathology), or 23 (late, established pathology) months of age. We found that the hippocampal GLT-1 expression and the steady state levels significantly decreased as AD-like neuropathology progressed in 3xTg-AD mice, but not in WT mice ( $p < 0.05$  and  $p < 0.01$ ; **Fig. 2-1A, C and D**). The steady-state levels of GLT-1 were significantly reduced especially at 12 months of age or older. We previously reported that GFAP steady state levels increase with age in 3xTg-AD mice<sup>174</sup>. In this study, we found that GFAP mRNA expression levels as well as the steady-state levels also increased with age in 3xTg-AD mice ( $p < 0.01$ ; **Fig. 2-1B, C and F**). Thus astrogliosis inversely correlated with significant GLT-1 decrease indicating that glial GLT-1 in synapses was less in the 3xTg-AD mice than that in age-matched WT mice. In comparison, the GLutamate ASpartate Transporter (GLAST) expression and steady state levels, also expressed on astrocytes, did not significantly decrease until 23 month of age ( $p < 0.05$  **Fig. 2-1C and E**).

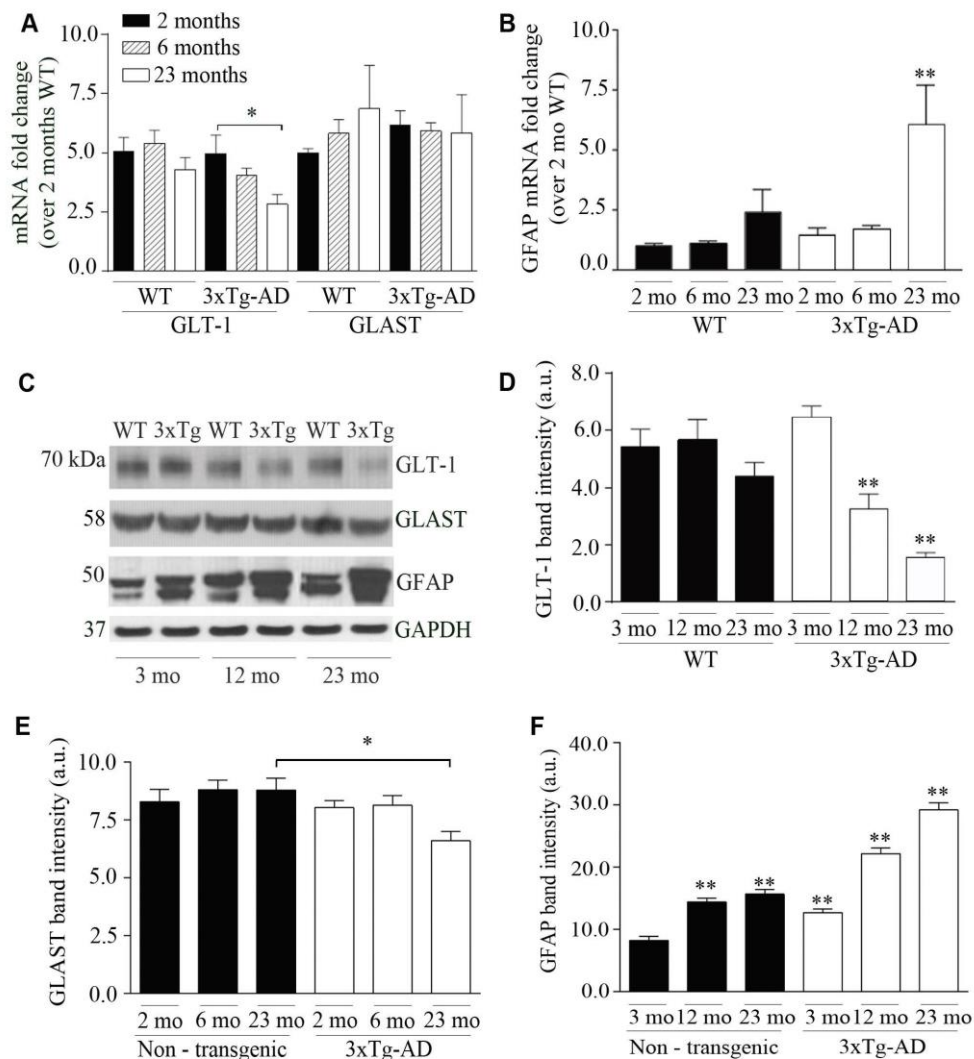


**Figure 2-1. GLT-1 decreases in an age-dependent manner in 3xTg-AD mice.** (A) RT-PCR analysis of GLT-1 mRNA levels in wild type (WT) and 3xTg-AD mice at 2, 6 and 23 month (mo) old mice. (B) RT-PCR analysis of GFAP mRNA levels in WT and 3xTg-AD 2, 6 and 23 month old mice. (C) Western blot analysis of protein extracts from 3, 12 and 23 month old WT and 3xTg-AD mice using GLT-1, GFAP and GAPDH antibodies. The densitometric analysis of the GLT-1 (D), GLAST (E) and GFAP (F) bands normalized to GAPDH shown in the graphs. Each bar is expressed as mean  $\pm$  standard error mean (S.E.M); \* $p < 0.05$  and \*\* $p < 0.01$  compared to the WT group or 2-3 months old 3xTg-AD group. The number of mice analyzed was  $n = 5-7$  per group.

Recent studies have demonstrated that synthetic oligomeric A $\beta$ 1-42 decreased GLT-1 expression or promoted mislocalization of GLT-1 from the cell surface of primary astrocytes, leading to glutamate dyshomeostasis in synapses<sup>168,178</sup>. Our in vivo evidence (Fig. 2-2), however, indicated a clear reduction of GLT-1; a reduction possibly through the decreased expression in astrocytes. To test whether A $\beta$  species subsequently alters GLT-1 expression, we utilized the primary neuron and astrocyte co-culture system to examine the role of naturally secreted A $\beta$  species on GLT-1 expression in vitro<sup>158</sup>. 1.85 nM of naturally secreted A $\beta$ 42 and 4.4 nM of naturally secreted A $\beta$ 40 in the conditioned medium (CM) from 7PA2 CHO cells (7PA2-CM)<sup>69</sup> were added to primary neuron/astrocyte co-culture for 48 hours (Fig. 2-2A). We found that the 48-hour treatment of 7PA2-CM

resulted in a significant decrease of the GLT-1 mRNA expression ( $p < 0.0001$  **Fig. 2-2B**) compared to cells treated with CM from CHO cells (CHO-CM; control). GLAST expression did not change under the same treatment (**Fig. 2-2B**, right). We also investigated the steady levels of GLT-1 and found that A $\beta$  species from the 7PA2-CM significantly decreased the steady state levels compared to CHO-CM ( $p < 0.0001$  **Fig. 2-2C**). Integrity of primary astrocyte and neuron co-cultures was consistently confirmed through immunofluorescence staining (**Fig. 2-2A**). These in vitro results suggest that A $\beta$  species are responsible for the loss of GLT-1 expression as a part of their toxicity to astrocytes.

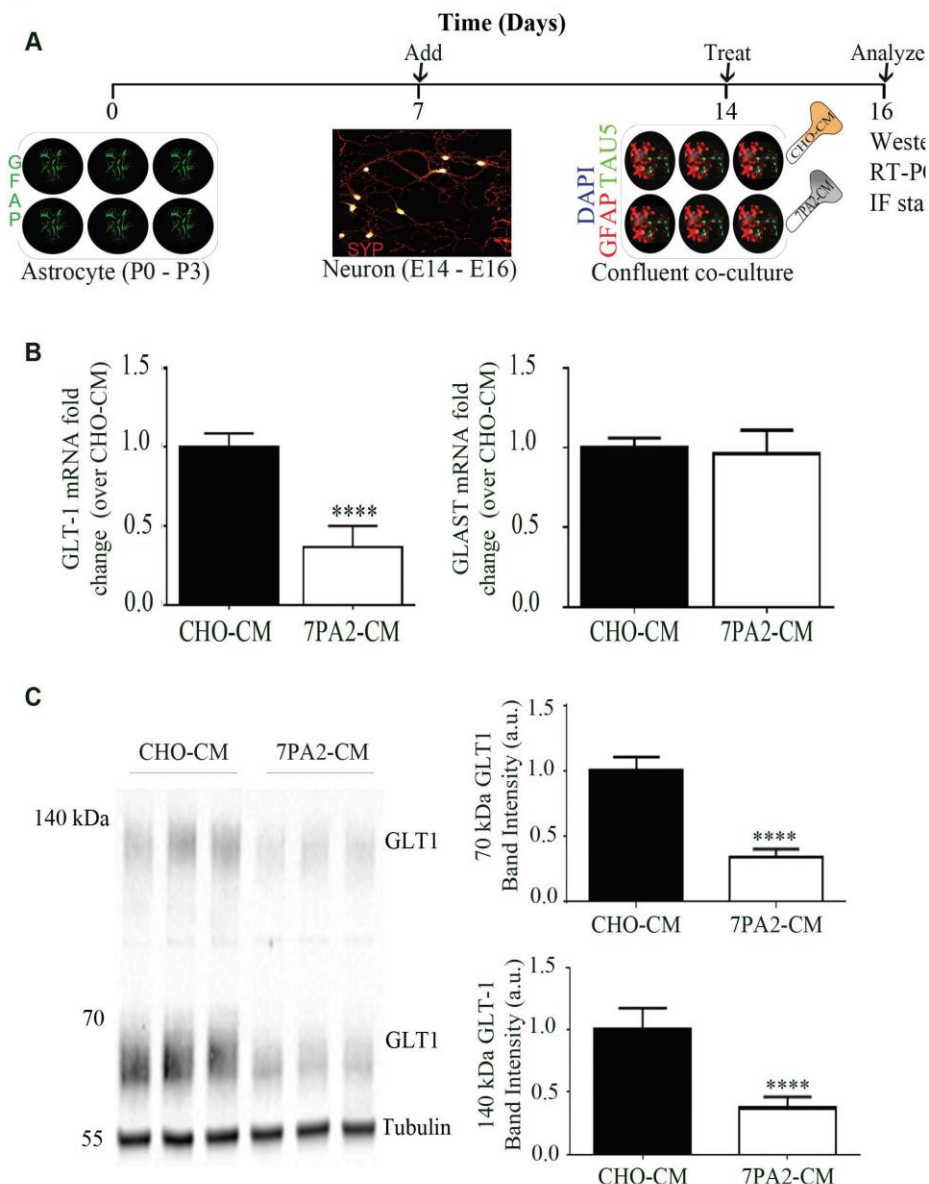


**Figure 2-2. Naturally secreted A $\beta$  decrease GLT-1 steady state levels.** (A) Experimental scheme for investigating GLT-1 expression in the primary astrocyte and neuron co-culture. Astrocytes extracted from the cortex and hippocampus of postnatal day 0 – day 3 (P0-P3) and detected with the GFAP antibody. Neurons were extracted from embryonic day 14 – 16 (E14 – E16) and detected with tau5 or SYP antibodies. 1.85 nM of naturally secreted A $\beta$ 42 and 4.4 nM of naturally secreted A $\beta$ 40 present in 7PA2-CM (quantified by ELISA) were added to the co-culture for 48 hours. (B) RT-PCR analysis of GLT-1 and GLAST mRNA levels from neuron and astrocyte co-cultures treated with

*CHO conditioned media (CHO-CM) or 7PA2 conditioned media (7PA2-CM) for 48 hrs. (C) Western blot of protein extracts from neuron and astrocyte co-cultures treated with 7PA2-CM or CHO-CM for 48 hours using GLT-1 and tubulin antibodies. The densitometric analysis of the 70 kDa and 140 kDa band from GLT shown in the graph. Each bar is expressed as mean  $\pm$  S.E.M.; \*\*\*\* $p < 0.0001$  7PA2-CM compared to CHO-CM. Three independent experiments performed each time in triplicates.*

Since a significant reduction of GLT-1 was evident in the hippocampus of 3xTg-AD mice at 12 months of age and our in vitro evidence suggested that its reduction was mediated by A $\beta$  species, we examined whether a chronic restoration of GLT-1 at this age would ameliorate downstream AD-like neuropathology and cognitive decline. We chronically treated 10 month old 3xTg-AD mice with either ceftriaxone (200 mg/kg i.p.) or saline (0.8% NaCl i.p.) daily for two months. Ceftriaxone is a beta lactam antibiotic shown to increase the astroglial GLT-1 expression both in vitro and in vivo<sup>157,179</sup>. Consistent with these previous reports, the ceftriaxone treatment in this study significantly increased GLT-1 protein expression levels compared to the age-matched vehicle group ( $p < 0.05$  for both 70 and 140 kDa bands; **Fig. 3**). GLT-1 western blots can show monomeric (70 kDa) and dimeric (140 kDa) forms as previously shown and described<sup>157,180</sup>.

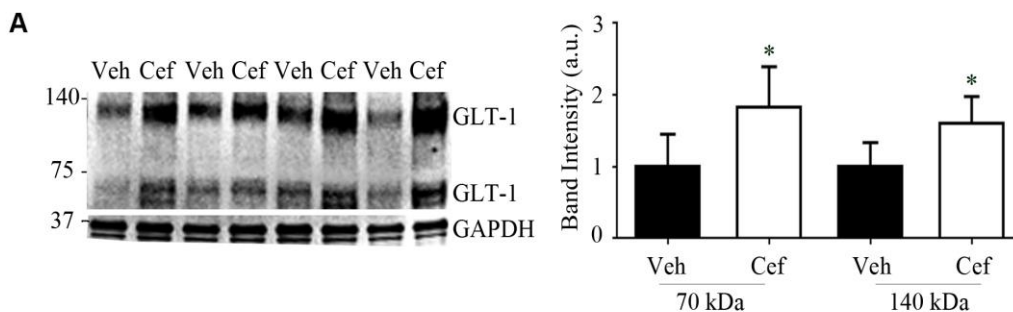


**Figure 2-3. Chronic ceftriaxone-treatment increases GLT-1 expression levels in 3xTg-AD mice.** (A) Western blot analysis of protein extracts from hippocampal tissue of 12 month old 3xTg-AD mice using GLT-1 and GAPDH (housekeeping) antibodies. Densitometric analysis of the GLT1 bands normalized to GAPDH shown in the graph. Each bar is expressed as mean  $\pm$  S.E.M.; \* $p < 0.05$ , ceftriaxone-treated 3xTg-AD mice compared with the vehicle-treated 3xTg-AD mice ( $n = 5$  mice per group). Molecular weight markers are in kDa. Veh = vehicle or saline-treatment and Cef = ceftriaxone treatment.

The effect of GLT-1 up-regulation on hippocampal-dependent cognition was evaluated by MWM and NOR immediately after treatment. During the acquisition training in the MWM, the vehicle 3xTg-AD group were capable of learning within the same day, but failed to retain spatial memory from day to day, which was consistent with previous findings<sup>181</sup>. In comparison, the ceftriaxone-treated 3xTg-AD group had better retention for the majority of the training days ( $p < 0.05$ ; **Fig. 2-4A**). This was later confirmed during the probe trial of MWM; the probe trial measures retention memory. During the probe trial, the ceftriaxone-treated group reached the platform location significantly faster than the vehicle group ( $p < 0.05$ ; **Fig. 2-4B**). In addition, ceftriaxone-treated mice crossed the platform location more than the vehicle group within the 60 sec of the probe trial, further suggesting that the retention memory was significantly rescued in the ceftriaxone-treated mice ( $p < 0.01$ ; **Fig. 2-4C**). Similarly, in the NOR, ceftriaxone-treated mice explored a novel object significantly longer than a familiar object ( $p < 0.05$ ; **Fig. 2-4D**). Therefore,



increasing GLT-1 in the 3xTg-AD mice rescued cognitive impairments as measured by two independent behavioral tests.

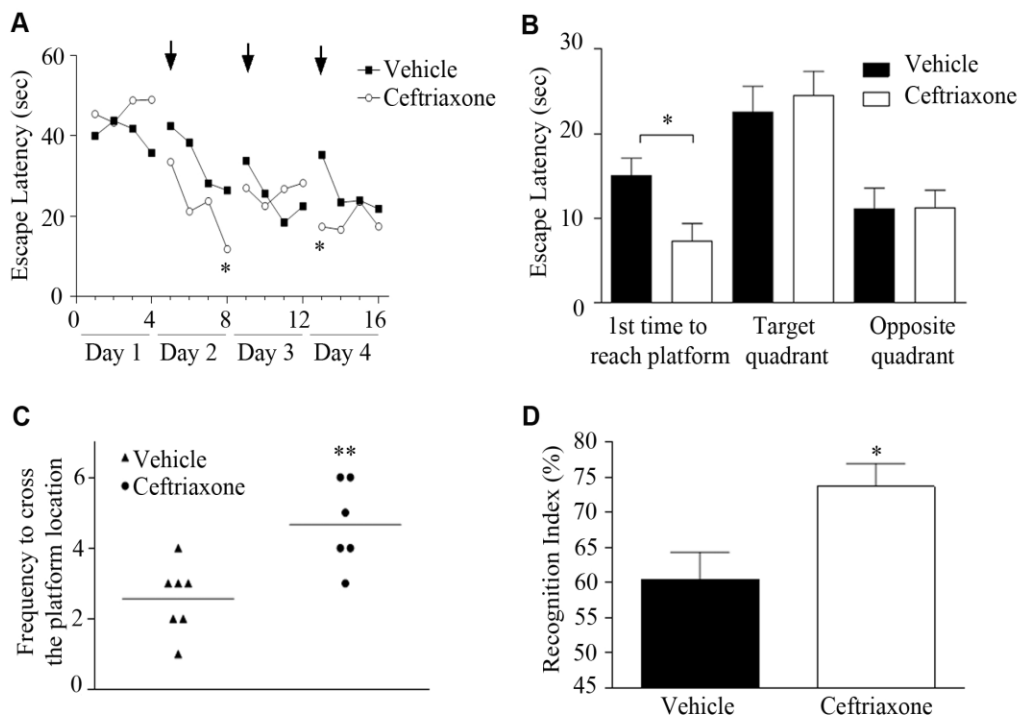
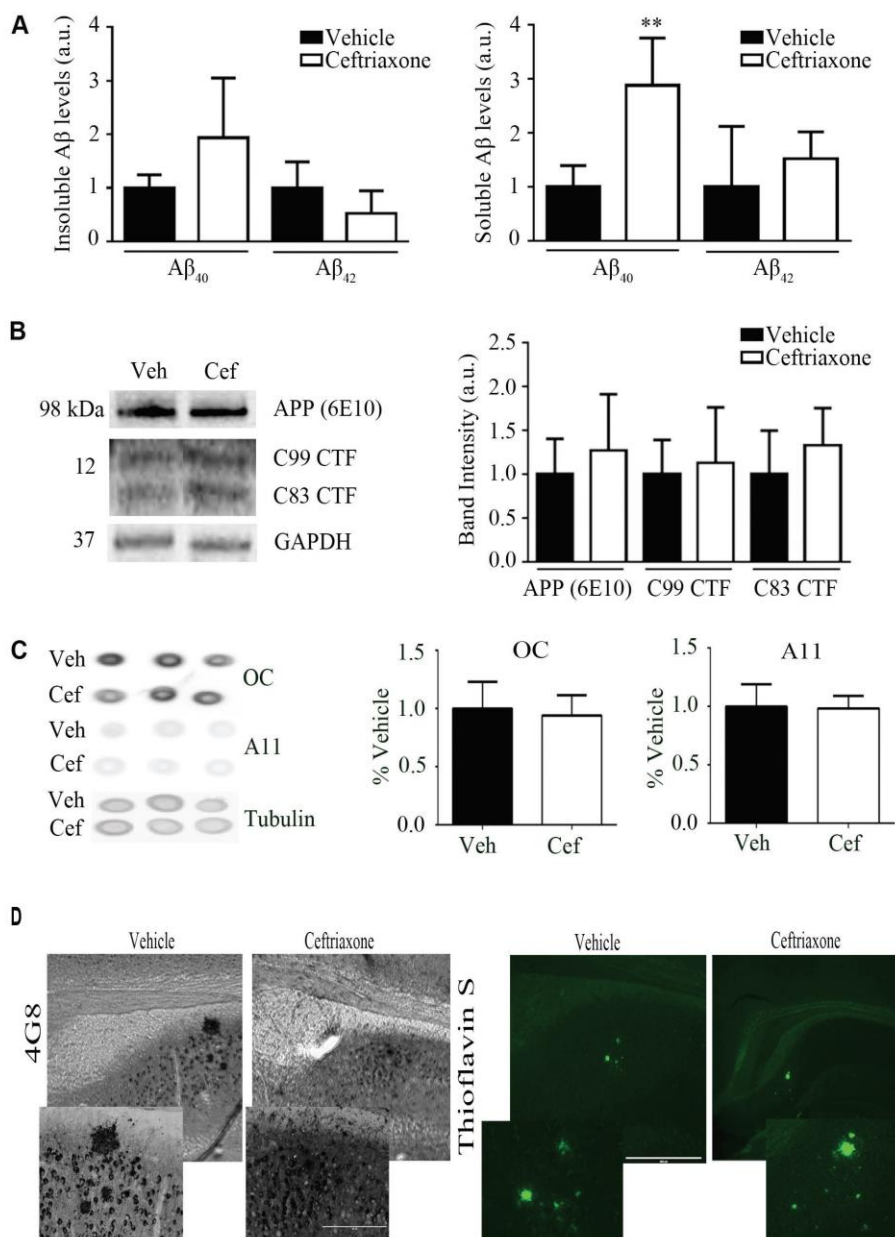


Figure 2-4. **Upregulation of GLT-1 by ceftriaxone ameliorates cognitive decline in 3xTg-AD mice.** (A) Acquisition curve during training of MWM expressed as average of all mice in each group. Arrowheads show the first training of the day. (B) Escape latency and (C) number of crosses on platform location for 24-hour retention trial in MWM. (D) NOR for the first minute of the test. Each bar is expressed as mean  $\pm$  S.E.M.; \* $p < 0.05$  and \*\* $p < 0.01$ , ceftriaxone-treated 3xTg-AD mice compared with the vehicle-treated 3xTg-AD mice ( $n = 5$  mice per group).

To better understand the molecular basis of the restoration of cognition in these behavioral tests, we examined the effects of GLT-1 up-regulation on A $\beta$  and tau pathology. Quantitative ELISA revealed no significant changes of detergent-insoluble A $\beta$ 40 and A $\beta$ 42 in the hippocampal tissues of 3xTg-AD mice (**Fig. 2-5A**). Detergent-soluble A $\beta$ 40 significantly ( $p < 0.01$ ; **Fig. 2-5A**) increased in ceftriaxone-treated mice, however there was no significance in detergent-soluble A $\beta$ 42 (**Fig. 2-5A**). APP expression or processing was not significantly altered by the treatment because the steady state levels of APP or C-terminal fragments of APP, specifically C99 and C83, were not changed among the treatment groups (**Fig. 2-5B**). We then used conformation specific antibodies, A11 and OC, to detect soluble pre-fibrillar and fibrillar A $\beta$  oligomers respectively<sup>182,183</sup>. Dot blot analysis of the cortical soluble fractions revealed no significant changes in A $\beta$  oligomer levels between the ceftriaxone-treated and vehicle-treated 3xTg-AD mice (**Fig. 2-5C**). Together with our in vitro data above, the presence of A $\beta$  species likely suppressed GLT-1 expression in the brain of 3xTg-AD mouse. In addition, histological analysis revealed that plaque burden in the hippocampus and subiculum of ceftriaxone-treated 3xTg-AD mice were not significantly different than the vehicle group, which in part supported the

quantitative ELISA data described above (**Fig. 2-5D**). While we do not know the exact mechanisms of increased soluble A $\beta$ 40 levels in the ceftriaxone-treated mice, collectively, these results suggest that GLT-1 dysfunction does not affect APP processing, overall A $\beta$  species levels and plaque pathology in the 3xTg-AD mice. These findings are consistent with a recent report in heterozygous knockout of GLT-1 in APP/PS1 mice<sup>150</sup>.



**Figure 2-5. Effect of GLT-1 up-regulation on A $\beta$  pathology in 3xTg-AD mice.** (A) Quantitative A $\beta$  ELISA in detergent-insoluble (formic acid soluble) brain hippocampal fraction and detergent soluble brain hippocampal fraction. (B) Westernblot analysis of APP processing in the hippocampus of the brain. The densitometric analysis of C99 and C83 fragments shown in the graph. (C) Dot blot analysis of soluble pre-fibrillar and fibrillar A $\beta$  oligomers in the cortical soluble fractions detected by the A11 and OC antibodies respectively. (D) Qualitative representation of the immunohistochemical staining with 4G8 and Thioflavin S

S to detect A $\beta$  plaques. Each bar is expressed in mean  $\pm$  S.E.M.; \*\* $p < 0.01$ , ceftriaxone-treated 3xTg-AD mice compared with the vehicle-treated 3xTg-AD mice ( $n = 4-5$  mice per group).

We previously demonstrated that altered inflammation such as gliosis in the brain exacerbated tau pathology in 3xTg-AD mice<sup>37,115</sup>. Accordingly we investigated pathological changes in tau following up-regulation of GLT-1. Histopathological analysis revealed that the ceftriaxone-treated mice showed significantly less CP13-positive tau (pSer202) bearing neurons than vehicle-treated mice in the cortex and hippocampus ( $p < 0.05$ ; **Fig. 2-6A**). Similarly, the mean intensity from immunofluorescence staining with the PHF-1 antibody (pSer396/Ser404) was significantly less than the vehicle group in the CA1 region of the hippocampus ( $p < 0.05$ ; **Fig. 2-6A**). No significant alteration in total tau levels by the HT7 antibody was detected in the same fields. Western blot analysis of the insoluble total tau levels in sarkosyl-insoluble fraction of the cortex was significantly lower in the ceftriaxone treated 3xTg-AD mice ( $p < 0.0001$ ; **Fig. 2-6B**). Western blot analysis of tau in detergent-soluble fraction of hippocampus showed a decreasing trend, though not significant, of phospho-specific tau using the PHF-1, AT8, CP13 and AT180 antibodies while the total tau levels remained unchanged (**Fig. 2-6C**). This discrepancy suggests decreased levels of insoluble or aggregated tau in the hippocampus of Ceftriaxone-treated 3xTg-AD mice. We investigated the kinases reported in the involvement of pathological tau phosphorylation<sup>184,185</sup>. Although we found a decreasing trend of phosphor-specific tau, the total steady state levels of cdk5 and GSK-3 $\beta$  were not significantly altered among the treatment groups (**Fig. 2-6D**). Taken together, these results highlights disease-modifying effects of GLT-1 on tau pathology in neurons.

3xTg-AD mice display an age-dependent dramatic loss of synapses without extensive neuronal loss<sup>176,186</sup>. Therefore, we examined whether a restoration of GLT-1 protected synaptic proteins in these mice. Synapse alterations were quantitatively analyzed by changes in synaptic markers SYP<sup>30,31,187,188</sup> and PSD95<sup>189</sup>. Significant changes of SYP and PSD95 immunoreactivity in subregions within hippocampus were observed by IF staining (**Fig. 2-7A-B**). Quantitative analysis of fluorescent signals revealed that synaptic proteins detected by the SYP and PSD95 antibodies was significantly preserved in the CA3 region of the hippocampus ( $p < 0.05$ ; **Fig. 2-7A-B**) of ceftriaxone-treated 3xTg-AD mice. In addition, a significant restoration of PSD95 immunoreactivity in CA1 hippocampus was also observed in the ceftriaxone-treated 3xTg-AD mice ( $p < 0.001$  and  $p < 0.05$ ; **Fig. 2-7B**). We also found the restoration of PSD95 had a tendency to correlate with augmented cognitive performance by MWM. Mice reaching the platform in 15 seconds or less had a high ( $>1.0$ ) synaptic protein intensity mean, and although not statistically significant, increased PSD95 mean fluorescent intensity negatively correlated with the escape latency in dentate gyrus (DG), CA1 and CA3 regions of hippocampus (**Fig. 2-7C**). These findings strongly indicate that GLT-1 is key to preserving synapses and crucial for neuron to neuron communication.

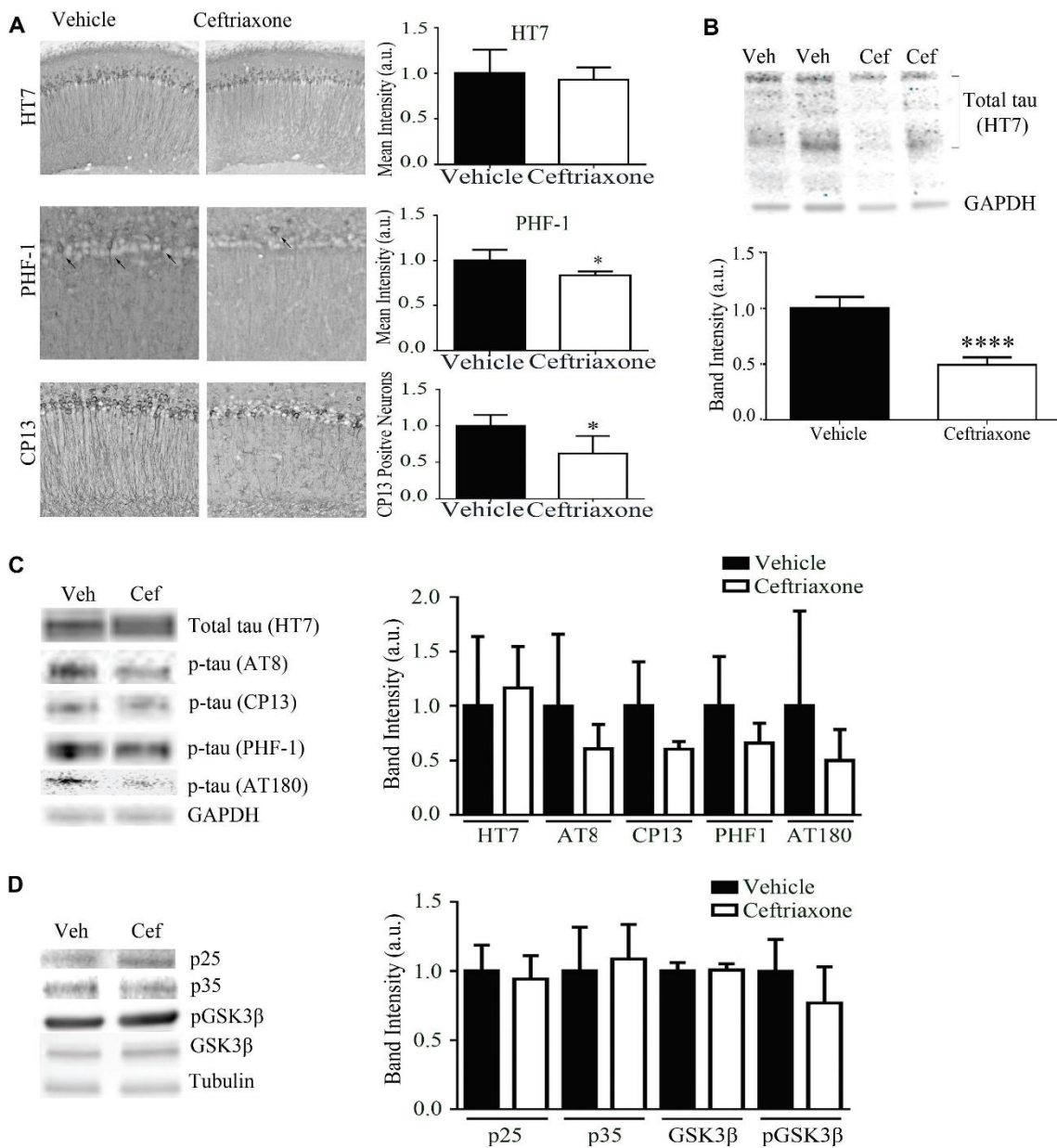


**Figure 2-6. Effect of GLT-1 up-regulation on tau pathology in 3xTg-AD mice.** (A) Representative IHC or IF staining with tau antibodies HT7, PHF-1 and CP13 antibodies. The mean intensities of HT7 and PHF-1 from immunofluorescence staining are shown in the graph along with the CP-13 positive neuron analysis. Arrows point to tau-positive neurons. (B) Representative western blot image of total human tau using HT7 antibody from the sarkosyl – insoluble cortical protein fraction. The densitometric analysis of all bands are shown in the graph. (C) Western blot analysis of total human tau using HT7 antibody and various phospho-specific tau using PHF1, AT8, CP13, AT180 and GAPDH (housekeeping protein) from the detergent-soluble hippocampal protein fraction. The densitometric analysis of PHF1, AT8, CP13 and AT180 are shown in the graph. (D) Western blot analysis of known tau kinases: p25, p35, phosphor-GSK3 $\beta$  (pGSK3 $\beta$ ), GSK3 $\beta$  and Tubulin (housekeeping protein) on detergent soluble hippocampal protein fraction. The densitometric analysis of p25, p35, phosphor-GSK3 $\beta$  and GSK3 $\beta$  are shown in the graph. Each bar is expressed as mean  $\pm$  S.E.M.; \* $p < 0.05$ , ceftriaxone-treated 3xTg-AD mice compared with the vehicle-treated 3xTg-AD mice ( $n = 4-5$  mice per group).

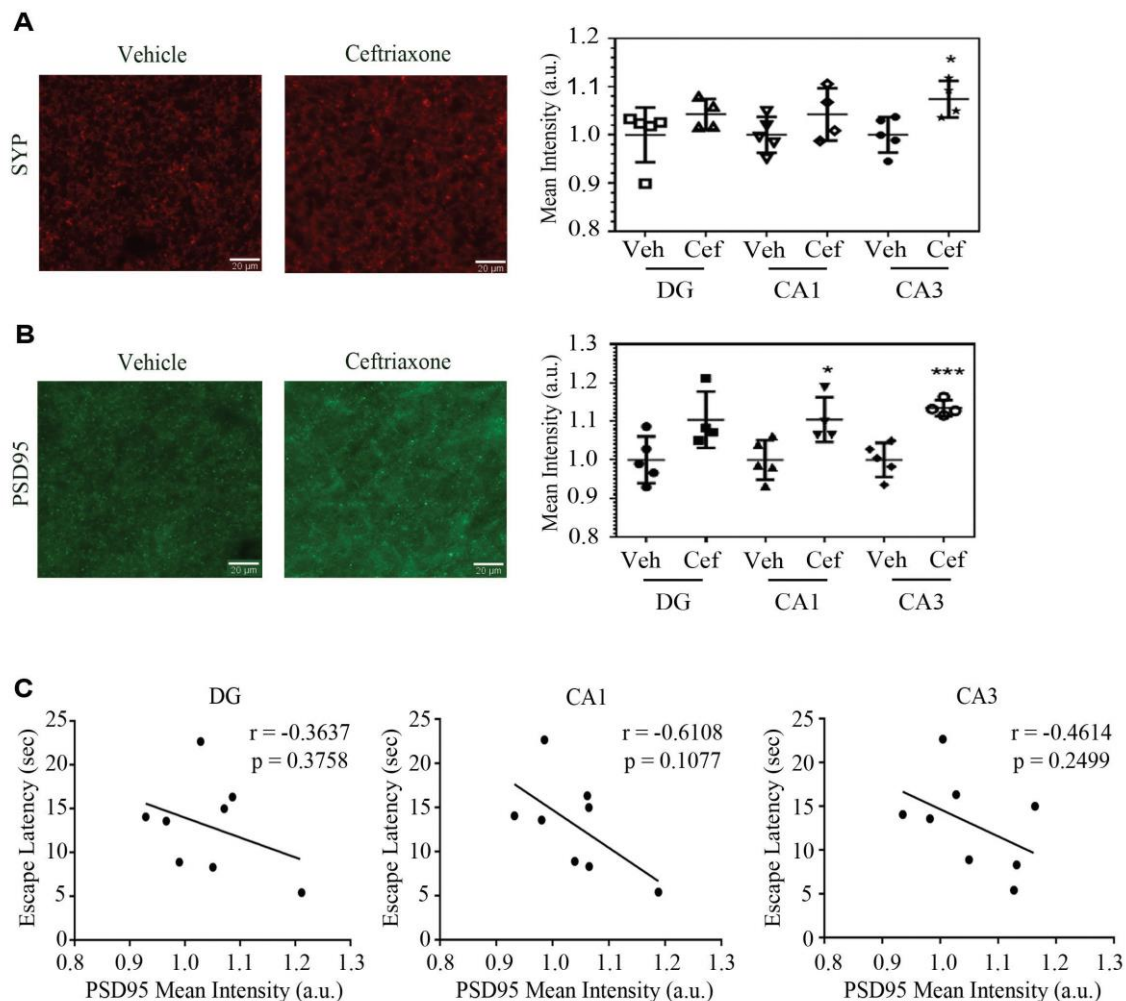


**Figure 2-7. Synaptic proteins restored in ceftriaxone-treated 3xTg-AD mice.** (A) Representative IF images of SYP in the CA3 region of the hippocampus and quantitative analysis of the average mean intensities from five IF (20  $\mu$ m) stained sections in the dentate gyrus (DG), CA1 and CA3 of the hippocampus. (B) Representative IF images of PSD95 in the CA3 region of the hippocampus and quantitative analysis of the average mean intensities from five IF (20  $\mu$ m) stained sections in the DG, CA1 and CA3 of the hippocampus. (C) Escape latency as a function of synaptic protein mean intensity graphs in the designated region of the hippocampus. Each shape represents one mouse and each bar is expressed as mean  $\pm$  S.E.M.; \* $p < 0.05$  and \*\*\* $p < 0.001$ , ceftriaxone-treated 3xTg-AD mice compared with the vehicle-treated 3xTg-AD mice ( $n = 3-5$  mice per group). Sec = seconds

## 2.5 Discussion

We report that astrocytic GLT-1 may be a key player that links A $\beta$  and tau pathology. Our findings show a significant correlation between the age-dependent decrease of astrocytic GLT-1 and the progression of AD-like neuropathology in 3xTg-AD mice regardless of astrogliosis. To test whether the loss of GLT-1 precede AD pathology and cognitive decline in 3xTg-AD mice, we pharmacologically overexpressed GLT-1 and examined its pathological and behavioral consequences *in vivo*. By doing so, we found that the chronic administration of ceftriaxone significantly increases GLT-1 expression, ameliorates cognitive deficits, preserves synaptic proteins and decreases tau pathology in aged 3xTg-

AD mice. These results strongly implicate and support the notion that astrocyte dysfunction have major implications in neurodegenerative disease particularly AD. Furthermore alteration of glutamate transporter expression occurs in the early stages of AD human patients – an important factor in finding a cure<sup>146</sup>.

Synaptic density significantly decreases in human AD brains<sup>27,31</sup> and AD mouse model brains<sup>174,190</sup>. Along with this, increasing evidence shows the active involvement of astrocytes in synapse formation, function and elimination<sup>129</sup>. Talantova and colleagues in particular showed the involvement of astrocytes in glutamate-induced synaptic damage via  $\alpha$ -7 nicotinic receptors stimulation and extrasynaptic NMDA-type glutamate receptors<sup>191</sup>. In comparison, our study focuses on glutamate regulation via GLT-1 expression. We show a positive and significant correlation between an increase in GLT-1 steady state levels and synaptic proteins (PSD-95 and SYP). In particular, a restoration of PSD95 is more evident and found in DG, CA1 and CA3 regions of hippocampus following ceftriaxone treatment, indicating a beneficial effect of GLT-1 in post-synaptic neurons. These results further support our hypothesis that the loss of GLT-1 triggers excitotoxicity and degeneration of post-synaptic neurons through aberrant calcium influx. Restoration of synaptic glutamate homeostasis attenuates post-synaptic degeneration more significantly and directly than pre-synapses. These changes in part contribute to the restoration of cognitive function in the ceftriaxone-treated 3xTg-AD mice as shown by the correlation curve (**Fig. 2-7C**).

As previous studies indicate, A $\beta$  species can induce toxicity to cells prior to plaque formation and synaptic loss<sup>64,66,69,190</sup>. In addition to those studies, we propose that A $\beta$  species also induce astrocyte dysfunction that affect pathology progression in AD. Our results clearly show that A $\beta$  species (including monomers and oligomers) downregulate GLT-1 expression *in vitro* and that GLT-1 restoration *in vivo* did not affect soluble A $\beta$  species levels (**Fig. 2-2 and 2-5**). Although GLT-1 is predominantly expressed on astrocytes, neurons also express GLT-1<sup>192,193</sup>. Thus further studies are needed to investigate the contribution of neuronal GLT-1 expression. Nonetheless A $\beta$ -induced GLT-1 dysfunction may occur in the early stages of AD. This effect can lead to glutamate dyshomeostasis and/or glutamate excitotoxicity. This phenomenon has been suggested in AD because AD patients have increasing glutamate levels in their cerebral spinal fluid (CSF) as dementia progresses<sup>194,195</sup>.

GLT-1 down-regulation also has important implications on tau propagation, phosphorylation and dephosphorylation as perturbation of this equilibrium can void tau's microtubule – associated function, lead to aberrant tau aggregates and increase neuron vulnerability in AD. Since GLT-1 indirectly affect calcium level influx, its dysfunction can impact tau calcium-dependent kinases, including GSK-3 $\beta$  and cdk5, and induce NFTs<sup>122,184,185</sup>. Additionally, an increase in calcium influx can lead to an increase in calcium-dependent tau inter-neuronal propagation<sup>196</sup>. Studies have also shown that tau can spread synaptically via connected glutamatergic neurons<sup>197,198</sup>. This presents the possibility that glutamate dyshomeostasis can be one of the driving forces of tau pathology.

NFTs correlate with cognitive decline<sup>199</sup> and are initiated by the abnormal accumulation and mislocalization of tau in somatodendritic compartments. Tau can also facilitate Fyn kinase to postsynaptic compartments whereby Fyn phosphorylates one of the NMDAR subunits, NR2b, thereby stabilizing its interaction with PSD95 thus causing a sustained activation of NMDAR<sup>123</sup>. Our study, however, showed no significant alterations in the NR2b subunit in the ceftriaxone-treated mice (data not shown). In addition GSK-3 $\beta$  and p25 were not significantly different in the ceftriaxone-treated 3xTg-AD mice. Overall, GLT-1 overexpression ameliorated tau pathology and cognition which suggests that GLT-1 is critical for AD progression.

The NF $\kappa$ B pathway is involved in Cef-induced GLT1 expression; ceftriaxone increases the NF $\kappa$ B binding to the GLT-1 promoter thus increasing its expression<sup>200</sup>. Ceftriaxone has also been shown to transport through the blood brain barrier<sup>201</sup>. Previous reports have shown that ceftriaxone impairs hippocampal learning and memory in rats or had no effect in mice<sup>202,203</sup>. Our study investigates the AD model while Matos-Ocasio et al., 2014 and Karaman et al., 2013 investigated WT animal models<sup>202,203</sup>. Opposite results may suggest adverse effects in normal conditions. As stated by Matos-Ocasio et al., 2014, GLT1 overexpression may be detrimental to normal neuronal activity<sup>202</sup>. In addition, our study chronically injected ceftriaxone for two months while the other two studies treated for only 8-9 days. Thus duration of ceftriaxone treatment may be crucial in improving learning and memory.

## 2.6 Conclusion

In conclusion, our study elucidates the involvement of the glial glutamate transporter in the pathogenesis of AD. We propose that A $\beta$  species prior to plaque or fibrillar formation initiate GLT-1 down-regulation in the early stages of AD. This accounts for the progressive decrease in GLT-1 expression seen in 3xTg-AD, unaffected progression of A $\beta$  pathology, and how the 7PA2 conditioned media containing A $\beta$  species decreased the steady state levels of GLT-1 *in vitro*. We also propose that A $\beta$ -induced GLT-1 dysfunction mediates downstream AD neuropathology including synaptic loss and tau pathology. Further studies, however, are needed to show underlying molecular mechanisms by which A $\beta$  affects GLT-1 down-regulation and alteration *in vivo*. Although further studies will also be needed to confirm any confounding variables from the pharmacological approach, this study determined an important role of astrocyte dysfunction in AD. Moreover, we find that the restoration of GLT-1 ameliorates tau pathology and cognitive deficits. Our study raises the possibility that targeting GLT-1 may result in disease modifying therapies for not only AD, but also other neurodegenerative disorders, such as tauopathies.

## Chapter 3: Inflammatory cytokine, IL-1 $\beta$ , regulates glial glutamate transporter via microRNA-181a in vitro.

### 3.1 Abstract

Glutamatergic neurotransmission plays a critical role in synaptic plasticity. However, glutamate overload triggers synaptic and neuronal loss that potentially contributes to neurodegenerative diseases including Alzheimer's disease (AD). Glutamate clearance and regulation at synaptic clefts is primarily mediated by astrocytic excitatory amino acid transporter 2 (EAAT-2) or its mouse homologue glutamate transporter 1 (GLT-1, herein collectively referred to as GLT-1). We sought to identify the key mechanism modulating GLT-1 and determine whether inflammation plays a pivotal role in this process. **Methods:** Primary murine astrocyte and neuron co-culture received 20 ng/mL IL-1 $\beta$ , TNF- $\alpha$  or IL-6 for 48 hours. Soluble proteins or total RNA were extracted after treatment for further analyses. **Results:** Inflammatory cytokines, IL-1 $\beta$  and TNF- $\alpha$ , significantly increased GLT-1 steady-state levels ( $p \leq 0.05$ ) while IL-6 showed no effect. These cytokines did not significantly affect GLT-1 mRNA, suggesting the cytokine-induced GLT-1 was regulated through post-transcriptional modifications. The primary interest of our lab focused our attention and the remainder of this report on IL-1 $\beta$ . Among the identified microRNAs predicted to modulate GLT-1 expression, microRNA-181 was significantly decreased following the IL-1 $\beta$  treatment ( $p \leq 0.05$ ) while other predicted microRNAs failed to show significance. Restoration of microRNA-181 in IL-1 $\beta$ -treated primary astrocytes and neurons significantly reduced the steady-state levels of GLT-1. In human AD brains, however, we did not observe a significant upregulation of mature microRNA-181 although GLT-1 was markedly reduced. **Conclusion:** Pro-inflammatory cytokine, IL-1 $\beta$ , upregulates astrocytic GLT-1 by suppressing microRNA-181. This novel pathway may be valuable to develop potential neuroprotective therapies for AD.

### 3.2 Introduction

Glutamate is a major excitatory neurotransmitter in the central nervous system and plays an important role in modulating synaptic plasticity, long-term potentiation (LTP), and learning and memory functions in hippocampus. Glutamate release, reuptake, and recycling are tightly maintained between neurons and astrocytes at tripartate synapses to evoke proper post-synaptic signal transduction. Disrupting one or more of these processes result in elevated synaptic or extrasynaptic glutamate levels that can aberrantly activate NMDA receptors (NMDARs) and lead to glutamate-induced, calcium-mediated excitotoxicity, and eventually to neurodegenerative diseases, such as Alzheimer's disease (AD)<sup>135</sup>. Overactivation of NMDARs or elevated neuronal activity has been shown to increase the production and release of amyloid-beta (A $\beta$ ) species from synapses<sup>204-206</sup>, further supporting the causal role of glutamate dyshomeostasis in AD.



Elevated levels of release glutamate is in part exacerbated by impaired glutamate uptake by astrocytes through the excitatory amino acid transporter 2 (EAAT2), which normally clears almost 90% of released glutamate in the synaptic cleft<sup>135</sup>. Loss of EAAT2 in hippocampus has been reported in AD brains<sup>147,149</sup>, and severity of cognitive decline in patients with mild cognitive impairment (MCI) and AD correlates with the loss of glutamatergic synapses, EAAT2, or elevated glutamate levels in cerebrospinal fluid<sup>145,146,207,208</sup>. In animal models, genetic knockdown of the glutamate transporter 1 (GLT-1), a mouse homologue of EAAT2, in AD mice further exacerbates cognitive decline, in part recapitulating the clinical observations described above<sup>150</sup>. In addition, we and others have recently shown that A $\beta$  species significantly reduces GLT-1 expression in the plasma membrane of astrocytes<sup>126,168,169</sup>, and pharmacological or genetic restoration of GLT-1 ameliorates A $\beta$  or tau neuropathology and rescues cognition in AD mouse models<sup>126,169</sup>. Thus, maintenance of functional GLT-1 in mouse or EAAT2 in human (herein collectively referred to as GLT-1) is important for survival of glutamatergic synapses. Furthermore, understanding the regulatory mechanisms of GLT-1 expression will help elucidate the role of glutamate transporter in physiological and pathological conditions.

Several lines of evidence suggest that GLT-1 expression is also modulated by the state of local inflammation in the brain<sup>135</sup>. This regulation appears to be particularly important during physiological conditions and normal brain functions as local elevation of several pro-inflammatory cytokines, such as IL-1 $\beta$ , TNF- $\alpha$ , and IL-6, has been shown to promote or suppress LTP in spatiotemporal manner<sup>209</sup>. While these cytokines are chronically elevated and dysregulated in AD<sup>101</sup>, contribution of acute or chronic input of cytokines to astrocytes and underlying mechanisms to control GLT-1 expression remain largely unknown. Our previous findings of an age-dependent decrease of GLT-1<sup>126</sup> in parallel with an increase of miR-181<sup>210</sup> in 3xTg-AD mouse model led us to specifically explore a potential mechanism involving GLT-1, microRNA and IL-1 $\beta$ . MicroRNAs are 19 to 22 nucleotides noncoding RNAs that bind to the 3'-UTR or coding regions of their respective mRNA target to control gene expression at the post-transcriptional level by modulating mRNA translation and its stability<sup>211</sup>. Alterations of microRNA have been implicated in human AD patients and may also contribute to synaptic function and plasticity<sup>212</sup>. Thus, this study investigates the role of inflammation and microRNAs on synaptic preservation via their control on GLT-1 expression.

In this study, we determined that microRNA-181a (miR-181a) controlled the expression of GLT-1 in astrocytes. When murine primary astrocytes and neurons were treated with IL-1 $\beta$  for 48 hours, GLT-1 was significantly upregulated while miR-181a was concomitantly down-regulated. GLT-1 was restored to the basal level in the co-culture when miR-181a mimics was co-treated with IL-1 $\beta$ . Application of miR-181a mimics alone sufficiently suppressed GLT-1 in a concentration dependent manner. In post-mortem hippocampal tissues from AD patients, we confirmed that GLT-1 is significantly decreased, and the ratio of mature miR-181a over primary miR-181a was elevated. Our results reveal that the expression of miR-181a regulates GLT-1 in astrocytes, and increased mature miR-181a may contribute to the loss of GLT-1 in AD.

### 3.3 Materials and Methods

#### 3.3.1 Primary astrocyte and neuron co-culture

As described previously<sup>126</sup>, primary astrocytes were extracted from the cortex and hippocampus of postnatal day 2-3 (P2-P3) mice from wildtype (WT) mice. Primary cells were grown in Dulbecco's modified Eagle's medium (DMEM) containing 10% fetal bovine serum (FBS), 50 units/mL penicillin and 50 $\mu$ g/mL streptomycin (P/S). Primary neurons were extracted from embryonic day 14-16 (E14-16) of WT mice. Primary neurons were added to confluent primary astrocytes in Neurobasal media with 2% B27 supplement, glutamine, and 5% FBS (plating media) for the first 24 hrs then the medium was changed to media of similar contents but with only 2.5% FBS (growth media). Primary cells were treated after day 7 (of neuron addition). The purity of primary astrocytes and the presence of neurons were consistently monitored by IF staining with GFAP and Tau5 respectively.

#### 3.3.2 Chinese hamster ovary and 7PA2 cell cultures

Naturally secreted A $\beta$  monomers and oligomers were obtained from the conditioned medium (CM) of 7PA2 CHO cells that express the V717F AD mutation in APP<sub>751</sub> (an APP isoform that is 751 amino acids in length, a kind gift from Dr. Edward Koo, UCSD)<sup>69</sup>. Both control CHO cells and 7PA2 cells were grown in the DMEM containing 10% FBS and P/S until ~90% confluency. Cells were washed and medium replaced with neuronal growth media (described above) for ~18 hrs. CM was collected and centrifuged at 1,000 x g for 10 minutes at 4°C to remove cell debris then used for treatment of astrocyte and neuron primary cell co-culture. CM from CHO cells and fresh growth media were used as controls. Recombinant Human Interleukin 1, beta (IL1 $\beta$ ;PHC0815 ThermoScientific, USA).

#### 3.3.3 Cytokine multiplex assay

Cytokines from CHO-CM, 7PA2-CM or growth media (NB) were quantified before and after 48 hours incubation with primary neuron and astrocyte co-cultures. The V-PLEX Proinflammatory Panel 1 (mouse) kits from Meso Scale Diagnostics (MSD, Gaithersburg, MD, USA) was used. The assay was performed according to the manufacturer's instructions and plates were analyzed on the MESO Quickplex SQ 120 (MSD). All standards and samples were measured in duplicate.

#### 3.3.4 Western Blot

Protein was extracted from primary murine astrocyte and neuron co-cultures using MPER while TPER was used to extract protein from human hippocampal tissue (Thermo Scientific). Bradford protein assay determined protein concentrations of MPER- or TPER-soluble fractions. Protein extracts were subsequently immunoblotted with the following

antibodies: GLT-1 (a kind gift from Dr. Jeffrey David Rothstein, Johns Hopkins University), tubulin and GAPDH (Abcam, Cambridge, MA) were used to control for protein loading or to confirm no cross-contamination of each fraction. Band intensity was measured using the Odyssey Image station and Image Studio (version 2.1, Li-Cor Biosciences, Lincoln, Nebraska) and normalized by corresponding loading control protein.

### 3.3.5 RNA Isolation, Reverse Transcription, and Real-time Polymerase Chain Reaction

Total RNA was isolated from primary cells or human hippocampal tissue using Direct-zol RNA MicroPrep and Direct-zol RNA Miniprep respectively according to manufacturer's protocol (Zymo Research Corp, Irvine, CA, USA). Total RNA concentrations were determined using a spectrophotometer (NanoDrop Lite, ThermoScientific, USA). Purity of samples was assessed with 2100 bioanalyzer (Agilent, USA). cDNA was produced from 1000 ng RNA using NCODE Vilo cDNA synthesis kit (microRNAs) or SuperScript III First-Strand Synthesis kit (mRNAs) following manufacturer's protocol (Life Technologies, USA). SYBR green detection for qPCR detailed protocol described previously<sup>126,210</sup>.

### 3.3.6 TaqMan Detection

cDNA was produced from 10ng RNA using TaqMan MicroRNA Reverse Transcription Kit (mature miRNA; Catalog# 4366596, ThermoFisher, USA) or High-Capacity cDNA Reverse Transcription Kit (primary miRNA; Catalog# 4368814, ThermoFisher, USA). Quantitative RT-PCR was performed using CFX Connect Real-Time System (Bio-Rad, USA) with the following TaqMan® miRNA assays (ThermoScientific, USA): hsa-miR-181a (assay ID: 000480), has-miR-181b (assay ID: 001098), U6 snRNA (control; assay ID: 001973), hsa-mir-181a-1 (assay ID: Hs03302966\_pri), hsa-mir-181a-2 (assay ID: Hs03302899\_pri), and 18S (assay ID: Hs99999901\_s1). Cycling for PCR amplification was as follows: enzyme activation at 95°C for 10 min, followed by 45 cycles at 95°C for 15 s and at 60°C for 60 s.

### 3.3.7 MiR-181a Mimic Transfection

Lipofectamine® RNAiMAX (Life Technologies) was utilized to transfect primary neuron and astrocyte co-culture with 25nM, 50nM or 100nM mirVana hsa-miR-29a-5p miRNA mimic or mirVana Negative Control #1 miRNA mimic (Ambion, Austin, TX, USA) per manufacturer's protocol. Protein or RNA were extracted 48 hours after transfection. To show that miR-181a mimics were upregulated in our cell culture after transfection, we extracted miRNAs after exposure and found higher levels of miR-181a in miR-181a (mimic) treated cells than the controls. Different concentrations of miR-181a were tested based on previous transfection reports<sup>161,210</sup>.

### 3.3.8 Statistics

All quantitative data are expressed as mean  $\pm$  SEM. Data analyses were obtained using unpaired, two-tailed *t* test or ANOVA followed by *post hoc* tests. The data were analyzed using Prism (GraphPad Prism Software) and values  $p \leq 0.05$  were considered significant.

## 3.4 Results

### 3.4.1 Inflammatory cytokines, IL-1 $\beta$ or TNF $\alpha$ , upregulate GLT-1 in astrocytes

We previously reported that conditioned media containing naturally secreted A $\beta_{40}$  and A $\beta_{42}$  species from 7PA2 cells (7PA2-CM) significantly downregulated the steady-state levels of GLT-1 compared to those from CHO cells lacking A $\beta$  species (CHO-CM) in primary astrocytes and neuronal co-culture<sup>126</sup>. While investigating a potential molecular mechanism, we found that GLT-1 was significantly elevated in primary astrocyte and neuronal co-cultures treated with CHO-CM by 47% while 7PA2-CM still significantly suppressed GLT-1 steady state levels by 36% compared to those in neurobasal media (control) (**Fig. 3-1**). To examine the rise in GLT-1 levels from CHO-CM compared to control, we hypothesized that cytokines may be involved in GLT-1 regulation since they have previously been shown to modulate GLT-1 expression<sup>135</sup>. We tested a panel of cytokines before and after the 48-hour treatment on our primary astrocytes and neuronal co-culture through MSD. While no difference was detected in cytokine levels among control, CHO-CM, and 7PA2-CM prior to the incubation with co-culture (**Fig. 3-2A**), significantly elevated levels of pro-inflammatory cytokines, IL-1 $\beta$ , IL-6, and TNF- $\alpha$ , were found in CHO-CM, but not in control or 7PA2-CM, after the 48-hour treatment with co-culture (**Fig. 3-2B - D**). We also detected elevated levels of IL-10 and IL-5 in CHO-CM, but no change was observed in IL-12p70, IFN- $\gamma$ , IL-2, and IL-4 (data not shown).

We then examined whether pro-inflammatory cytokine, IL-1 $\beta$ , TNF $\alpha$ , or IL-6, alone could modulate the levels of GLT-1. Treatment with recombinant IL-1 $\beta$  or TNF- $\alpha$  (20 ng/ml) significantly increased GLT-1 levels by 35% and 69%, respectively while recombinant IL-6 did not (**Fig. 3-3**). Cytokine treatment did not alter GLT-1 mRNA measured by qRT-PCR (data not shown). These results show that, in our treatment paradigm on primary neuron and astrocyte co-cultures, specific cytokines upregulate GLT-1 steady state levels while having no significant effect on GLT-1 mRNA.

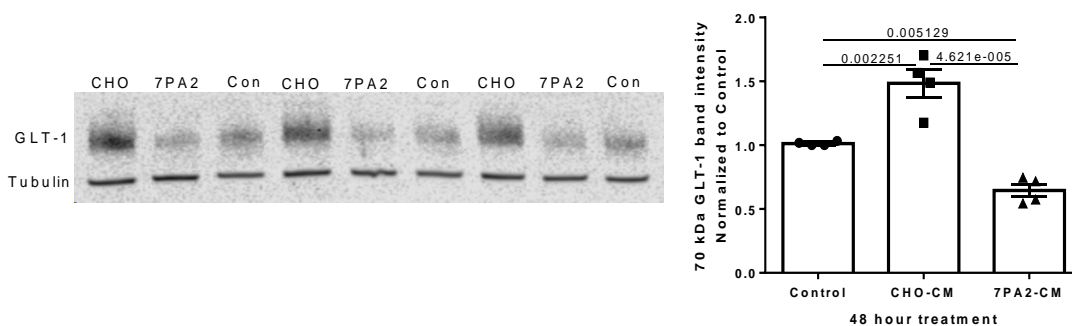


Figure 3-1. Primary astrocyte and neuron co-culture treated with CHO-CM elevated GLUT-1 steady state levels while 7PA2-CM decreased GLUT-1 steady state levels relative to regular neurobasal growth media (control) after 48 hours treatment. GLUT-1 mean  $\pm$  std. error: Control =  $1.01 \pm 0.00816$ , CHO-CM =  $1.48 \pm 0.111$ , 7PA2-CM =  $0.645 \pm .0506$ , Control vs CHO  $p = 0.0023$ , Control vs 7PA2-CM  $p = 0.0051$  and CHO-CM vs 7PA2-CM  $p < 0.0001$ ,  $n = 4$  independent experiments in triplicates.  $p \leq 0.05$  considered significant by one-way ANOVA followed by Holm-Sidak's post hoc multiple comparisons test. Abbreviations: CHO = Chinese hamster ovary; 7PA2 = CHO cells that express the V717F AD mutation in APP751 (an APP isoform that is 751 amino acids in length); CM = conditioned media; GLUT-1 = glutamate transporter 1.

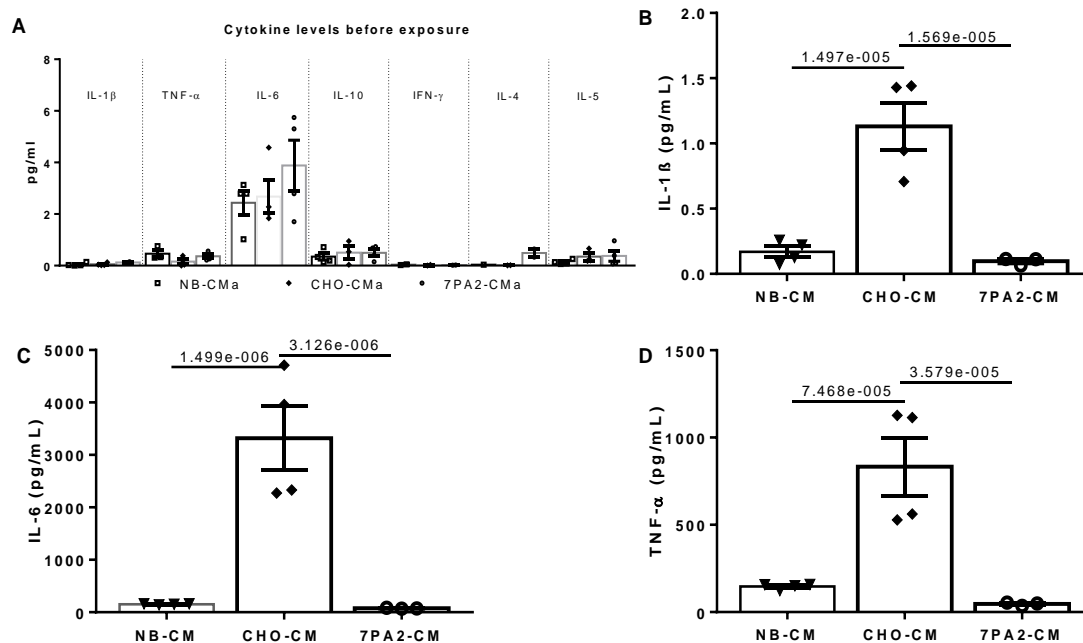


Figure 3-2. Significant differences in cytokine profile between CHO- and 7PA2- CM after 48 hours exposure. (A) No significant differences in cytokine profile between Neurobasal, CHO-CM and 7PA2-CM prior to incubation. 48 hours exposure showed significant levels (pg/mL) of (B) IL-1 $\beta$  (mean  $\pm$  std. error: Control =  $0.170 \pm 0.0422$ , CHO-CM =  $1.13 \pm 0.182$ , 7PA2-CM =  $0.0969 \pm 0.0165$ ), (C) IL-6 mean  $\pm$  std. error: Control =  $154 \pm 4.79$  CHO-CM =  $3320 \pm 607$ , 7PA2 =  $75.2 \pm 5.03$ , (D) TNF- $\alpha$  mean  $\pm$  std. error: Control =  $147 \pm 8.17$  CHO-CM =  $833 \pm 166$ , 7PA2 =  $46.5 \pm 5.92$ .  $n = 3-4$  independent experiments in duplicates.  $p \leq 0.05$  considered significant by one-way ANOVA followed by Sidak's

posthoc multiple comparison's test.

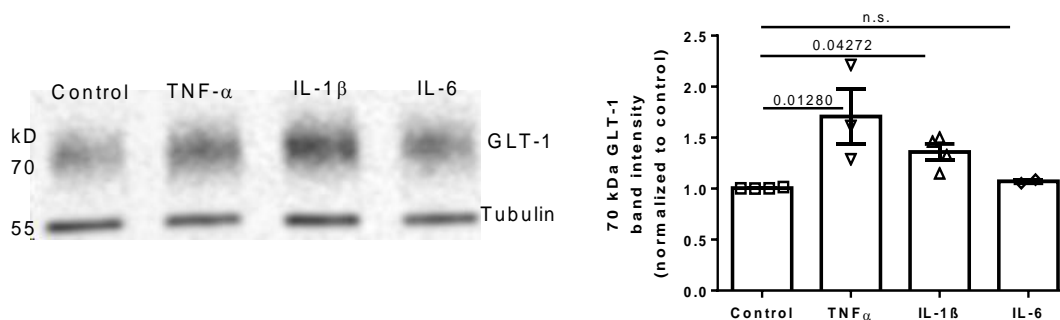


Figure 3-3. 48 hours of 20ng/mL IL-1 $\beta$  or TNF- $\alpha$  increases GLT-1 while IL-6 has no effect. GLT-1 mean  $\pm$  std. error: Control = 1.01  $\pm$  0.00332, IL-1 $\beta$  = 1.36  $\pm$  0.0797; p = 0.0427, TNF- $\alpha$  = 1.71  $\pm$  0.271; p = 0.0128, IL-6 = 1.07  $\pm$  0.0172; p > 0.9999. n = 2-4 independent experiments in duplicates or triplicates. p  $\leq$  0.05 considered significant by one-way ANOVA followed by Dunn's post hoc multiple comparison's test.

### 3.4.2 MicroRNA-181a mediates IL-1 $\beta$ -induced GLT-1 upregulation in astrocytes

We continued to investigate the underlying molecular mechanism by which IL-1 $\beta$  upregulated GLT-1 in the primary co-culture system. MicroRNAs regulate gene expression post-transcriptionally, and several microRNAs have been reported to modulate GLT-1 expression<sup>158,161,213</sup>. Based on these reports and results from Targetscan prediction search, we selected 5 candidate microRNAs (20a, 29a, 107, 124a, and 181a) to screen for IL-1 $\beta$ -induced GLT-1 upregulation. Among these candidate miRNAs, we found 69% reduction in miR-181a after 48 hours of 20 ng/mL IL-1 $\beta$  treatment in primary astrocyte and neuron co-culture compared to the untreated control (**Fig. 3-4A**). The reduction of miR-181a by IL-1 $\beta$  was further confirmed by TaqMan miR181a probes, which indicated 34% reduction (**Fig. 3-4B**).

We then determined whether miR-181a directly suppressed GLT-1 steady state levels *in vitro*. We transfected miR-181a mimics to primary astrocyte and neuron co-culture for 48 hrs and found miR-181a mimics decreased the steady-state levels of GLT-1 by 32% in a concentration-dependent manner compared to the vehicle (**Fig. 3-4C**). We confirmed that cells transfected with 70 nM miR-181a contained higher levels of miR-181a specifically than the control via RT-PCR (Ct<sub>control</sub> = 27 and Ct<sub>70nM Mir-181a</sub> = 20). Accordingly, we co-treated co-culture with 20 ng/mL IL-1 $\beta$  and 70 nM miR-181a mimic for 48 hrs, and miR-181a mimics counteracted with the effect by IL-1 $\beta$  and reduced GLT-1 steady-state levels by 48% compared to 20 ng/mL IL-1 $\beta$  treatment alone (**Fig. 3-4D**). These results show IL-1 $\beta$  as an external source to downregulate miR-181a in cells to increase GLT-1 expression.

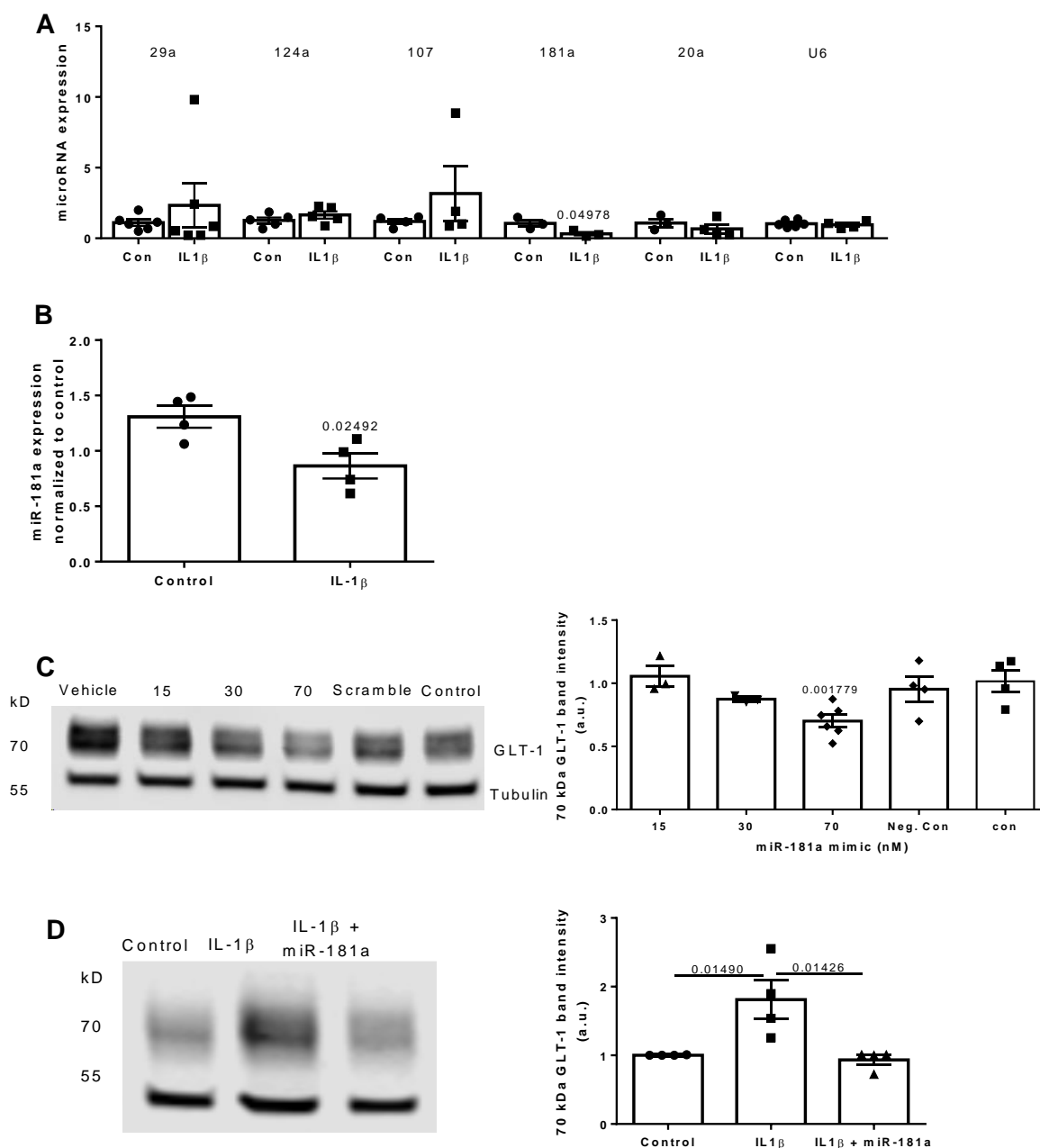


Figure 3-4 miR-181a decreases after 20ng/mL IL-1b expression. 48-hour exposure of 20ng/mL IL-1b on primary astrocyte and neuron co-culture. (A) SYBR® Chemistry for Real-Time PCR using miRNA primers known to regulate GLT-1 or synaptic function. GLT-1 mean  $\pm$  std. error: Control =  $1.05 \pm 0.234$  and IL-1 $\beta$  =  $0.324 \pm 0.117$ ,  $p = 0.0498$ .  $n = 2-3$  independent experiments with 1-3 samples per group.  $p \leq 0.05$  considered significant by unpaired t-test performed for each microRNA between control and IL-1 $\beta$  (presented on a single graph for presentation). (B) TaqMan® Chemistry for Real-Time PCR using miR-181a primer confirms IL-1 $\beta$  downregulates miR-181a; GLT-1 mean  $\pm$  std. error: Control =  $1.31 \pm 0.0980$  and IL-1 $\beta$  =  $0.864 \pm 0.113$ ,  $p = 0.0249$ .  $n = 4$  independent experiments in triplicates.  $p \leq 0.05$  considered significant by unpaired t-test. (C) miR-181a mimic decreases GLT-1 expression in a concentration-dependent manner after 48 hours. GLT-1 mean  $\pm$  std. error: Vehicle =  $1.03 \pm 0.0102$ , Control =  $1.02 \pm 0.0882$ , 15nM =  $1.056 \pm 0.0813$ , 30nM =  $0.875 \pm 0.0149$ , 70nM =  $0.701 \pm 0.0509$  ( $p =$

0.0102), negative control =  $0.953 \pm .0983$ .  $n = 5$  independent experiments with duplicates or triplicates for 3 experiments, 1 exploratory experiment and 1 experiment with vehicle and 70nM miR-181a mimic for confirmation.  $p \leq 0.05$  considered significant by one-way ANOVA followed by Dunn's post hoc multiple comparison's test. (D) Co-treatment of 70nM hsa-miR-181a-5p mimic with 20 ng/mL IL-1 $\beta$  after 48 hours returned GLT-1 steady state levels relatively close to control levels. GLT-1 mean  $\pm$  std. error: Control =  $1.00 \pm 0.00241$ , IL-1 $\beta$  =  $1.81 \pm 0.280$ , IL-1 $\beta$  and miR-181a mimic =  $0.935 \pm 0.0705$ ; Control vs IL-1 $\beta$  ( $p = 0.0149$ ), IL-1 $\beta$  vs IL-1 $\beta$  and 70nM miR-181a mimic ( $p = 0.0143$ ).  $n = 4$  independent experiments in duplicates or triplicates.  $p \leq 0.05$  considered significant by one-way ANOVA followed by Holm-Sidak's post hoc multiple comparison's test. miR-181a mimic = mirVana hsa-miR-181a-5p and scramble = mirVana Negative Control #1 microRNA mimic.

### 3.4.3 Primary and mature miR-181a in human AD brain

The loss of GLT-1 has been observed in post-mortem AD brains<sup>147,149</sup>. To examine whether the loss of GLT-1 in AD was mediated in part by miR-181a, we assessed primary and mature miR-181a expression and GLT-1 steady-state levels in hippocampal tissues from AD patients and age-matched cognitively normal individuals (Table 1 for patient information). We show that GLT-1 steady-state levels were significantly reduced in AD brains by 72% (**Fig. 5A**), consistent with previously reported observations. To correlate the loss of GLT-1 with increased mature miR-181a, we quantitatively measured both mature and primary miR-181a in these tissues. The miR-181 family consists of four mature miRNAs (miR-181a, miR-181b, miR-181c and miR-181d) with miR-181a being transcribed from pri-miR-181a-1 and pri-miR-181a-2 genes<sup>162</sup>. While the mean of mature miR-181a between non-demented individuals and AD was not different (**Fig. 5B**) we found lower levels of pri-miR-181a-1 in AD brains compared to age matched controls by 46% (**Fig. 5C**) but not pri-miR-181a-2 (**Fig. 5D**) suggesting that, overall, less miR-181 transcript is being produced in AD patients. Consequently, the ratio of mature miR-181a over immature form had a trend towards increasing in AD patients compared to controls (**Fig. 5E**).



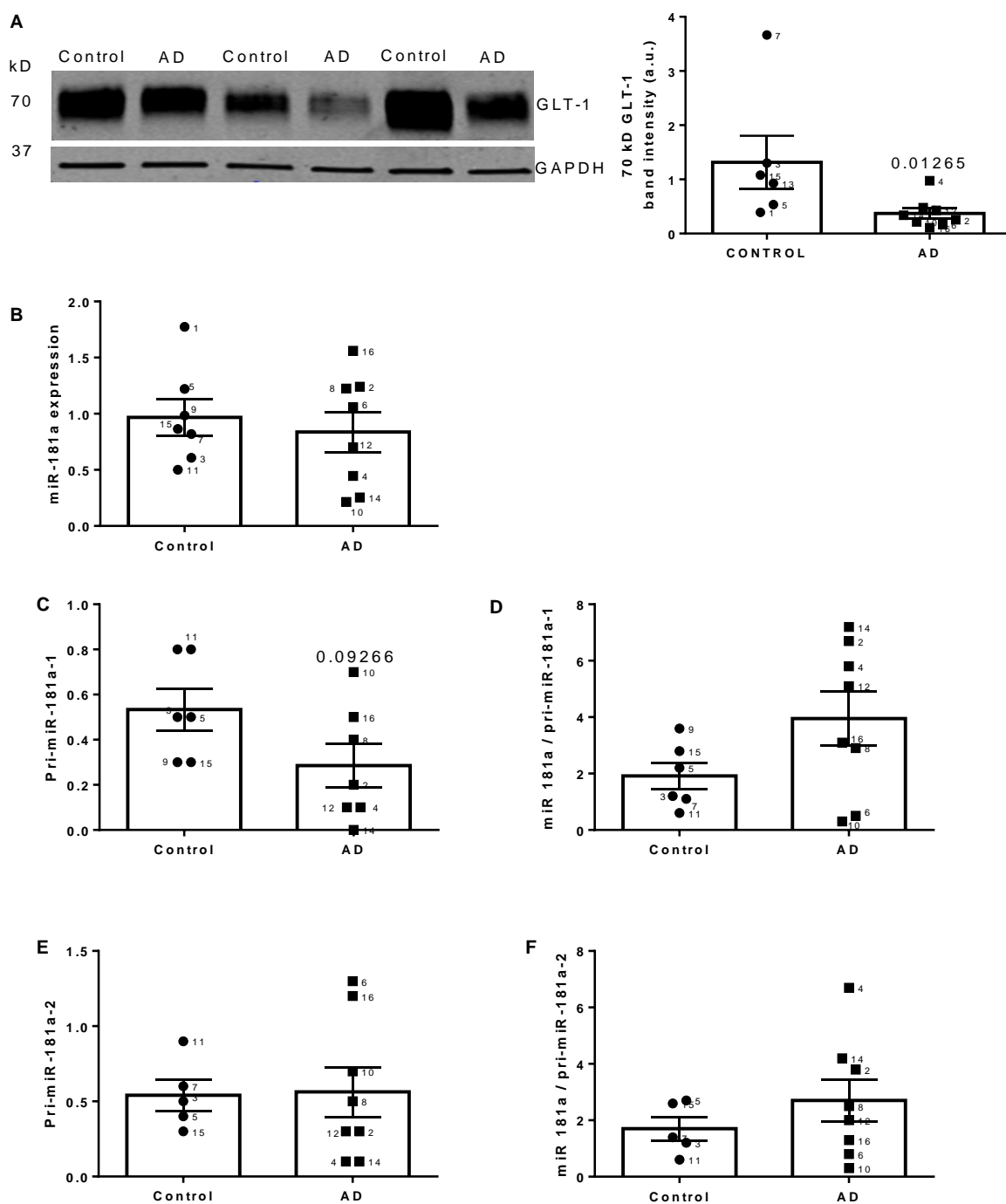


Figure 3-5 GLUT-1 steady state levels and microRNA levels from hippocampal human AD patients compared to age-matched controls. (A) GLUT-1 steady state levels significantly decrease in AD human patients compared to age-matched human controls. GLUT-1 mean  $\pm$  std. mean error: Control =  $1.32 \pm 0.489$  and AD =  $0.370 \pm 0.0975$  ( $p = 0.0127$ ).  $p = 0.0127$ . (B) no significant differences between mature miR-181a levels from AD patients compared to age-matched control. miR-181a mean  $\pm$  std. mean error: Control =  $0.967 \pm 0.162$  and AD =  $0.837 \pm 0.179$  ( $p = 0.7789$ ).

(C) Decrease of immature miR-181a levels in AD compared to age matched control. pri-miR-181a-1 mean  $\pm$  std. mean error: Control =  $0.533 \pm 0.0919$ , AD =  $0.2857 \pm 0.0962$  ( $p = 0.0927$ ) (D) Ratio of mature miR-181a and pri-miR181a-1 is higher in AD compared to age matched control groups. Control =  $1.92 \pm 0.469$ , AD =  $3.95 \pm 0.944$  ( $p = 0.228$ ). (E) no differences in pri-miR-181a-2 levels between AD and age matched controls. pri-miR-181a-2 mean  $\pm$  std. mean error: Control =  $0.540 \pm 0.103$ , AD =  $0.563 \pm 0.166$  ( $p = 0.758$ ) and (F) ratio of miR-181a and pri-miR-181-a-2  $\pm$  std. mean error: Control =  $1.70 \pm 0.410$ , AD =  $2.70 \pm 0.748$  ( $p = 0.622$ ). Each symbol represents 1 human sample with an ID corresponding to the number next to the symbol (ntotal = 5 – 8 samples).  $p \leq 0.05$  considered significant by unpaired t-test. Immature miR-181a corresponds to primary miR-181a.

Table 1. Human samples information

Neuropathology Dx	Mean age	MMSE	Plaque Stage	Tangle Stage
Control	83 – 87	22 – 30	A-C	3-5
AD	80 – 90	10 – 17	A-C	4-6

### 3.5 Discussion

In this study, we report that inflammatory cytokines control GLT-1 translation in astrocytes via miR-181a. Recombinant IL-1 $\beta$  or TNF- $\alpha$ , but not IL-6, showed marked increase of GLT-1 levels in the primary neuron and astrocyte co-culture, and screening of microRNAs identified miR-181a as a regulator of GLT-1 particularly via IL-1 $\beta$ . Application of miR-181a mimics effectively decreased GLT-1 steady-state levels. Lastly, in agreement with previous studies<sup>146,147,149</sup>, GLT-1 levels decreased in the hippocampus from AD patients compared to age-matched non-demented individuals. Furthermore, we found a trend towards increasing ratio of mature miR-181a over primary miR-181 in AD brains when compared to age-matched control brains.

Cytokine-mediated GLT-1 regulation elicits varying effects because of the involvement of various pathways and duration of exposure. In accordance with some of our results, application of recombinant 20 ng/mL TNF- $\alpha$  upregulate the steady-state levels of GLT-1 in primary astrocytes<sup>214</sup>. On the other hand, others have shown that IL-1 $\beta$  or TNF- $\alpha$  decreases GLT-1 mRNA levels acting on pathways through NF- $\kappa$ B<sup>155,156,215</sup>. This dichotomous effect of cytokines on GLT-1 may further be in part owing to the concentration of cytokines<sup>209</sup>, diversity of models (single versus co-cultures)<sup>216</sup>, exposure time<sup>209,216</sup>, serum use<sup>217</sup>, and differential regulation between protein and mRNA. In addition, the binding of IL-1 $\beta$  to the IL-1 receptor 1 (IL-1R1) followed by recruitment of accessory protein subunit expressed on astrocytes can ultimately activate transcription factors including NF- $\kappa$ B<sup>218-220</sup>. NF- $\kappa$ B in turn can bind to multiple binding sites available on the GLT-1 promoter however distinct pathways can repress or activate GLT-1 expression depending on the co-factors present<sup>135,156</sup>. Similarly, TNF- $\alpha$  receptor subtype 2 activation during neuroinflammation can activate either caspases or transcription factors including NF- $\kappa$ B<sup>214</sup>. Further complicating a succinct conclusion among reports but indicating a need to explore other regulatory pathways mediated by cytokines.

The duration of our experimental conditions performed in our *in vitro* studies is acute and not in the chronic state of IL-1 $\beta$  treatment that mimics the disease state commonly observed in AD. In this regard, our experimental condition may represent in part a physiological

state with transient elevation of IL-1 $\beta$  and other local cytokines. Such acute treatment of cytokines, specifically IL-1 $\beta$ , may relay essential signals from local microenvironment to astrocytes to adapt their functions. In the presence of astrocytes, GLT-1 upregulation can be a compensatory mechanism to prevent sustained NMDAR activity indicating a neuron-glia crosstalk. As others have demonstrated that IL-1 $\beta$  increases activity of NMDAR in a manner sufficient to increase neuronal cell death in neuronal cultures<sup>221</sup>. The effect of IL-1 $\beta$  seen in our treatment paradigm on astrocytes and neurons may be to control glutamate levels by modulating astrocytic GLT-1 expression at the synapse.

At the tripartite synapse, we hypothesize that IL-1 $\beta$  can act as a local messenger to both neurons and astrocytes to modulate LTP and synaptic plasticity through GLT-1 expression. While IL-1 $\beta$  has been shown to suppress LTP on primary neuronal cultures and hippocampal slices<sup>125,209,222,223</sup>, other studies show that IL-1 $\beta$  is important and essential for LTP. Specifically, IL-1R1 deficient mice develop memory impairment and/or LTP inhibition<sup>224,225</sup>. This impairment was rescued by introducing wildtype astrocytes in the IL-1R1 deficient mice<sup>226</sup>. In addition, GLT-1 is responsible for glutamate uptake during (late) LTP and pharmacological inhibition of astrocytic GLT-1 activity reduced LTP and prevented induction of additional LTP in hippocampal slices and cell culture experiments<sup>227</sup>, suggesting that GLT-1 plays an important role in synaptic plasticity. MiR-181a is enriched in neurons and astrocytes particularly in the hippocampus and is critically involved in synaptic plasticity and memory processing<sup>162,210,211,228,229</sup>. Mature microRNA is generated from the sequential processing of the primary microRNA in the nucleus to a precursor microRNA in the cytoplasm. Recent growing bodies of evidence strongly implicate spatiotemporal maturation of precursor microRNA to mature miR-181a during low-frequency stimulation, which subsequently down-regulates CAMKII (Sambandan et al., 2017). Other critical synaptic proteins regulated by miR-181a include cFos and SIRT1<sup>210,228</sup>. Thus, at the tripartite synapse, miR-181a appears to negatively modulate plasticity, while inhibition of miR-181a may promote to strengthen synapses and LTP. We speculate that IL-1 $\beta$ -mediated upregulation of GLT-1 via downregulation of miR-181a is part of the mechanisms involved in enhanced LTP and synaptic plasticity. Augmented levels of GLT-1 would be required to deal with the increased activity associated with strengthened synapses and avoid neurotoxicity. Further studies, however, are needed to validate our results under relevant physiological conditions using appropriate *in vivo* models.

In addition to its role in dynamic physiological mechanisms, microRNAs are increasingly recognized as important biomarker for various diseases<sup>230</sup>. In AD, reduction of miR-181a was initially reported in the cerebrospinal fluid compared to the age-matched controls<sup>231</sup>. More recently, as a part of identification of plasma biomarkers for AD, miR-181a appeared as one of the novel microRNAs that are significantly different when compared between control and MCI or early-stage AD, but not established AD<sup>232</sup>, suggesting that miR-181a may be involved in the prodromal or early stages of AD pathogenesis, possibly when synaptic abnormalities are being triggered. We attempted to determine the levels of mature miR-181a in post-mortem AD brains. Although we detected an increasing trend of mature miR-181a ratio in AD, it failed to show statistical significance, possibly because these brains were from relatively advanced stages of AD. Further studies will be needed to

extensively analyze the microRNA profile in brain tissues from MCI and early stages of AD patients.

### 3.6 Conclusion

Insurmountable evidence of GLT-1's importance in maintaining a healthy microenvironment in normal aging brains and the consequences that may result from its dysfunction has led to GLT-1 being a potential target for therapeutic interventions for AD. Our approach simplifies a very complex system but has allowed us to focus on important components that unveil a potential molecular mechanism that affect GLT-1 steady state level expression. Our *in vitro* study is a primary step to unveiling a potential and important molecular mechanism that regulates GLT-1 steady state levels. Further studies are needed to extrapolate our results and apply them in a more complex model. In conclusion, we provide a beneficial role of inflammatory cytokines and suggest that this may be a defense mechanism against a possible neurotoxic environment.

## Chapter 4: Future projects

### 4.1 Abstract

The pharmacological or genetic restoration of GLT-1 by our lab and others markedly ameliorates the development of AD-like neuropathology and rescues cognition in AD mouse models, suggesting that GLT-1 is a molecular link between A $\beta$  and downstream tau pathology. To further determine the molecular action of GLT-1 in AD, we genetically decreased GLT-1 in established AD mouse models that express either A $\beta$  or tau pathology and examine the temporal progression of pathology. We hypothesized that the loss of GLT-1 will accelerate the buildup of A $\beta$  and tau pathology, synaptic loss, and cognitive impairment in these mice. Unexpectedly, mice with heterozygous knock-down of GLT-1 gene and APP or tau transgene significantly lowered survival rate. We managed to run several qualitative assessments on 7 months old mice and showed that haplotype insufficient GLT-1 exhibited an increasing trend of A $\beta$  and tau pathology. Despite the low sample size, the preliminary results suggest a possible increase in pathology due to GLT-1 reduction which encourages our hypothesis and provides preliminary data for future projects.

### 4.2 Introduction

Astrocytes tightly control glutamate homeostasis in glutamatergic synapses by forming tripartite synapses and expressing glutamate transporters<sup>128,131,233</sup>. Among these transporters, the excitatory amino acid transporter 2 (EAAT-2), or its mouse homologue glutamate transporter 1 (GLT-1, herein collectively referred to as GLT-1), is responsible for clearing almost 90% of released glutamate in the synapses, allowing precise pulse of excitatory neurotransmission to the post-synaptic neuron. GLT-1 prevents sustained excitatory signals and excitotoxicity in the post-synaptic neuron<sup>135,140</sup>. A significant reduction of GLT-1 activity has been reported in an early stage of AD as well as mild cognitive impaired (MCI) patients and correlates well with synaptic loss and cognitive decline<sup>146</sup>. In addition, protein levels are significantly reduced in the hippocampus of AD patients<sup>147-149</sup>. Recent studies further support the involvement of GLT-1 in AD by showing that the heterozygous knockdown of GLT-1 in an AD mouse model exacerbates cognitive decline and that astrocytic GLT-1 dysfunction plays an important role in human AD pathogenesis<sup>150,151</sup>. In contrast, GLT-1 restoration in AD mice models ameliorates cognitive decline<sup>126,169</sup>. Thus, the loss of GLT-1 evidently plays an active role in exacerbating downstream AD pathology however consequences of GLT-1 reduction on A $\beta$  pathology is unclear.

Recent evidence suggests that GLT-1 downregulation can result in a generation of aberrant glutamate-induced neuronal excitatory activity that subsequently exacerbates A $\beta$  or tau pathology. Neuronal hyperactivity significantly exacerbates A $\beta$  production<sup>234</sup> in hippocampal slice cultures and in animal models of AD<sup>167</sup> suggesting A $\beta$  can propagate through neuronal activity. Our *in vivo* study has shown pharmacological restoration of GLT-1 ameliorates tau-like pathology in an AD mouse model suggesting GLT-1

dyfunction may contribute to tau pathology<sup>126</sup>. In clinical studies, a pattern of high neuronal activity in MCI patients, the prodromal phase of AD, is detected<sup>164,165,235</sup> suggesting that abnormal hyperactivity of neurons may be an early disease phenomenon and can be triggered by the loss of GLT-1 and subsequent glutamate dyshomeostasis. In cell culture models, we and others found that GLT-1 is downregulated or mislocalized in the presence of (synthetic or naturally secreted) A $\beta$  species<sup>126,168,169</sup>. Consequently, A $\beta$ -induced GLT-1 downregulation can result in glutamate-induced excitotoxicity and neuronal excitability<sup>170,171</sup> further potentiating the spread of A $\beta$  or tau. Thus, we hypothesize that the loss of GLT-1 is an upstream of A $\beta$  and tau propagation and generates a vicious feedback loop to increase the production and secretion of toxic A $\beta$  or tau in the brain. Our previous study used pharmacological restoration of GLT-1 in a mouse model of AD to show the disease modifying effects. In this chapter, we used genetic ablation of GLT-1 in two mouse models and assess the progression of A $\beta$  and tau pathology in the brain.

The loss of GLT-1 was achieved by a conditional knockdown of GLT-1 (NST-GLT1-KD) in the forebrain, originally generated by Dr. Ko-ichi Tanaka, Tokyo Medical and Dental University. This mouse model knocked in the Neomycin resistant cassette-STOP sequence-TetO (NST) within the endogenous GLT-1 promoter region, achieving over 90% of knock-down of GLT-1 in homozygous mouse (K. Tanaka, unpublished observations). We crossed this NST-GLT1-KD mice in C57BL/6 background with J20 APP overexpressing transgenic mouse model of AD (C57BL/6 background) or human wildtype tau overexpressing mouse (htau, C57BL/6 background) from Jackson Laboratories, and created APP or tau overexpressed mice with GLT-1 haplotype deficiency. We observed an increasing trend of A $\beta$  and tau pathology in our double transgenic mice at 7 months of age. In addition, initial analysis of dendritic spine morphology in the stratum radiatum (s.r.) of the CA1 of the hippocampus was not significant however future studies investigating other parts of the hippocampus will confirm if neuronal morphology is altered. These results suggest GLT-1 reduction in part plays a role in A $\beta$  and tau exacerbation.

## 4.3 Methods

### 4.3.1 Animals

All experiments were carried out in accordance with the Institutional Animal Care and Use Committee at the University of California and were consistent with Federal guidelines. All mice were housed on a 12-hour light/dark schedule with ad libitum access to food and water. Mice utilized were commercially available AD transgenic mouse model, J20 and a forebrain specific knock-down of GLT-1 (NST-GLT1-KD, a generous gift from Dr. Ko-ichi Tanaka, Tokyo Medical and Dental University). WT mice are C57BL/6 strains.

To identify the genotype of the animals, we used the polymerase chain reaction on tail samples with their respective primers.

Table 2. Mouse acronym

Acronym	Meaning
C57BL/6J = B6	Background recipient mouse strain name; B6 widely used and characterized.
B6.Cg- Tg(PDGFBAPPSwInd)20Lms/2Mmjax Also known as “J20”	. = Backcrossed to recipient inbred strain for more than 5 generations Cg = Donor strain Tg = Transgenic PDGFB = human platelet derived growth factor, B polypeptide promoter APPSwInd = mutant human amyloid protein precursor APPSwInd, which bears both the Swedish (K670N/M671L) and the Indiana (V717F) mutations 20 = Founder line Lms = creator lab code (Lennart Mucke <sup>190</sup> ) 2Mmjax = Holding site lab code
B6.Cg- Mapt <sup>tm1(EGFP)Klt</sup> Tg(MAPT)8cPdav/J Also known as “hTau”	Mapt = microtubule associated protein tau, homolog in mouse Tm = targeted mutation 1 = allele# EGFP = mutant allele Klt = creator lab code MAPT = microtubule associated protein tau, human (transgenic) 8c = Founder line Pdav = Creator lab code /J = holding site code
APPsw/ind(Tg/0). Also known as “J20”	Overexpresses human APP with two familial AD mutations – the Swedish (APP KM670/671NL) and Indiana (APP V717F) <sup>190</sup> . The Swedish mutation is located next to the $\beta$ -secretase site in APP consequently increasing total A $\beta$ levels; Swedish mutation increases overall A $\beta$ production <sup>49,52,236</sup> . Indiana mutation consequently increases A $\beta$ <sub>42</sub> /A $\beta$ <sub>40</sub> ratio thus increasing A $\beta$ 's propensity to aggregate <sup>53,54</sup> .
hTau	Overexpression of human tau; hemizygous for the transgene express all six isoforms (including both 3R and 4R forms) of human MAPT. Hyperphosphorylated tau in soma and dendrites <sup>237</sup> .

NST-GLT1-KD	Knocked in the Neomycin resistant cassette-STOP sequence-TetO (NST) within the endogenous GLT-1 promoter region, achieving over 90% of knock-down of GLT-1 in homozygous mouse (K. Tanaka, unpublished observations).
-------------	---

#### 4.3.2 Immunostaining

Each half brain was cut into 40  $\mu\text{m}$  slices using a microtome and stored in PBS with 0.05% sodium azide. Free-floating sections were washed with TBS, permeablized with 0.1% triton X-100 and blocked with 3% BSA in TBS. For A $\beta$  plaque burden, free-floating sections were pre-treated with 90% formic acid for 3 minutes prior to the incubation with primary antibodies. Sections were then incubated with antibodies against 82E1 (1:200). Sections were washed the following day and incubated with 3% BSA and 1% triton X-100 in TBS then 1 hr incubation with corresponding secondary antibody conjugated with Alexa Fluor 488, Alexa Fluor 555 and/or Alexa Fluor 633 with DAPI for nuclear staining.

#### 4.3.3 Thioflavin S staining

Thioflavin S For immunofluorescent staining with thioflavin S (Sigma, St. Louis, MO), free-floating sections were mounted on a Superfrost Plus™ microscope slide (Fisher Scientific, Waltham, MA) to dry overnight. To hydrate, fixed sections were immersed twice in 100% ethanol for 2 minutes, twice in 95% ethanol for 2 minutes, once in 70% ethanol for two minutes then once in 50% ethanol for two minutes. Sections were then incubated with 0.5% thioflavin S in 50% ethanol for 10 minutes (in the dark). Sections were washed twice with 50% ethanol for 3 minutes and twice with water for 3 minutes. Staining was visualized using a digital inverted microscope (EVOS-*fl*, Advanced Microscopy Group).

#### 4.3.4 Golgi Staining

For Golgi staining, mice were perfused transcardially with 0.1 M phosphate-buffered saline (pH 7.4) and brains were processed using superGolgi Kit (Bioenno Tech LLC, Santa Ana, CA, USA). According to the manufacturer's and collaborators protocol, brains were incubated for 11 days in impregnation solutions, followed by 2 days incubation in post-impregnation solution. Once impregnation of neurons was complete, thick (150  $\mu\text{m}$ ) free-floating sections were obtained using a HA752 vibratome (Campden Instruments Ltd, Lafayette, IN, USA) and serially collected in a mounting buffer (provided by the kit). Sections mounted on coated slides were stained and post-stained, respectively for 20 minutes, dehydrated in graded ethanol, cleared with xylene and coverslipped with dibutylphthalate polystyrene xylene (DPX) mounting medium<sup>238</sup>.



NeuronStudio software (NeuronStudio Documentation © CNIC, Mount Sinai School of Medicine, New York, NY) was utilized to examine the dendritic spine in the CA1 of the hippocampus. Thus, stereological quantifications were performed using Stereo-Investigator software from Microbrightfield Bioscience (MBF Bioscience, Williston, VT, USA) to determine the number of spines in the CA1 region of the hippocampus. CA1 of the hippocampus was defined using a 5× objective and spines were counted using a 100x/1.4 objective. NeuronStudio software was utilized to determine the number of spines per dendritic length. Briefly, 10–13 images stacks were collected from J20, WT, J20/GLT-1KD and GLT-1KD. The images were collected, using 100x/1.4 oil objective from a Zeiss AxioImager M2 microscope (Zeiss, Thornwood, NY, USA). Next, images were modified to greyscale with 8 bit-depth using Image J (NIH, Bethesda, MD) 1.36b software. Then, NeuronStudio software was used to perform unbiased and automatic spines quantification per dendritic length<sup>238</sup>.

#### 4.3.5 Statistics

Based on the normal distribution of t-test power analysis, with the standard deviation of 25%, power = 0.9 and  $\alpha$  error = 0.05, at least 10 mice per group will provide statistical significance for this study. We applied unpaired t-test when comparing two groups or ANOVA with post hoc test when comparing more than two groups. Due to the low numbers, no statistical significance was detected. Graphs are shown as the mean for each group  $\pm$  standard error mean.

### 4.4 Results

#### 4.4.1 Breeding scheme to generate GLT-1 knockdown with A $\beta$ or tau pathology.

We maintained 2-3 breeding pairs to obtain double transgenic mice expressing either A $\beta$  pathology with GLT-1 knockdown or tau pathology with GLT-1 knockdown. The breeding scheme to generate the desired double transgenic mice are depicted in **Fig. 4-2** and **4-3**. Of the 73 total pups, only 7 were GLT-1 knockdown in APP overexpression ((NST-GLT-1+/-, APP<sup>sw/ind</sup>(Tg/0)). From the 7, only 5 survived to 7 months of age – 9.6% was markedly lower than expected Mendelian inheritance. Litter size was generally less than 5 pups and foster mothers were used for poor breeders. Although GLT-1 heterozygous knockdown has been shown to appear phenotypically normal<sup>140</sup>, the overexpression of A $\beta$  or tau with GLT-1 knockdown showed high mortality. Thus, the pups produced were like those reported with GLT-1 homozygous knockout<sup>140</sup> suggesting glutamate excitotoxicity may play a role with the high mortality rate.

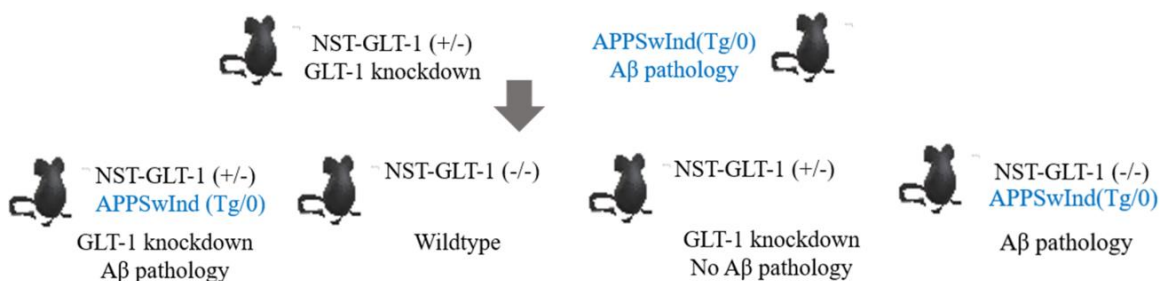


**Figure 4-1 Aβ and GLT-1 knockdown breeding scheme.** Double transgenic mice were born from heterozygous crosses at the frequency predicted by Mendelian ratios. Expected 25% heterozygous GLT-1 knockdown and hemizygous Aβ, 25% wild type, 25% GLT-1 knockdown and 25% hemizygous Aβ. Tg/0 = hemizygous for the mutated APP transgene; 0 = no transgene.

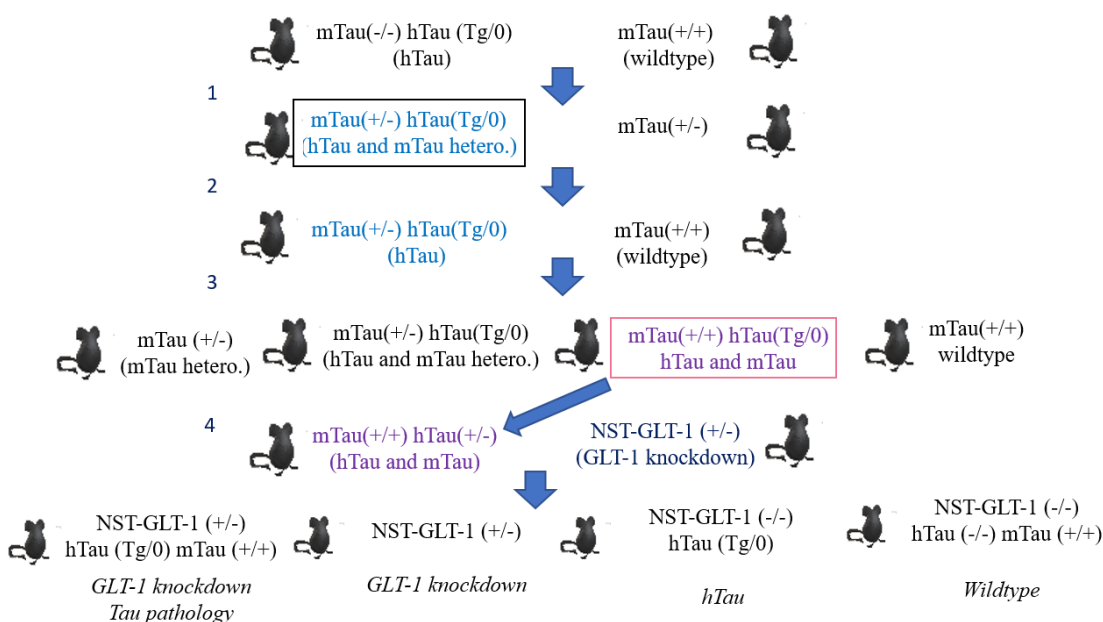


**Figure 4-2 Tau pathology and GLT-1 knockdown breeding scheme;** Double transgenic mice were born from heterozygous crosses at the frequency predicted by Mendelian ratios. Expected 25% heterozygous GLT-1 knockdown and hemizygous human tau, 25% wild type, 25% GLT-1 knockdown and 25% hemizygous human tau. Tg/0 = hemizygous for the mutated APP transgene; 0 = no transgene.

#### 4.4.2 Pathological analyses of NST-GLT-1(+/-)/APPswind(Tg/0) mice

We qualitatively assessed Aβ pathology through immunostaining of the cortex and hippocampus. We observed the presence of amyloid fibrils and Aβ specific plaques using Thioflavin S and 82E1 antibody respectively at 7 months of age. Thioflavin S binds to amyloid fibrils and gives a distinct fluorescence emission. We found an increasing trend of Aβ plaque pathology in the double transgenic based in our analysis. These results suggest that GLT-1 knockdown may increase Aβ however the limited number of mice prevents us from making a definitive conclusion.

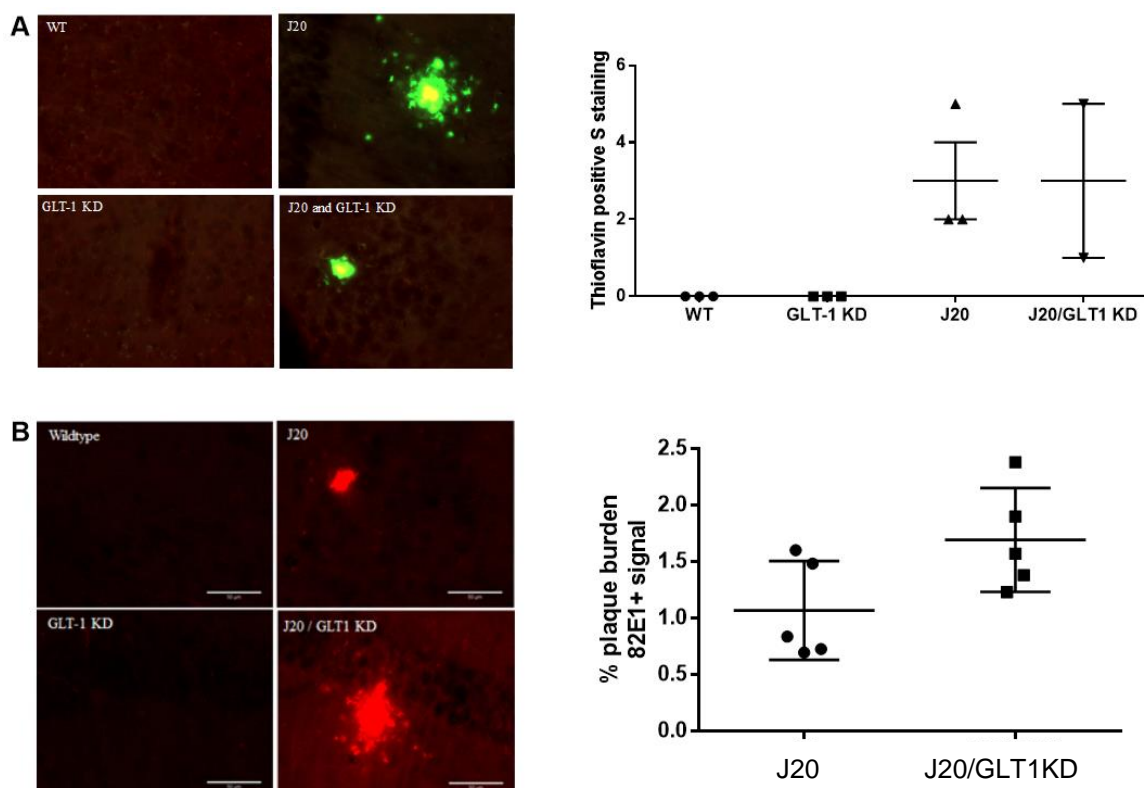


**Figure 4-3** Effect of *GLT-1* knock down on  $A\beta$  pathology in double transgenic mice. Qualitative representation of the immunostaining with (A) Thioflavin S (green) and (b) 82E1 antibody (red) to detect  $A\beta$  plaques in the cortex and hippocampus.  $n = 4-5$  mice per group; blind experiment to detect plaques. *GLT1KD* = *NST-GLT-1(+/-)* and *J20* = *APPsweind(Tg/0)*

The density of dendritic spines in the stratum radiatum (s.r.) area of the CA1 pyramidal cells were investigated in the current study. We started with the s.r. region because it is one of the initial positions in the hippocampus affected in AD<sup>239</sup>. Dendritic spines are protrusions from neuronal dendrites that represent the post-synaptic compartment; these spines receive synaptic input from an axon at the synapse<sup>240</sup>. We identified the dendritic spines based on anatomical studies of fixed brain tissues that report shapes as thin, stubby, mushroom, filopodia and branched<sup>241-243</sup>. We found no significant differences in the total dendritic spine density between our single and double transgenic animals in the s.r. of the CA1 in the hippocampus.

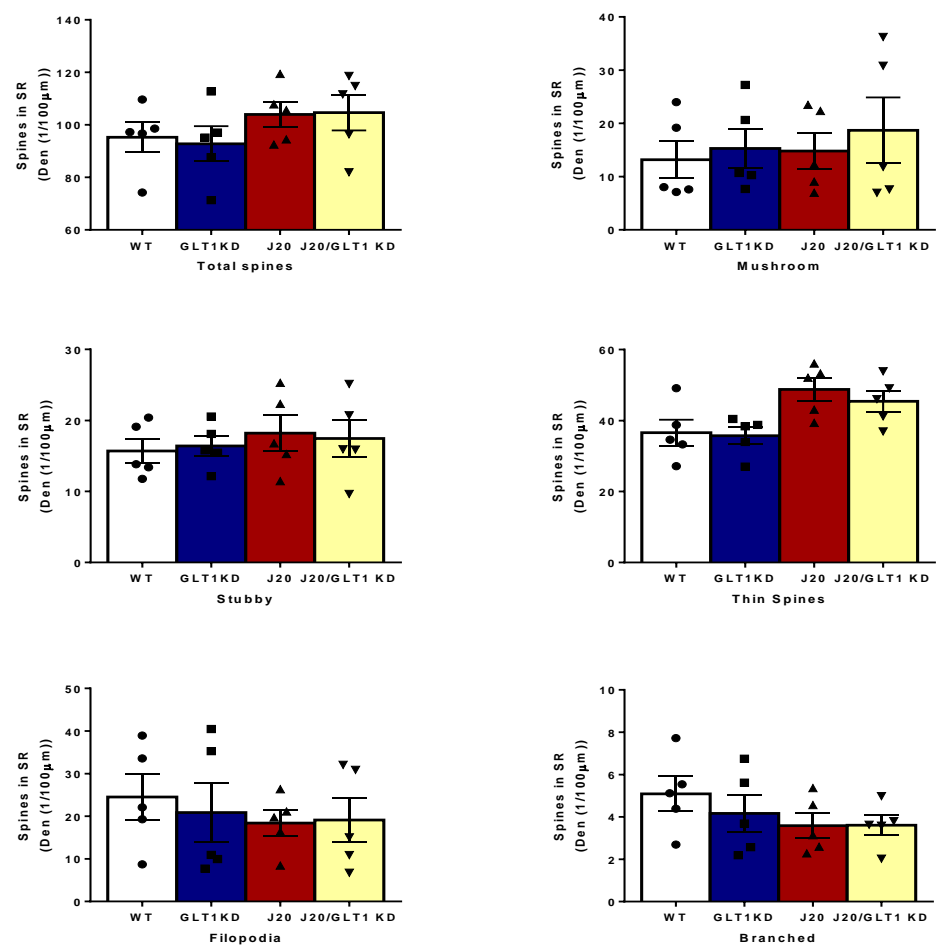
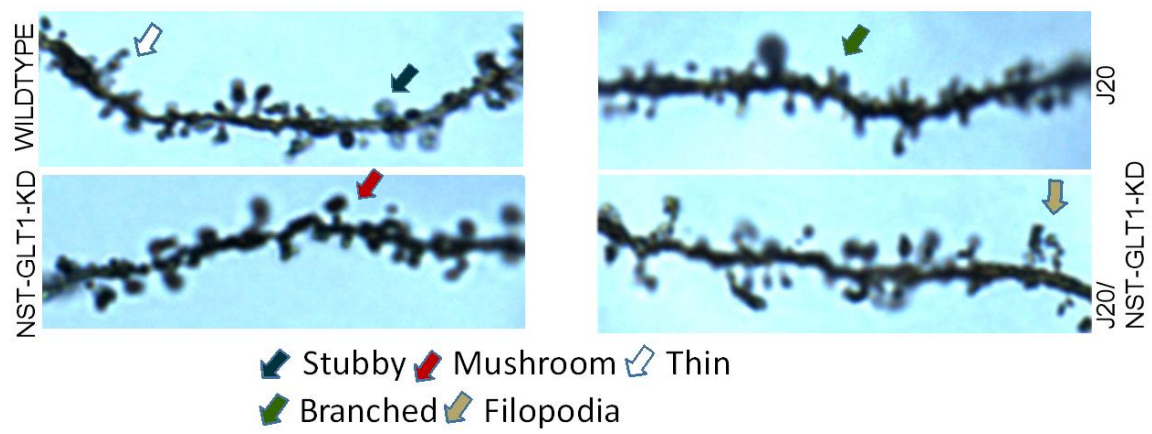


Figure 4-4 Spine densities (spines/100µm) in stratum radiatum area of CA1. (A) Light microscopy images of dendritic spines on pyramidal cells in CA1 subfield of in wildtype, GLT-1 knockdown, J20 and GLT-1 knockdown with Aβ mice at 6-7 months of age. (B) Quantification of spine density

(spines/ $\mu\text{m}$ ) based on types of spines (including mushroom, thin and stubby). The framed area is 100x. sr = stratum radiatum. GLT1KD = NST-GLT-1(+/-) and J20 = APP<sup>sweind</sup>(Tg/0)

#### 4.4.3 Tau pathology in NST-GLT-1(+/-)/htau(Tg/0)

We assessed tau pathology through immunohistochemical staining using phospho-specific tau antibodies. Our results indicated very low tau-positive staining in all areas of the hippocampus and in all groups at 7 months of age which suggests age of assessment may be too early in age. Detection of tau was only limited to certain areas of the hippocampus. Specifically, we found an increasing trend in tau pathology using the PHF-1 specific antibody in the dentate gyrus.

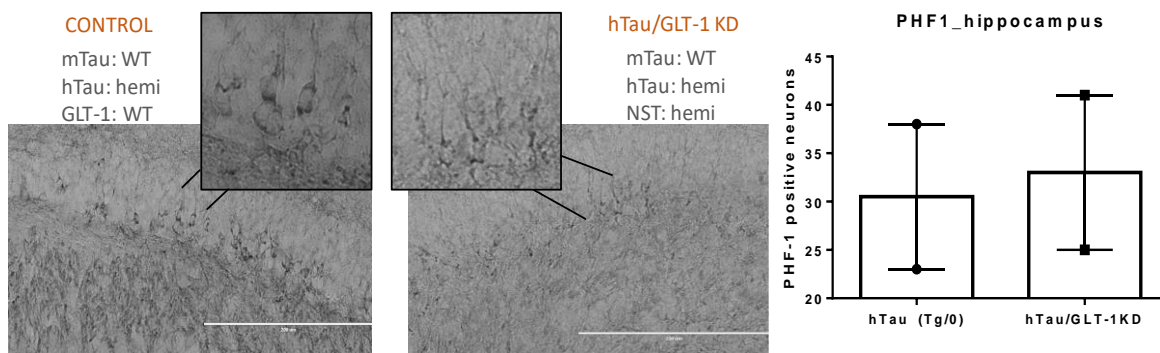


Figure 4-5 Tau pathology preliminary assessment using PHF-1 antibody found in the dentate gyrus. Phosphorylation at serine 396 and 404<sup>237</sup>.  $n = 2$  mice per group (indicated by symbol). GLT-1KD = NST-GLT-1(+/-) Scale bar: 200 $\mu\text{m}$ .

## 4.5 Discussion

The purpose of this study is to validate the mechanism of GLT-1 dysfunction regarding A $\beta$  and tau pathology. Independent generation of A $\beta$  or tau with GLT-1 knockdown eliminated potential interactions between A $\beta$  and tau that may cover the effect of GLT-1 on these pathologies. In this study, we provide preliminary observations of the double transgenic mice expressing A $\beta$  or tau with GLT-1 knockdown. We find an increasing trend of A $\beta$  and tau pathology. Further studies however are needed to confirm our hypothesis but our preliminary results are encouraging in this direction.

GLT-1 reduction can exacerbate A $\beta$  pathology through aberrant neuronal activity. Currently, the pathological buildup of A $\beta$  in the brain is thought to be mediated by increased production and aggregation of A $\beta$  species and/or impaired clearance of A $\beta$  from brain parenchyma. The former mechanism is particularly true in early-onset familial AD cases as all known disease-causing mutations promote increased A $\beta$  production or aggregation<sup>13,49,52</sup>. In late-onset sporadic AD cases, certain known risk factors, such as history of traumatic brain injuries, are found to increase the APP expression, hence A $\beta$  production may be enhanced. However, a recent *in vitro* study concluded that the APP

processing was virtually unaltered when AD susceptible genes, which were identified by the genome-wide association studies, were knocked-out<sup>244</sup>. In addition, examining patients' cerebral spinal fluid confirmed a significant reduction of A $\beta$  clearance in AD<sup>95</sup>. Interestingly, increased neuronal activity could also facilitate the secretion and deposition of A $\beta$ . When channel rhodopsin was expressed in cortical projection neurons in the lateral entorhinal cortex that are projecting to dentate gyrus through the perforant pathway, repeated light stimulation caused a long-lasting neuronal activity in these neurons. This resulted in an increased (~24%) A $\beta$  deposition in its presynaptic projection area<sup>167</sup>, suggesting activity-dependent buildup of A $\beta$ . This finding is particularly exciting as hyperexcitability of neurons, seizures, and latent epileptic activity are reported in early AD or MCI patients<sup>164,245</sup>. These clinical signs may further foster AD neuropathology. Thus, we hypothesized that the increase of glutamatergic input due to the loss of GLT-1 would exacerbate A $\beta$  pathology. We observed an increasing trend of A $\beta$  plaques in mice with GLT-1 knockdown, however, more studies are required to draw a solid conclusion. In addition, we need to evaluate any potential selection bias of these mice due to the high mortality of the target transgenic mice.

Glial dysfunction can result in cognitive loss associated with AD. Mookherjee and colleagues demonstrated that partial loss of GLT-1 resulted in cognitive spatial deficits in young AD mouse model exhibiting A $\beta$  pathology<sup>150</sup>. In the same study, they show that cognitive deficits were not associated with changes in overall APP expression or processing as indicated from their western blots utilizing 22C11 (APP N-terminal ectodomain), 6E10 (human specific A $\beta$  domain) and C-term (intracellular APP C-terminal domain) but rather by the loss of GLT-1. Other glutamate transporters expressed on astrocytes (GLAST) and neurons (EAAC1) were not changed further implicating GLT-1 loss specifically expressed on astrocytes as the primary culprit. These results support our pharmacological approach that GLT-1 restoration restored cognitive decline in 3xTg-AD<sup>126</sup>. Furthermore, their study showed that insoluble A $\beta_{42/40}$  ratio increased because of GLT-1 loss supporting our results that neuronal activity caused by GLT-1 downregulation can exacerbate A $\beta$  pathology.

GLT-1 reduction can exacerbate tau propagation through aberrant neuronal activity. Human autopsy observations note that NFTs appear in the entorhinal cortex (EC) then the hippocampus and spread to the limbic and association cortices<sup>33</sup> suggesting a synaptically connected pattern of tau pathology. In animal models, propagation of tau through synaptically connected neurons was reported using mouse models overexpressing human tau (P301L) under the control of a EC specific promoter showing that hyperphosphorylated tau can be present from the EC to neighboring neurons then to the hippocampal neurons (not expressing the transgene) or extend to the neocortex in an age dependent manner<sup>118,246</sup>. The exact mechanism by which tau can propagate through synapses is unknown. It's been suggested that tau can be internalized by endocytosis and transported through neurons in anterograde or retrograde manner<sup>247</sup>. Furthermore, models show stimulating action potentials in channel rhodopsin expressing neuronal cells by blue light for 30 minutes increased tau levels in the media and later in neighboring cells indicating neuronal activity can induce tau release and propagation *in vitro*<sup>248</sup>. From these

studies, we hypothesized that mice with GLT-1 haplotype insufficiency would exacerbate tau pathology. We found an increasing trend of tau pathology in mice with GLT-1 haplotype insufficiency however more studies are required to draw a solid conclusion.

The double transgenic mice expressing A $\beta$  or tau with GLT-1 knockdown was obtained by crossing commercially available transgenic mice with knock in mice provided by our collaborators. Thus, the breeding pairs of our mice consisted of the very well established, characterized and utilized J20, hTau and GLT1-NST-KD mice. It is important to note that generation of the double transgenic mice is a slow process because of the small litter size and high mortality rate. Despite of this, our strategy was straightforward and encompassed the necessary phenotypes to test our hypothesis.

#### 4.6 Conclusion

We hypothesized that GLT-1 expression will exacerbate AD-like pathology in AD mouse models. Our major findings indicate that GLT-1 reduction shows an increasing trend of A $\beta$  and tau pathology. However, the above results remain inconclusive as there were not enough pups to compare pathologies. Though the models explored here are at a preliminary stage, they encourage a new line of inquiry that will help future studies to determine whether the loss of GLT-1 in astrocytes is the key factor to trigger and exacerbate tau pathology and cognitive decline *in vivo*.

## Chapter 5: Conclusion

The excitatory amino acid transporter 2, or its mouse homologue glutamate transporter 1 (GLT-1), is a major glutamate transporter primarily expressed on astrocytes and plays an essential role in maintaining the glutamate homeostasis in the synaptic cleft. The levels and activity of GLT-1 have been shown to be significantly decreased in AD brains. Its loss is evident even in early or prodromal stages of AD and correlates well with cognitive impairment. It remains unclear, however, whether the loss of the glutamate transporter directly contributes to the pathological buildup of amyloid  $\beta$  ( $A\beta$ ) and neurofibrillary tau tangles (NFTs) - two key pathological hallmarks of AD. The established amyloid cascade hypothesis posits  $A\beta$ , in oligomeric form, as the initiator of AD. Along with this, glutamate excitotoxicity is one of the potential mechanisms hypothesized to result in synapse and neuronal loss. Since the glutamate transporter is the major regulator of glutamate at the synapse, its loss compromises the surrounding cellular environment. Thus, I hypothesized that an  $A\beta$ -induced GLT-1 decrease leads to downstream AD pathology including synapse loss, tau pathology and cognitive decline.

To test my hypothesis, we first determine the temporal change of GLT-1 in the 3xTg-AD mouse model, a well-established and widely used AD mouse model with plaques and tangles. GLT-1 was significantly downregulated as 3xTg-AD mouse aged, recapitulating the phenomenon occurring in AD brains. However, this finding alone did not support the role of GLT-1 in AD neuropathology. Thus, we restored GLT-1 in 3xTg-AD mice with ceftriaxone, a  $\beta$ -lactam antibiotic that has been well documented to upregulate GLT-1 in rodent models<sup>126,179,201,249</sup>. Chronic treatment with ceftriaxone 1) ameliorated cognitive deficits as seen from the Morris Water maze test, 2) preserved synaptic proteins as seen from quantitative analysis of immunostaining with synaptophysin and post-synaptic density protein, and 3) decreased phosphor-specific tau proteins representing AD-like pathology in the 3xTgAD mouse model. There were no significant differences in  $A\beta$  pathology which suggested  $A\beta$  may be upstream of GLT-1 dysfunction. Interestingly, another group reported that the pharmacological and genetic restoration of GLT-1 in another transgenic mouse model of AD rescued cognition and  $A\beta$  pathology<sup>169</sup>. While this particular mouse model does not develop tau pathology, it would be important to examine any alterations of phosphorylation state of tau as even mouse endogenous tau could contribute to the cognition and dysfunction of neuronal activity<sup>250</sup>. Collectively, these findings strongly support the link between the loss of GLT-1 and AD neuropathology and cognitive decline. The exact mechanism, however, by which GLT-1 is down-regulated in AD remains to be determined.

To determine the underlying molecular and cellular mechanisms of GLT-1 regulation during the disease course, we performed a series of *in vitro* experiments. We identified  $A\beta$  species to decrease GLT-1 expression while several inflammatory cytokines surprisingly upregulated GLT-1 in primary murine astrocyte and neuronal co-cultures.  $A\beta$ -induced GLT-1 downregulation support our hypothesis and results from the *in vivo* model. However, cytokine-mediated upregulation of GLT-1 was initially puzzling since pro-



inflammatory cytokines are implicated to play pivotal roles in the neuropathological hallmarks of AD<sup>101</sup>. These discrepancies however may be due to chronic and acute exposure of pro-inflammatory cytokines that can be a consequence or a benefit to cells. Our co-culture exhibits acute exposure compared to the chronic exposure seen in AD.

IL-1 $\beta$  may play a role in neuroprotection via microRNA-181a. This idea stems from Chapter 3 that shows IL-1 $\beta$  upregulates GLT-1 steady state levels post-transcriptionally via downregulation of microRNA-181a. microRNA-181a is enriched in astrocytes<sup>162,229</sup> and decreased in microRNA-181a increases astrocyte survival<sup>251</sup> thus explained why IL-1 $\beta$  decreases miR-181a to increase GLT-1. Whether IL-1 $\beta$  directly acts on miR-181a remains to be elucidated.

In conclusion, this dissertation provides compelling evidence that GLT-1 is a key player in AD pathogenesis but further clinical or *in vivo* studies are needed to confirm our results. We show that GLT-1 steady state levels decrease in human hippocampal samples from AD patients and their age-matched controls (Chapter 3). These findings support our *in vivo* findings (Chapter 2) that show GLT-1 decrease in an AD mouse model. Furthermore, we quantitatively assess changes in pathology to show the importance of GLT-1 in AD (Chapter 2 and 4). Thus, GLT-1 restoration may be an effective therapeutic strategy for AD.

## References

- 1 Kenneth D. Kochanek, S. L. M., Jiaquan Xu, and Betzaida Tejada-Vera. Deaths: Final Data for 2014. *National Vital Statistics Reports* **65**, 71 (2016).
- 2 Control, C. f. D. & Statistics, N. C. f. H. (2015).
- 3 Hebert, L. E., Weuve, J., Scherr, P. A. & Evans, D. A. Alzheimer disease in the United States (2010–2050) estimated using the 2010 census. *Neurology* **80**, 1778-1783, doi:10.1212/WNL.0b013e31828726f5 (2013).
- 4 Hurd , M. D., Martorell , P., Delavande , A., Mullen , K. J. & Langa , K. M. Monetary Costs of Dementia in the United States. *New England Journal of Medicine* **368**, 1326-1334, doi:10.1056/NEJMsa1204629 (2013).
- 5 Association, A. s. 2017 Alzheimer's disease facts and figures. *Alzheimer's & Dementia* (2017).
- 6 Hampel, H. *et al.* Biological markers of amyloid  $\beta$ -related mechanisms in Alzheimer's disease. *Experimental neurology* **223**, 334-346, doi:10.1016/j.expneurol.2009.09.024 (2010).
- 7 Association, A. s. (2016).
- 8 Selkoe, D. J. & Hardy, J. The amyloid hypothesis of Alzheimer's disease at 25 years. *EMBO Molecular Medicine* **8**, 595-608, doi:10.15252/emmm.201606210 (2016).
- 9 Doody, R. S. *et al.* Phase 3 Trials of Solanezumab for Mild-to-Moderate Alzheimer's Disease. *New England Journal of Medicine* **370**, 311-321, doi:10.1056/NEJMoa1312889 (2014).
- 10 Doody, R. S. *et al.* A Phase 3 Trial of Semagacestat for Treatment of Alzheimer's Disease. *New England Journal of Medicine* **369**, 341-350, doi:10.1056/NEJMoa1210951 (2013).
- 11 Coric, V. *et al.* Safety and tolerability of the  $\gamma$ -secretase inhibitor avagacestat in a phase 2 study of mild to moderate Alzheimer disease. *Archives of Neurology* **69**, 1430-1440 (2012).
- 12 Martorana, A., Esposito, Z. & Koch, G. Beyond the cholinergic hypothesis: do current drugs work in Alzheimer's disease? *CNS neuroscience & therapeutics* **16**, 235-245 (2010).
- 13 Tanzi, R. E. The Genetics of Alzheimer Disease. *Cold Spring Harbor Perspectives in Medicine* **2**, a006296, doi:10.1101/cshperspect.a006296 (2012).
- 14 Folstein, M. F., Folstein, S. E. & McHugh, P. R. "Mini-mental state": a practical method for grading the cognitive state of patients for the clinician. *Journal of psychiatric research* **12**, 189-198 (1975).
- 15 Webster, S. J., Bachstetter, A. D., Nelson, P. T., Schmitt, F. A. & Van Eldik, L. J. Using mice to model Alzheimer's dementia: an overview of the clinical disease and the preclinical behavioral changes in 10 mouse models. *Frontiers in Genetics* **5**, 88, doi:10.3389/fgene.2014.00088 (2014).

- 16 Albert, M. S. *et al.* The diagnosis of mild cognitive impairment due to Alzheimer's disease: Recommendations from the National Institute on Aging-Alzheimer's Association workgroups on diagnostic guidelines for Alzheimer's disease. *Alzheimer's & dementia* **7**, 270-279 (2011).
- 17 Miller-Thomas, M. M. *et al.* Multimodality Review of Amyloid-related Diseases of the Central Nervous System. *RadioGraphics* **36**, 1147-1163, doi:10.1148/rg.2016150172 (2016).
- 18 Clifford R. Jack, J. Alzheimer Disease: New Concepts on Its Neurobiology and the Clinical Role Imaging Will Play. *Radiology* **263**, 344-361, doi:10.1148/radiol.12110433 (2012).
- 19 Mosconi, L. & McHugh, P. F. FDG- and amyloid-PET in Alzheimer's disease: is the whole greater than the sum of the parts? *The Quarterly Journal of Nuclear Medicine and Molecular Imaging* **55**, 250-264 (2011).
- 20 Bobinski, M. *et al.* The histological validation of post mortem magnetic resonance imaging-determined hippocampal volume in Alzheimer's disease. *Neuroscience* **95**, 721-725 (1999).
- 21 Fagan, A. M. *et al.* Inverse relation between in vivo amyloid imaging load and cerebrospinal fluid A $\beta$ 42 in humans. *Annals of neurology* **59**, 512-519 (2006).
- 22 DeKosky, S. T. & Scheff, S. W. Synapse loss in frontal cortex biopsies in Alzheimer's disease: Correlation with cognitive severity. *Annals of Neurology* **27**, 457-464, doi:10.1002/ana.410270502 (1990).
- 23 Scheff, S. W., DeKosky, S. T. & Price, D. A. Quantitative assessment of cortical synaptic density in Alzheimer's disease. *Neurobiology of aging* **11**, 29-37 (1990).
- 24 Scheff, S. W. & Price, D. A. Synapse loss in the temporal lobe in Alzheimer's disease. *Annals of neurology* **33**, 190-199 (1993).
- 25 Masliah, E. *et al.* Synaptic and neuritic alterations during the progression of Alzheimer's disease. *Neuroscience letters* **174**, 67-72, doi:[https://doi.org/10.1016/0304-3940\(94\)90121-X](https://doi.org/10.1016/0304-3940(94)90121-X) (1994).
- 26 Samuel, W., Masliah, E., Hill, L. R., Butters, N. & Terry, R. Hippocampal connectivity and Alzheimer's dementia: Effects of synapse loss and tangle frequency in a two-component model. *Neurology* **44**, 2081, doi:10.1212/wnl.44.11.2081 (1994).
- 27 Scheff, S. W., Price, D. A., Schmitt, F. A. & Mufson, E. J. Hippocampal synaptic loss in early Alzheimer's disease and mild cognitive impairment. *Neurobiology of aging* **27**, 1372-1384 (2006).
- 28 Goto, S. & Hirano, A. Neuronal inputs to hippocampal formation in Alzheimer's disease and in parkinsonism-dementia complex on Guam. *Acta neuropathologica* **79**, 545-550 (1990).
- 29 Hyman, B., Van Hoesen, G., Kromer, L. & Damasio, A. Perforant pathway changes and the memory impairment of Alzheimer's disease. *Annals of neurology* **20**, 472-481 (1986).
- 30 Sze, C.-I. *et al.* Loss of the presynaptic vesicle protein synaptophysin in hippocampus correlates with cognitive decline in Alzheimer disease. *Journal of Neuropathology & Experimental Neurology* **56**, 933-944 (1997).

- 31 Terry, R. D. *et al.* Physical basis of cognitive alterations in Alzheimer's disease: synapse loss is the major correlate of cognitive impairment. *Annals of neurology* **30**, 572-580 (1991).
- 32 Selkoe, D. J. Alzheimer's disease is a synaptic failure. *Science* **298**, 789-791 (2002).
- 33 Braak, H. & Braak, E. Staging of alzheimer's disease-related neurofibrillary changes. *Neurobiology of aging* **16**, 271-278, doi:[https://doi.org/10.1016/0197-4580\(95\)00021-6](https://doi.org/10.1016/0197-4580(95)00021-6) (1995).
- 34 Braak, H. & Braak, E. Neuropathological staging of Alzheimer-related changes. *Acta Neuropathol* **82**, doi:10.1007/bf00308809 (1991).
- 35 Vijg, J. & Hasty, P. in *Handbook of Models for Human Aging* 601-618 (Academic Press, 2006).
- 36 St George-Hyslop, P. *et al.* The genetic defect causing familial Alzheimer's disease maps on chromosome 21. *Science* **235**, 885-890, doi:10.1126/science.2880399 (1987).
- 37 Kitazawa, M. *et al.* Blocking Interleukin-1 Signaling Rescues Cognition, Attenuates Tau Pathology, and Restores Neuronal  $\beta$ -Catenin Pathway Function in an Alzheimer's Disease Model. *Journal of immunology (Baltimore, Md. : 1950)* **187**, 6539-6549, doi:10.4049/jimmunol.1100620 (2011).
- 38 Linder, C. C. Genetic Variables That Influence Phenotype. *ILAR Journal* **47**, 132-140, doi:10.1093/ilar.47.2.132 (2006).
- 39 Glenner, G. G. & Wong, C. W. Alzheimer's disease: Initial report of the purification and characterization of a novel cerebrovascular amyloid protein. *Biochemical and Biophysical Research Communications* **120**, 885-890, doi:[http://dx.doi.org/10.1016/S0006-291X\(84\)80190-4](http://dx.doi.org/10.1016/S0006-291X(84)80190-4) (1984).
- 40 Müller, U. C. & Zheng, H. Physiological functions of APP family proteins. *Cold Spring Harbor perspectives in medicine* **2**, a006288 (2012).
- 41 Müller, U. C., Deller, T. & Korte, M. Not just amyloid: physiological functions of the amyloid precursor protein family. *Nature Reviews Neuroscience* (2017).
- 42 Walsh, D. M. *et al.* The APP family of proteins: similarities and differences. *Biochemical Society Transactions* **35**, 416-420, doi:10.1042/bst0350416 (2007).
- 43 Nalivaeva, N. N. & Turner, A. J. The amyloid precursor protein: A biochemical enigma in brain development, function and disease. *FEBS Letters* **587**, 2046-2054, doi:<https://doi.org/10.1016/j.febslet.2013.05.010> (2013).
- 44 Kang, J. *et al.* The precursor of Alzheimer's disease amyloid A4 protein resembles a cell-surface receptor. *Nature* **325**, 733-736 (1987).
- 45 Busciglio, J., Gabuzda, D. H., Matsudaira, P. & Yankner, B. A. Generation of beta-amyloid in the secretory pathway in neuronal and nonneuronal cells. *Proceedings of the National Academy of Sciences of the United States of America* **90**, 2092-2096 (1993).
- 46 Haass, C., Kaether, C., Thinakaran, G. & Sisodia, S. Trafficking and Proteolytic Processing of APP. *Cold Spring Harbor Perspectives in Medicine* **2**, a006270, doi:10.1101/cshperspect.a006270 (2012).

- 47 Haass, C. & Selkoe, D. J. Soluble protein oligomers in neurodegeneration: lessons from the Alzheimer's amyloid  $\beta$ -peptide. *Nature reviews Molecular cell biology* **8**, 101-112 (2007).
- 48 Mucke, L. & Selkoe, D. J. Neurotoxicity of Amyloid  $\beta$ -Protein: Synaptic and Network Dysfunction. *Cold Spring Harbor Perspectives in Medicine* **2**, a006338, doi:10.1101/cshperspect.a006338 (2012).
- 49 Citron, M. *et al.* Mutation of the [beta]-amyloid precursor protein in familial Alzheimer's disease increases [beta]-protein production. *Nature* **360**, 672-674 (1992).
- 50 Murrell, J., Farlow, M., Ghetti, B. & Benson, M. A mutation in the amyloid precursor protein associated with hereditary Alzheimer's disease. *Science* **254**, 97-99, doi:10.1126/science.1925564 (1991).
- 51 Mullan, M. *et al.* A pathogenic mutation for probable Alzheimer's disease in the APP gene at the N-terminus of  $\beta$ -amyloid. *Nature genetics* **1**, 345-347 (1992).
- 52 Johnston, J. A. *et al.* Increased  $\beta$ -amyloid release and levels of amyloid precursor protein (APP) in fibroblast cell lines from family members with the Swedish Alzheimer's disease APP670/671 mutation. *FEBS Letters* **354**, 274-278, doi:10.1016/0014-5793(94)01137-0 (1994).
- 53 Tamaoka, A. *et al.* APP717 missense mutation affects the ratio of amyloid beta protein species (A beta 1-42/43 and a beta 1-40) in familial Alzheimer's disease brain. *Journal of Biological Chemistry* **269**, 32721-32724 (1994).
- 54 Suzuki, N. *et al.* An increased percentage of long amyloid beta protein secreted by familial amyloid beta protein precursor (beta APP717) mutants. *Science* **264**, 1336-1340, doi:10.1126/science.8191290 (1994).
- 55 Clark, R. F. *et al.* The structure of the presenilin 1 (S182) gene and identification of six novel mutations in early onset AD families. *Nat Genet* **11**, 219-222 (1995).
- 56 Finckh, U. *et al.* Novel mutations and repeated findings of mutations in familial Alzheimer disease. *Neurogenetics* **6**, 85-89, doi:10.1007/s10048-005-0211-x (2005).
- 57 Margallo-Lana, M. *et al.* Fifteen-year follow-up of 92 hospitalized adults with Down's syndrome: incidence of cognitive decline, its relationship to age and neuropathology. *Journal of Intellectual Disability Research* **51**, 463-477 (2007).
- 58 Wisniewski, K., Wisniewski, H. & Wen, G. Occurrence of neuropathological changes and dementia of Alzheimer's disease in Down's syndrome. *Annals of neurology* **17**, 278-282 (1985).
- 59 Wisniewski, K. E., Dalton, A. J., McLachlan, D. R. C., Wen, G. Y. & Wisniewski, H. M. Alzheimer's disease in Down's syndrome: Clinicopathologic studies. *Neurology* **35**, 957, doi:10.1212/wnl.35.7.957 (1985).
- 60 Sleegers, K. *et al.* APP duplication is sufficient to cause early onset Alzheimer's dementia with cerebral amyloid angiopathy. *Brain* **129**, 2977-2983 (2006).
- 61 Jonsson, T. *et al.* A mutation in APP protects against Alzheimer's disease and age-related cognitive decline. *Nature* **488**, 96-99 (2012).
- 62 Dickson, D. W. *et al.* Identification of normal and pathological aging in prospectively studied nondemented elderly humans. *Neurobiology of aging* **13**, 179-189 (1992).

- 63 LaFerla, F. M. & Green, K. N. Animal Models of Alzheimer Disease. *Cold Spring Harbor Perspectives in Medicine* **2**, a006320, doi:10.1101/cshperspect.a006320 (2012).
- 64 Cleary, J. P. *et al.* Natural oligomers of the amyloid- $\beta$  protein specifically disrupt cognitive function. *Nature neuroscience* **8**, 79-84 (2004).
- 65 Li, S. *et al.* Soluble oligomers of amyloid  $\beta$  protein facilitate hippocampal long-term depression by disrupting neuronal glutamate uptake. *Neuron* **62**, 788-801 (2009).
- 66 Townsend, M., Shankar, G. M., Mehta, T., Walsh, D. M. & Selkoe, D. J. Effects of secreted oligomers of amyloid  $\beta$ -protein on hippocampal synaptic plasticity: a potent role for trimers. *The Journal of Physiology* **572**, 477-492, doi:10.1113/jphysiol.2005.103754 (2006).
- 67 Glabe, C. G. Structural classification of toxic amyloid oligomers. *Journal of Biological Chemistry* **283**, 29639-29643 (2008).
- 68 Tomic, J. L., Pensalfini, A., Head, E. & Glabe, C. G. Soluble fibrillar oligomer levels are elevated in Alzheimer's disease brain and correlate with cognitive dysfunction. *Neurobiology of disease* **35**, 352-358 (2009).
- 69 Walsh, D. M. *et al.* Naturally secreted oligomers of amyloid  $\beta$  protein potently inhibit hippocampal long-term potentiation in vivo. *Nature* **416**, 535-539 (2002).
- 70 Shankar, G. M. *et al.* Natural Oligomers of the Alzheimer Amyloid- $\beta$  Protein Induce Reversible Synapse Loss by Modulating an NMDA-Type Glutamate Receptor-Dependent Signaling Pathway. *The Journal of Neuroscience* **27**, 2866-2875, doi:10.1523/jneurosci.4970-06.2007 (2007).
- 71 Shankar, G. M. *et al.* Amyloid- $\beta$  protein dimers isolated directly from Alzheimer's brains impair synaptic plasticity and memory. *Nat Med* **14**, 837-842, doi:[http://www.nature.com/nm/journal/v14/n8/suppinfo/nm1782\\_S1.html](http://www.nature.com/nm/journal/v14/n8/suppinfo/nm1782_S1.html) (2008).
- 72 Jin, M. *et al.* Soluble amyloid  $\beta$ -protein dimers isolated from Alzheimer cortex directly induce Tau hyperphosphorylation and neuritic degeneration. *Proceedings of the National Academy of Sciences of the United States of America* **108**, 5819-5824, doi:10.1073/pnas.1017033108 (2011).
- 73 Tyan, S.-H. *et al.* Amyloid precursor protein (APP) regulates synaptic structure and function. *Molecular and Cellular Neuroscience* **51**, 43-52, doi:<https://doi.org/10.1016/j.mcn.2012.07.009> (2012).
- 74 Zheng, H. *et al.*  $\beta$ -amyloid precursor protein-deficient mice show reactive gliosis and decreased locomotor activity. *Cell* **81**, 525-531, doi:[http://dx.doi.org/10.1016/0092-8674\(95\)90073-X](http://dx.doi.org/10.1016/0092-8674(95)90073-X) (1995).
- 75 Luo, J. J., Wallace, M. S., Hawver, D. B., Kusiak, J. W. & Wallace, W. C. Characterization of the neurotrophic interaction between nerve growth factor and secreted  $\alpha$ -amyloid precursor protein. *Journal of neuroscience research* **63**, 410-420 (2001).
- 76 Mattson, M. P. *et al.* Evidence for excitoprotective and intraneuronal calcium-regulating roles for secreted forms of the  $\beta$ -amyloid precursor protein. *Neuron* **10**, 243-254 (1993).

- 77 Lüscher, C. & Malenka, R. C. NMDA receptor-dependent long-term potentiation and long-term depression (LTP/LTD). *Cold Spring Harbor perspectives in biology* **4**, a005710 (2012).
- 78 Meziane, H. *et al.* Memory-enhancing effects of secreted forms of the  $\beta$ -amyloid precursor protein in normal and amnesic mice. *Proceedings of the National Academy of Sciences* **95**, 12683-12688, doi:10.1073/pnas.95.21.12683 (1998).
- 79 Xiong, M. *et al.* Secreted amyloid precursor protein-alpha can restore novel object location memory and hippocampal LTP in aged rats. *Neurobiology of Learning and Memory* **138**, 291-299, doi:<https://doi.org/10.1016/j.nlm.2016.08.002> (2017).
- 80 Moreno, L. *et al.* sA $\beta$ PP $\alpha$  Improves Hippocampal NMDA-Dependent Functional Alterations Linked to Healthy Aging. *Journal of Alzheimer's Disease* **48**, 927-935 (2015).
- 81 Chasseigneaux, S. *et al.* Secreted amyloid precursor protein  $\beta$  and secreted amyloid precursor protein  $\alpha$  induce axon outgrowth in vitro through Egr1 signaling pathway. *PloS one* **6**, e16301 (2011).
- 82 Chasseigneaux, S. & Allinquant, B. Functions of A $\beta$ , sAPP $\alpha$  and sAPP $\beta$ : similarities and differences. *Journal of neurochemistry* **120**, 99-108 (2012).
- 83 Turner, A. J., Belyaev, N. D. & Nalivaeva, N. N. Mediator: the missing link in amyloid precursor protein nuclear signalling. *EMBO Reports* **12**, 180-181, doi:10.1038/embor.2011.25 (2011).
- 84 Cao, X. & Südhof, T. C. A transcriptively active complex of APP with Fe65 and histone acetyltransferase Tip60. *Science* **293**, 115-120 (2001).
- 85 Li, H. *et al.* Soluble amyloid precursor protein (APP) regulates transthyretin and Klotho gene expression without rescuing the essential function of APP. *Proceedings of the National Academy of Sciences* **107**, 17362-17367, doi:10.1073/pnas.1012568107 (2010).
- 86 Kerridge, C., Belyaev, N. D., Nalivaeva, N. N. & Turner, A. J. The A $\beta$ -clearance protein transthyretin, like neprilysin, is epigenetically regulated by the amyloid precursor protein intracellular domain. *Journal of neurochemistry* **130**, 419-431, doi:10.1111/jnc.12680 (2014).
- 87 Leissring, M. A. *et al.* A physiologic signaling role for the  $\gamma$ -secretase-derived intracellular fragment of APP. *Proceedings of the National Academy of Sciences of the United States of America* **99**, 4697-4702, doi:10.1073/pnas.072033799 (2002).
- 88 Belyaev, N. D., Nalivaeva, N. N., Makova, N. Z. & Turner, A. J. Neprilysin gene expression requires binding of the amyloid precursor protein intracellular domain to its promoter: implications for Alzheimer disease. *EMBO Reports* **10**, 94-100, doi:10.1038/embor.2008.222 (2009).
- 89 Puzzo, D. *et al.* Endogenous amyloid- $\beta$  is necessary for hippocampal synaptic plasticity and memory. *Annals of neurology* **69**, 819-830 (2011).
- 90 Puzzo, D. *et al.* Picomolar amyloid- $\beta$  positively modulates synaptic plasticity and memory in hippocampus. *Journal of Neuroscience* **28**, 14537-14545 (2008).
- 91 Lawrence, J. L. M. *et al.* Regulation of Presynaptic Ca<sup>2+</sup>, Synaptic Plasticity and Contextual Fear Conditioning by a N-terminal  $\beta$ -Amyloid

- Fragment. *The Journal of Neuroscience* **34**, 14210-14218, doi:10.1523/jneurosci.0326-14.2014 (2014).
- 92 Yankner, B. A., Duffy, L. K. & Kirschner, D. A. Neurotrophic and Neurotoxic Effects of Amyloid (beta) Protein: Reversal by Tachykinin Neuropeptides. *Science* **250**, 279 (1990).
- 93 Giuffrida, M. L. *et al.*  $\beta$ -Amyloid Monomers Are Neuroprotective. *The Journal of Neuroscience* **29**, 10582-10587, doi:10.1523/jneurosci.1736-09.2009 (2009).
- 94 Nicolas, M. & Hassan, B. A. Amyloid precursor protein and neural development. *Development* **141**, 2543-2548, doi:10.1242/dev.108712 (2014).
- 95 Mawuenyega, K. G. *et al.* Decreased Clearance of CNS  $\beta$ -Amyloid in Alzheimer's Disease. *Science* **330**, 1774-1774, doi:10.1126/science.1197623 (2010).
- 96 Huang, Y. & Mucke, L. Alzheimer Mechanisms and Therapeutic Strategies. *Cell* **148**, 1204-1222, doi:10.1016/j.cell.2012.02.040 (2012).
- 97 Hardy, J. & Selkoe, D. J. The amyloid hypothesis of Alzheimer's disease: progress and problems on the road to therapeutics. *Science* **297**, 353-356 (2002).
- 98 Guerreiro, R. *et al.* TREM2 variants in Alzheimer's disease. *New England Journal of Medicine* **368**, 117-127 (2013).
- 99 Bradshaw, E. M. *et al.* CD33 Alzheimer's disease locus: altered monocyte function and amyloid biology. *Nature neuroscience* **16**, 848-850 (2013).
- 100 Griciuc, A. *et al.* Alzheimer's Disease Risk Gene CD33 Inhibits Microglial Uptake of Amyloid Beta. *Neuron* **78**, 631-643, doi:<https://doi.org/10.1016/j.neuron.2013.04.014> (2013).
- 101 Heneka, M. T. *et al.* Neuroinflammation in Alzheimer's disease. *The Lancet Neurology* **14**, 388-405 (2015).
- 102 Bamberger, M. E., Harris, M. E., McDonald, D. R., Husemann, J. & Landreth, G. E. A cell surface receptor complex for fibrillar  $\beta$ -amyloid mediates microglial activation. *Journal of Neuroscience* **23**, 2665-2674 (2003).
- 103 Paresce, D. M., Ghosh, R. N. & Maxfield, F. R. Microglial cells internalize aggregates of the Alzheimer's disease amyloid  $\beta$ -protein via a scavenger receptor. *Neuron* **17**, 553-565 (1996).
- 104 Stewart, C. R. *et al.* CD36 ligands promote sterile inflammation through assembly of a Toll-like receptor 4 and 6 heterodimer. *Nature immunology* **11**, 155-161 (2010).
- 105 Liu, Y. *et al.* LPS receptor (CD14): a receptor for phagocytosis of Alzheimer's amyloid peptide. *Brain* **128**, 1778-1789 (2005).
- 106 Wang, Y. *et al.* TREM2-mediated early microglial response limits diffusion and toxicity of amyloid plaques. *The Journal of Experimental Medicine* **213**, 667-675, doi:10.1084/jem.20151948 (2016).
- 107 Koistinaho, M. *et al.* Apolipoprotein E promotes astrocyte colocalization and degradation of deposited amyloid-[beta] peptides. *Nat Med* **10**, 719-726, doi:[http://www.nature.com/nm/journal/v10/n7/supinfo/nm1058\\_S1.html](http://www.nature.com/nm/journal/v10/n7/supinfo/nm1058_S1.html) (2004).
- 108 Halle, A. *et al.* The NALP3 inflammasome is involved in the innate immune response to amyloid- $\beta$ . *Nature immunology* **9**, 857-865, doi:10.1038/ni.1636 (2008).



- 109 Kanekiyo, T., Xu, H. & Bu, G. ApoE and A $\beta$  in Alzheimer's Disease: Accidental Encounters or Partners? *Neuron* **81**, 740-754, doi:<https://doi.org/10.1016/j.neuron.2014.01.045> (2014).
- 110 Cho, M.-H. *et al.* Autophagy in microglia degrades extracellular  $\beta$ -amyloid fibrils and regulates the NLRP3 inflammasome. *Autophagy* **10**, 1761-1775, doi:10.4161/auto.29647 (2014).
- 111 Farris, W. *et al.* Insulin-degrading enzyme regulates the levels of insulin, amyloid  $\beta$ -protein, and the  $\beta$ -amyloid precursor protein intracellular domain in vivo. *Proceedings of the National Academy of Sciences* **100**, 4162-4167 (2003).
- 112 Eckman, E. A., Reed, D. K. & Eckman, C. B. Degradation of the Alzheimer's amyloid  $\beta$  peptide by endothelin-converting enzyme. *Journal of Biological Chemistry* **276**, 24540-24548 (2001).
- 113 Liddelw, S. A. *et al.* Neurotoxic reactive astrocytes are induced by activated microglia. *Nature* **541**, 481-487, doi:10.1038/nature21029 <http://www.nature.com/nature/journal/v541/n7638/abs/nature21029.html#supplementary-information> (2017).
- 114 Yoshiyama, Y. *et al.* Synapse Loss and Microglial Activation Precede Tangles in a P301S Tauopathy Mouse Model. *Neuron* **53**, 337-351, doi:<https://doi.org/10.1016/j.neuron.2007.01.010> (2007).
- 115 Kitazawa, M., Oddo, S., Yamasaki, T. R., Green, K. N. & LaFerla, F. M. Lipopolysaccharide-Induced Inflammation Exacerbates Tau Pathology by a Cyclin-Dependent Kinase 5-Mediated Pathway in a Transgenic Model of Alzheimer's Disease. *The Journal of Neuroscience* **25**, 8843-8853, doi:10.1523/jneurosci.2868-05.2005 (2005).
- 116 Wang, Y. & Mandelkow, E. Tau in physiology and pathology. *Nature Reviews Neuroscience* **17**, 22-35 (2016).
- 117 Wolfe, M. S. Tau mutations in neurodegenerative diseases. *Journal of Biological Chemistry* **284**, 6021-6025 (2009).
- 118 Liu, L. *et al.* Trans-Synaptic Spread of Tau Pathology In Vivo. *PLoS ONE* **7**, e31302, doi:10.1371/journal.pone.0031302 (2012).
- 119 Wu, J. W. *et al.* Neuronal activity enhances tau propagation and tau pathology in vivo. *Nat Neurosci* **19**, 1085-1092, doi:10.1038/nn.4328 <http://www.nature.com/neuro/journal/v19/n8/abs/nn.4328.html#supplementary-information> (2016).
- 120 Asai, H. *et al.* Depletion of microglia and inhibition of exosome synthesis halt tau propagation. *Nat Neurosci* **18**, 1584-1593, doi:10.1038/nn.4132 <http://www.nature.com/neuro/journal/v18/n11/abs/nn.4132.html#supplementary-information> (2015).
- 121 Holtzman, D. M. *et al.* Tau: From research to clinical development. *Alzheimer's & Dementia* **12**, 1033-1039, doi:<https://doi.org/10.1016/j.jalz.2016.03.018> (2016).
- 122 Blurton-Jones, M. & LaFerla, F. M. Pathways by which A facilitates tau pathology. *Current Alzheimer Research* **3**, 437-448 (2006).
- 123 Ittner, L. M. *et al.* Dendritic function of tau mediates amyloid- $\beta$  toxicity in Alzheimer's disease mouse models. *Cell* **142**, 387-397 (2010).

- 124 Hong, S. *et al.* Complement and microglia mediate early synapse loss in Alzheimer mouse models. *Science* **352**, 712-716, doi:10.1126/science.aad8373 (2016).
- 125 Prieto, G. A. *et al.* Synapse-specific IL-1 receptor subunit reconfiguration augments vulnerability to IL-1 $\beta$  in the aged hippocampus. *Proceedings of the National Academy of Sciences* **112**, E5078-E5087, doi:10.1073/pnas.1514486112 (2015).
- 126 Zumkehr, J. *et al.* Ceftriaxone ameliorates tau pathology and cognitive decline via restoration of glial glutamate transporter in a mouse model of Alzheimer's disease. *Neurobiology of Aging* **36**, 2260-2271, doi:<http://dx.doi.org/10.1016/j.neurobiolaging.2015.04.005> (2015).
- 127 Kimelberg, H. K. & Nedergaard, M. Functions of astrocytes and their potential as therapeutic targets. *Neurotherapeutics* **7**, 338-353, doi:10.1016/j.nurt.2010.07.006 (2010).
- 128 Sofroniew, M. V. & Vinters, H. V. Astrocytes: biology and pathology. *Acta Neuropathologica* **119**, 7-35, doi:10.1007/s00401-009-0619-8 (2010).
- 129 Clarke, L. E. & Barres, B. A. Emerging roles of astrocytes in neural circuit development. *Nat Rev Neurosci* **14**, 311-321, doi:10.1038/nrn3484 (2013).
- 130 Chung, W.-S., Allen, N. J. & Eroglu, C. Astrocytes Control Synapse Formation, Function, and Elimination. *Cold Spring Harbor Perspectives in Biology* **7**, a020370, doi:10.1101/cshperspect.a020370 (2015).
- 131 Barres, B. A. The Mystery and Magic of Glia: A Perspective on Their Roles in Health and Disease. *Neuron* **60**, 430-440, doi:<http://dx.doi.org/10.1016/j.neuron.2008.10.013> (2008).
- 132 Araque, A., Parpura, V., Sanzgiri, R. P. & Haydon, P. G. Tripartite synapses: glia, the unacknowledged partner. *Trends in Neurosciences* **22**, 208-215, doi:[https://doi.org/10.1016/S0166-2236\(98\)01349-6](https://doi.org/10.1016/S0166-2236(98)01349-6) (1999).
- 133 Tani, H. *et al.* A Local Glutamate-Glutamine Cycle Sustains Synaptic Excitatory Transmitter Release. *Neuron* **81**, 888-900, doi:<https://doi.org/10.1016/j.neuron.2013.12.026> (2014).
- 134 Butterfield, D. A. & Pocernich, C. B. The glutamatergic system and Alzheimer's disease. *CNS drugs* **17**, 641-652 (2003).
- 135 Kim, K. *et al.* Role of Excitatory Amino Acid Transporter-2 (EAAT2) and glutamate in neurodegeneration: Opportunities for developing novel therapeutics. *Journal of cellular physiology* **226**, 2484-2493 (2011).
- 136 Martinez-Hernandez, A., Bell, K. & Norenberg, M. Glutamine synthetase: glial localization in brain. *Science* **195**, 1356-1358, doi:10.1126/science.14400 (1977).
- 137 Kvamme, E., Roberg, B. & Torgner, I. A. Phosphate-activated glutaminase and mitochondrial glutamine transport in the brain. *Neurochemical research* **25**, 1407-1419 (2000).
- 138 Takahashi, K., Foster, J. B. & Lin, C.-L. G. Glutamate transporter EAAT2: regulation, function, and potential as a therapeutic target for neurological and psychiatric disease. *Cellular and Molecular Life Sciences* **72**, 3489-3506, doi:10.1007/s00018-015-1937-8 (2015).

- 139 Freneau, R. T., Voglmaier, S., Seal, R. P. & Edwards, R. H. VGLUTs define subsets of excitatory neurons and suggest novel roles for glutamate. *Trends in neurosciences* **27**, 98-103 (2004).
- 140 Tanaka, K. *et al.* Epilepsy and exacerbation of brain injury in mice lacking the glutamate transporter GLT-1. *Science* **276**, 1699-1702 (1997).
- 141 Rothstein, J. D. *et al.* Localization of neuronal and glial glutamate transporters. *Neuron* **13**, 713-725, doi:[https://doi.org/10.1016/0896-6273\(94\)90038-8](https://doi.org/10.1016/0896-6273(94)90038-8) (1994).
- 142 Eroglu, C. & Barres, B. A. Regulation of synaptic connectivity by glia. *Nature* **468**, 223-231, doi:10.1038/nature09612 (2010).
- 143 Witcher, M. R., Kirov, S. A. & Harris, K. M. Plasticity of perisynaptic astroglia during synaptogenesis in the mature rat hippocampus. *Glia* **55**, 13-23, doi:10.1002/glia.20415 (2007).
- 144 Anggono, V., Tsai, L.-H. & Götz, J. Glutamate Receptors in Alzheimer's Disease: Mechanisms and Therapies. *Neural plasticity* **2016** (2016).
- 145 Bell, K. F., Bennett, D. A. & Cuello, A. C. Paradoxical upregulation of glutamatergic presynaptic boutons during mild cognitive impairment. *Journal of Neuroscience* **27**, 10810-10817 (2007).
- 146 Masliah, E., Hansen, L., Alford, M., Deteresa, R. & Mallory, M. Deficient glutamate transport is associated with neurodegeneration in Alzheimer's disease. *Annals of neurology* **40**, 759-766 (1996).
- 147 Li, S., Mallory, M., Alford, M., Tanaka, S. & Masliah, E. Glutamate transporter alterations in Alzheimer disease are possibly associated with abnormal APP expression. *Journal of Neuropathology & Experimental Neurology* **56**, 901-911 (1997).
- 148 Tian, G., Kong, Q., Lai, L., Ray-Chaudhury, A. & Lin, C.-I. G. Increased expression of cholesterol 24S-hydroxylase results in disruption of glial glutamate transporter EAAT2 association with lipid rafts: a potential role in Alzheimer's disease. *Journal of Neurochemistry* **113**, 978-989, doi:10.1111/j.1471-4159.2010.06661.x (2010).
- 149 Jacob, C. *et al.* Alterations in expression of glutamatergic transporters and receptors in sporadic Alzheimer's disease. *Journal of Alzheimer's Disease* **11**, 97-116 (2007).
- 150 Mookherjee, P. *et al.* GLT-1 loss accelerates cognitive deficit onset in an Alzheimer's disease animal model. *Journal of Alzheimer's Disease* **26**, 447-455 (2011).
- 151 Woltjer, R. L. *et al.* Aberrant detergent-insoluble excitatory amino acid transporter 2 accumulates in Alzheimer disease. *Journal of neuropathology and experimental neurology* **69**, 667 (2010).
- 152 Figiel, M., Maucher, T., Rozyczka, J., Bayatti, N. & Engele, J. Regulation of glial glutamate transporter expression by growth factors. *Experimental Neurology* **183**, 124-135, doi:[https://doi.org/10.1016/S0014-4886\(03\)00134-1](https://doi.org/10.1016/S0014-4886(03)00134-1) (2003).
- 153 Zeleniaia, O. *et al.* Epidermal Growth Factor Receptor Agonists Increase Expression of Glutamate Transporter GLT-1 in Astrocytes through Pathways Dependent on Phosphatidylinositol 3-Kinase and Transcription Factor NF- $\kappa$ B. *Molecular Pharmacology* **57**, 667-678, doi:10.1124/mol.57.4.667 (2000).

- 154 Filosa, A. *et al.* Neuron-glia communication via EphA4/ephrin-A3 modulates LTP through glial glutamate transport. *Nature neuroscience* **12**, 1285-1292 (2009).
- 155 Su, Z.-z. *et al.* Insights into glutamate transport regulation in human astrocytes: Cloning of the promoter for excitatory amino acid transporter 2 (EAAT2). *Proceedings of the National Academy of Sciences* **100**, 1955-1960, doi:10.1073/pnas.0136555100 (2003).
- 156 Sitcheran, R., Gupta, P., Fisher, P. B. & Baldwin, A. S. Positive and negative regulation of EAAT2 by NF- $\kappa$ B: a role for N-myc in TNF $\alpha$ -controlled repression. *The EMBO journal* **24**, 510-520 (2005).
- 157 Rothstein, J. D. *et al.*  $\beta$ -Lactam antibiotics offer neuroprotection by increasing glutamate transporter expression. *Nature* **433**, 73-77 (2005).
- 158 Yang, Y. *et al.* Pre-synaptic regulation of astroglial excitatory neurotransmitter transporter GLT1. *Neuron* **61**, 880-894, doi:10.1016/j.neuron.2009.02.010 (2009).
- 159 Wahid, F., Shehzad, A., Khan, T. & Kim, Y. Y. MicroRNAs: Synthesis, mechanism, function, and recent clinical trials. *Biochimica et Biophysica Acta (BBA) - Molecular Cell Research* **1803**, 1231-1243, doi:<https://doi.org/10.1016/j.bbamcr.2010.06.013> (2010).
- 160 Chendrimada, T. P. *et al.* TRBP recruits the Dicer complex to Ago2 for microRNA processing and gene silencing. *Nature* **436**, 740-744 (2005).
- 161 Morel, L. *et al.* Neuronal Exosomal miRNA-dependent Translational Regulation of Astroglial Glutamate Transporter GLT1. *Journal of Biological Chemistry* **288**, 7105-7116, doi:10.1074/jbc.M112.410944 (2013).
- 162 Ouyang, Y.-B., Xu, L., Liu, S. & Giffard, R. G. Role of astrocytes in delayed neuronal death: GLT-1 and its novel regulation by microRNAs. *Advances in neurobiology* **11**, 171-188, doi:10.1007/978-3-319-08894-5\_9 (2014).
- 163 Yang, Z.-B. *et al.* Up-regulation of brain-enriched *miR-107* promotes excitatory neurotoxicity through down-regulation of glutamate transporter-1 expression following ischaemic stroke. *Clinical Science* **127**, 679-689, doi:10.1042/cs20140084 (2014).
- 164 Hämäläinen, A. *et al.* Increased fMRI responses during encoding in mild cognitive impairment. *Neurobiology of Aging* **28**, 1889-1903, doi:<http://dx.doi.org/10.1016/j.neurobiolaging.2006.08.008> (2007).
- 165 Dickerson, B. C. *et al.* Increased hippocampal activation in mild cognitive impairment compared to normal aging and AD. *Neurology* **65**, 404-411, doi:10.1212/01.wnl.0000171450.97464.49 (2005).
- 166 Bookheimer, S. Y. *et al.* Patterns of Brain Activation in People at Risk for Alzheimer's Disease. *New England Journal of Medicine* **343**, 450-456, doi:doi:10.1056/NEJM200008173430701 (2000).
- 167 Yamamoto, K. *et al.* Chronic optogenetic activation augments A $\beta$  pathology in a mouse model of Alzheimer disease. *Cell reports* **11**, 859-865 (2015).
- 168 Scimemi, A. *et al.* Amyloid- $\beta$ 1-42 slows clearance of synaptically released glutamate by mislocalizing astrocytic GLT-1. *The Journal of Neuroscience* **33**, 5312-5318 (2013).

- 169 Takahashi, K. *et al.* Restored glial glutamate transporter EAAT2 function as a potential therapeutic approach for Alzheimer's disease. *The Journal of Experimental Medicine* **212**, 319-332, doi:10.1084/jem.20140413 (2015).
- 170 Parsons, Matthew P. & Raymond, Lynn A. Extrasynaptic NMDA Receptor Involvement in Central Nervous System Disorders. *Neuron* **82**, 279-293, doi:<http://dx.doi.org/10.1016/j.neuron.2014.03.030> (2014).
- 171 Lai, T. W., Zhang, S. & Wang, Y. T. Excitotoxicity and stroke: Identifying novel targets for neuroprotection. *Progress in Neurobiology* **115**, 157-188, doi:<http://dx.doi.org/10.1016/j.pneurobio.2013.11.006> (2014).
- 172 Pooler, A. M., Phillips, E. C., Lau, D. H., Noble, W. & Hanger, D. P. Physiological release of endogenous tau is stimulated by neuronal activity. *EMBO reports* **14**, 389-394 (2013).
- 173 Yamada, K. *et al.* Neuronal activity regulates extracellular tau in vivo. *Journal of Experimental Medicine*, jem. 20131685 (2014).
- 174 Oddo, S. *et al.* Triple-transgenic model of Alzheimer's disease with plaques and tangles: intracellular A $\beta$  and synaptic dysfunction. *Neuron* **39**, 409-421 (2003).
- 175 Kitazawa, M. *et al.* Blocking IL-1 signaling rescues cognition, attenuates tau pathology, and restores neuronal  $\beta$ -catenin pathway function in an Alzheimer's disease model. *The Journal of Immunology* **187**, 6539-6549 (2011).
- 176 Blurton-Jones, M. *et al.* Neural stem cells improve cognition via BDNF in a transgenic model of Alzheimer disease. *Proceedings of the National Academy of Sciences* **106**, 13594-13599 (2009).
- 177 Langmann, T., Mauerer, R. & Schmitz, G. Human ATP-binding cassette transporter TaqMan low-density array: analysis of macrophage differentiation and foam cell formation. *Clinical chemistry* **52**, 310-313 (2006).
- 178 Abdul, H. M. *et al.* Cognitive decline in Alzheimer's disease is associated with selective changes in calcineurin/NFAT signaling. *Journal of Neuroscience* **29**, 12957-12969 (2009).
- 179 Lee, S.-G. *et al.* Mechanism of Ceftriaxone Induction of Excitatory Amino Acid Transporter-2 Expression and Glutamate Uptake in Primary Human Astrocytes. *The Journal of biological chemistry* **283**, 13116-13123, doi:10.1074/jbc.M707697200 (2008).
- 180 Danbolt, N. C. Glutamate uptake. *Progress in Neurobiology* **65**, 1-105, doi:[https://doi.org/10.1016/S0301-0082\(00\)00067-8](https://doi.org/10.1016/S0301-0082(00)00067-8) (2001).
- 181 Billings, L. M., Oddo, S., Green, K. N., McGaugh, J. L. & LaFerla, F. M. Intraneuronal A $\beta$  Causes the Onset of Early Alzheimer's Disease-Related Cognitive Deficits in Transgenic Mice. *Neuron* **45**, 675-688, doi:<https://doi.org/10.1016/j.neuron.2005.01.040> (2005).
- 182 Kaye, R. *et al.* Common Structure of Soluble Amyloid Oligomers Implies Common Mechanism of Pathogenesis. *Science* **300**, 486-489, doi:10.1126/science.1079469 (2003).
- 183 Kaye, R. *et al.* Fibril specific, conformation dependent antibodies recognize a generic epitope common to amyloid fibrils and fibrillar oligomers that is absent in prefibrillar oligomers. *Molecular Neurodegeneration* **2**, 18, doi:10.1186/1750-1326-2-18 (2007).

- 184 Götz, J., Ittner, L. M., Schonrock, N. & Cappai, R. An update on the toxicity of  
A $\beta$  in Alzheimer's disease. *Neuropsychiatric Disease and Treatment* **4**, 1033-  
1042 (2008).
- 185 Dhavan, R. & Tsai, L.-H. A decade of CDK5. *Nature reviews Molecular cell  
biology* **2**, 749-759 (2001).
- 186 LaFerla, F. M. & Oddo, S. Alzheimer's disease: A $\beta$ , tau and synaptic dysfunction.  
*Trends in Molecular Medicine* **11**, 170-176,  
doi:<http://dx.doi.org/10.1016/j.molmed.2005.02.009> (2005).
- 187 Dickson, D. W. *et al.* Correlations of synaptic and pathological markers with  
cognition of the elderly. *Neurobiology of aging* **16**, 285-298 (1995).
- 188 Masliah, E. *et al.* Altered expression of synaptic proteins occurs early during  
progression of Alzheimer's disease. *Neurology* **56**, 127-129 (2001).
- 189 Zhao, L. *et al.* Role of p21-activated kinase pathway defects in the cognitive  
deficits of Alzheimer disease. *Nat Neurosci* **9**, 234-242,  
doi:[http://www.nature.com/neuro/journal/v9/n2/supinfo/n1630\\_S1.html](http://www.nature.com/neuro/journal/v9/n2/supinfo/n1630_S1.html) (2006).
- 190 Mucke, L. *et al.* High-level neuronal expression of A $\beta$ 1-42 in wild-type human  
amyloid protein precursor transgenic mice: synaptotoxicity without plaque  
formation. *Journal of Neuroscience* **20**, 4050-4058 (2000).
- 191 Talantova, M. *et al.* A $\beta$  induces astrocytic glutamate release, extrasynaptic  
NMDA receptor activation, and synaptic loss. *Proceedings of the National  
Academy of Sciences* **110**, E2518-E2527, doi:10.1073/pnas.1306832110 (2013).
- 192 Chen, W. *et al.* Expression of a variant form of the glutamate transporter GLT1 in  
neuronal cultures and in neurons and astrocytes in the rat brain. *The Journal of  
neuroscience* **22**, 2142-2152 (2002).
- 193 Chen, W. *et al.* The glutamate transporter GLT1a is expressed in excitatory axon  
terminals of mature hippocampal neurons. *The Journal of neuroscience* **24**, 1136-  
1148 (2004).
- 194 Jimenez-Jimenez, F. *et al.* Neurotransmitter amino acids in cerebrospinal fluid of  
patients with Alzheimer's disease. *Journal of neural transmission* **105**, 269-277  
(1998).
- 195 Kaiser, E. *et al.* Cerebrospinal fluid concentrations of functionally important  
amino acids and metabolic compounds in patients with mild cognitive impairment  
and Alzheimer's disease. *Neurodegenerative Diseases* **7**, 251-259 (2010).
- 196 Pooler, A. M., Phillips, E. C., Lau, D. H. W., Noble, W. & Hanger, D. P.  
Physiological release of endogenous tau is stimulated by neuronal activity. *EMBO  
reports* **14**, 389-394, doi:10.1038/embor.2013.15 (2013).
- 197 de Calignon, A. *et al.* Propagation of Tau Pathology in a Model of Early  
Alzheimer's Disease. *Neuron* **73**, 685-697,  
doi:<http://dx.doi.org/10.1016/j.neuron.2011.11.033> (2012).
- 198 Liu, L. *et al.* Trans-Synaptic Spread of Tau Pathology *In Vivo*.  
*PLoS ONE* **7**, e31302, doi:10.1371/journal.pone.0031302 (2012).
- 199 Giannakopoulos, P. *et al.* Tangle and neuron numbers, but not amyloid load,  
predict cognitive status in Alzheimer's disease. *Neurology* **60**, 1495-1500 (2003).

- 200 Lee, S.-G. *et al.* Mechanism of ceftriaxone induction of excitatory amino acid transporter-2 expression and glutamate uptake in primary human astrocytes. *Journal of Biological Chemistry* **283**, 13116-13123 (2008).
- 201 Spector, R. Ceftriaxone Transport through the Blood-Brain Barrier. *The Journal of Infectious Diseases* **156**, 209-211, doi:10.2307/30136528 (1987).
- 202 Matos-Ocasio, F., Hernández-López, A. & Thompson, K. J. Ceftriaxone, a GLT-1 transporter activator, disrupts hippocampal learning in rats. *Pharmacology Biochemistry and Behavior* **122**, 118-121 (2014).
- 203 Karaman, I., Kizilay-Ozfidan, G., Karadag, C. H. & Ulugol, A. Lack of effect of ceftriaxone, a GLT-1 transporter activator, on spatial memory in mice. *Pharmacology Biochemistry and Behavior* **108**, 61-65 (2013).
- 204 Lesné, S. *et al.* NMDA Receptor Activation Inhibits  $\alpha$ -Secretase and Promotes Neuronal Amyloid- $\beta$  Production. *The Journal of Neuroscience* **25**, 9367-9377, doi:10.1523/jneurosci.0849-05.2005 (2005).
- 205 Bordji, K., Becerril-Ortega, J., Nicole, O. & Buisson, A. Activation of Extrasynaptic, But Not Synaptic, NMDA Receptors Modifies Amyloid Precursor Protein Expression Pattern and Increases Amyloid- $\beta$  Production. *The Journal of Neuroscience* **30**, 15927-15942, doi:10.1523/jneurosci.3021-10.2010 (2010).
- 206 Yamamoto, K. *et al.* Chronic Optogenetic Activation Augments A $\beta$  Pathology in a Mouse Model of Alzheimer Disease. *Cell Reports* **11**, 859-865, doi:<http://dx.doi.org/10.1016/j.celrep.2015.04.017> (2015).
- 207 Jiménez-Jiménez, F. J. *et al.* Neurotransmitter amino acids in cerebrospinal fluid of patients with Alzheimer's disease. *Journal of Neural Transmission* **105**, 269-277, doi:10.1007/s007020050056 (1998).
- 208 Csernansky, J. G., Bardgett, M. E., Sheline, Y. I., Morris, J. C. & Olney, J. W. CSF excitatory amino acids and severity of illness in Alzheimer's disease. *Neurology* **46**, 1715-1720, doi:10.1212/wnl.46.6.1715 (1996).
- 209 Prieto, G. A. & Cotman, C. W. Cytokines and cytokine networks target neurons to modulate long-term potentiation. *Cytokine & Growth Factor Reviews* **34**, 27-33, doi:<https://doi.org/10.1016/j.cytogfr.2017.03.005> (2017).
- 210 Rodriguez-Ortiz, C. J., Baglietto-Vargas, D., Martinez-Coria, H., LaFerla, F. M. & Kitazawa, M. Upregulation of miR-181 decreases c-Fos and SIRT-1 in the hippocampus of 3xTg-AD mice. *Journal of Alzheimer's Disease* **42**, 1229-1238 (2014).
- 211 Schrott, G. microRNAs at the synapse. *Nat Rev Neurosci* **10**, 842-849, doi:[http://www.nature.com/nrn/journal/v10/n12/supinfo/nrn2763\\_S1.html](http://www.nature.com/nrn/journal/v10/n12/supinfo/nrn2763_S1.html) (2009).
- 212 Femminella, G. D., Ferrara, N. & Rengo, G. The emerging role of microRNAs in Alzheimer's disease. *Frontiers in Physiology* **6**, 40, doi:10.3389/fphys.2015.00040 (2015).
- 213 Yang, Z.-B. *et al.* Up-regulation of brain-enriched miR-107 promotes excitatory neurotoxicity through down-regulation of glutamate transporter-1 expression following ischaemic stroke. *Clinical Science* **127**, 679-689 (2014).
- 214 Dumont, A. O., Goursaud, S., Desmet, N. & Hermans, E. Differential Regulation of Glutamate Transporter Subtypes by Pro-Inflammatory Cytokine TNF- $\alpha$  in

- Cortical Astrocytes from a Rat Model of Amyotrophic Lateral Sclerosis. *PLOS ONE* **9**, e97649, doi:10.1371/journal.pone.0097649 (2014).
- 215 Hu, S., Sheng, W. S., Ehrlich, L. C., Peterson, P. K. & Chao, C. C. Cytokine Effects on Glutamate Uptake by Human Astrocytes. *Neuroimmunomodulation* **7**, 153-159 (2000).
- 216 Pinteaux, E., Trotter, P. & Simi, A. Cell-specific and concentration-dependent actions of interleukin-1 in acute brain inflammation. *Cytokine* **45**, 1-7 (2009).
- 217 Zhang, Y. *et al.* Purification and Characterization of Progenitor and Mature Human Astrocytes Reveals Transcriptional and Functional Differences with Mouse. *Neuron* **89**, 37-53, doi:10.1016/j.neuron.2015.11.013 (2016).
- 218 Parker, L. C., Luheshi, G. N., Rothwell, N. J. & Pinteaux, E. IL-1 $\beta$  signalling in glial cells in wildtype and IL-1RI deficient mice. *British journal of pharmacology* **136**, 312-320 (2002).
- 219 Chao, C. C., Lokensgard, J. R., Sheng, W. S., Hu, S. & Peterson, P. K. IL-1-induced iNOS expression in human astrocytes via NF- $\kappa$ B. *Neuroreport* **8**, 3163-3166 (1997).
- 220 Stanimirovic, D., Zhang, W., Howlett, C., Lemieux, P. & Smith, C. Inflammatory gene transcription in human astrocytes exposed to hypoxia: roles of the nuclear factor- $\kappa$ B and autocrine stimulation. *Journal of neuroimmunology* **119**, 365-376 (2001).
- 221 Viviani, B. *et al.* Interleukin-1 $\beta$  Enhances NMDA Receptor-Mediated Intracellular Calcium Increase through Activation of the Src Family of Kinases. *The Journal of Neuroscience* **23**, 8692-8700 (2003).
- 222 Ross, F. M., Allan, S. M., Rothwell, N. J. & Verkhratsky, A. A dual role for interleukin-1 in LTP in mouse hippocampal slices. *Journal of neuroimmunology* **144**, 61-67, doi:<https://doi.org/10.1016/j.jneuroim.2003.08.030> (2003).
- 223 Goshen, I. *et al.* A dual role for interleukin-1 in hippocampal-dependent memory processes. *Psychoneuroendocrinology* **32**, 1106-1115, doi:<https://doi.org/10.1016/j.psyneuen.2007.09.004> (2007).
- 224 Avital, A. *et al.* Impaired interleukin-1 signaling is associated with deficits in hippocampal memory processes and neural plasticity. *Hippocampus* **13**, 826-834, doi:10.1002/hipo.10135 (2003).
- 225 Schneider, H. *et al.* A neuromodulatory role of interleukin-1 $\beta$  in the hippocampus. *Proceedings of the National Academy of Sciences of the United States of America* **95**, 7778-7783 (1998).
- 226 Ben Menachem-Zidon, O. *et al.* Astrocytes support hippocampal-dependent memory and long-term potentiation via interleukin-1 signaling. *Brain, Behavior, and Immunity* **25**, 1008-1016, doi:<https://doi.org/10.1016/j.bbi.2010.11.007> (2011).
- 227 Pita-Almenar, J. D., Zou, S., Colbert, C. M. & Eskin, A. Relationship between increase in astrocytic GLT-1 glutamate transport and late-LTP. *Learning & Memory* **19**, 615-626, doi:10.1101/lm.023259.111 (2012).
- 228 Sambandan, S. *et al.* Activity-dependent spatially localized miRNA maturation in neuronal dendrites. *Science* **355**, 634-637 (2017).



- 229 Hutchison, E. R. *et al.* Involvement of miR-181 in Neuroinflammatory Responses of Astrocytes. *Glia* **61**, 1018-1028, doi:10.1002/glia.22483 (2013).
- 230 Kiko, T. *et al.* MicroRNAs in plasma and cerebrospinal fluid as potential markers for Alzheimer's disease. *Journal of Alzheimer's Disease* **39**, 253-259 (2014).
- 231 Cogswell, J. P. *et al.* Identification of miRNA changes in Alzheimer's disease brain and CSF yields putative biomarkers and insights into disease pathways. *Journal of Alzheimer's disease* **14**, 27-41 (2008).
- 232 Nagaraj, S. *et al.* Profile of 6 microRNA in blood plasma distinguish early stage Alzheimer's disease patients from non-demented subjects. *Oncotarget* **8**, 16122 (2017).
- 233 Chung, W.-S., Allen, N. J. & Eroglu, C. Astrocytes Control Synapse Formation, Function, and Elimination. *Cold Spring Harbor perspectives in biology* (2015).
- 234 Kamenetz, F. *et al.* APP Processing and Synaptic Function. *Neuron* **37**, 925-937, doi:[https://doi.org/10.1016/S0896-6273\(03\)00124-7](https://doi.org/10.1016/S0896-6273(03)00124-7) (2003).
- 235 Bookheimer, S. Y. *et al.* Patterns of Brain Activation in People at Risk for Alzheimer's Disease. *New England Journal of Medicine* **343**, 450-456, doi:10.1056/nejm200008173430701 (2000).
- 236 Cai, X., Golde, T. & Younkin, S. Release of excess amyloid beta protein from a mutant amyloid beta protein precursor. *Science* **259**, 514-516, doi:10.1126/science.8424174 (1993).
- 237 Andorfer, C. *et al.* Hyperphosphorylation and aggregation of tau in mice expressing normal human tau isoforms. *Journal of neurochemistry* **86**, 582-590, doi:10.1046/j.1471-4159.2003.01879.x (2003).
- 238 Baglietto-Vargas, D. *et al.* Short-term modern life-like stress exacerbates A $\beta$ -pathology and synapse loss in 3xTg-AD mice. *Journal of neurochemistry* **134**, 915-926, doi:10.1111/jnc.13195 (2015).
- 239 Kerchner, G. A. *et al.* Hippocampal CA1 apical neuropil atrophy and memory performance in Alzheimer's disease. *NeuroImage* **63**, 194-202, doi:10.1016/j.neuroimage.2012.06.048 (2012).
- 240 Hering, H. & Sheng, M. Dendritic spines : structure, dynamics and regulation. *Nat Rev Neurosci* **2**, 880-888 (2001).
- 241 Chang, F.-L. F. & Greenough, W. T. Transient and enduring morphological correlates of synaptic activity and efficacy change in the rat hippocampal slice. *Brain Research* **309**, 35-46, doi:[http://dx.doi.org/10.1016/0006-8993\(84\)91008-4](http://dx.doi.org/10.1016/0006-8993(84)91008-4) (1984).
- 242 Penazzi, L. *et al.* A $\beta$ -mediated spine changes in the hippocampus are microtubule-dependent and can be reversed by a subnanomolar concentration of the microtubule-stabilizing agent epothilone D. *Neuropharmacology* **105**, 84-95, doi:10.1016/j.neuropharm.2016.01.002 (2016).
- 243 van der Zee, E. A. Synapses, spines and kinases in mammalian learning and memory, and the impact of aging. *Neuroscience & Biobehavioral Reviews* **50**, 77-85, doi:<http://dx.doi.org/10.1016/j.neubiorev.2014.06.012> (2015).
- 244 Bali, J., Gheinani, A. H., Zurbriggen, S. & Rajendran, L. Role of genes linked to sporadic Alzheimer's disease risk in the production of  $\beta$ -amyloid peptides.

- Proceedings of the National Academy of Sciences* **109**, 15307-15311, doi:10.1073/pnas.1201632109 (2012).
- 245 Amatniek, J. C. *et al.* Incidence and Predictors of Seizures in Patients with Alzheimer's Disease. *Epilepsia* **47**, 867-872, doi:10.1111/j.1528-1167.2006.00554.x (2006).
- 246 de Calignon, A. *et al.* Propagation of tau pathology in a model of early Alzheimer's disease. *Neuron* **73**, 685-697 (2012).
- 247 Wu, J. W. *et al.* Small misfolded Tau species are internalized via bulk endocytosis and anterogradely and retrogradely transported in neurons. *Journal of Biological Chemistry* **288**, 1856-1870 (2013).
- 248 Wu, J. W. *et al.* Neuronal activity enhances tau propagation and tau pathology in vivo. *Nature neuroscience* **19**, 1085-1092, doi:10.1038/nn.4328 (2016).
- 249 Hu, Y.-Y. *et al.* Ceftriaxone modulates uptake activity of glial glutamate transporter-1 against global brain ischemia in rats. *Journal of neurochemistry* **132**, 194-205, doi:10.1111/jnc.12958 (2015).
- 250 Roberson, E. D. *et al.* Reducing Endogenous Tau Ameliorates Amyloid  $\beta$ -Induced Deficits in an Alzheimer's Disease Mouse Model. *Science* **316**, 750-754, doi:10.1126/science.1141736 (2007).
- 251 Ouyang, Y.-B. *et al.* miR-181 regulates GRP78 and influences outcome from cerebral ischemia in vitro and in vivo. *Neurobiology of disease* **45**, 555-563, doi:10.1016/j.nbd.2011.09.012 (2012).